NUI MAYNOOTH

Ollscoil na hÉireann Má Nuad

A control theoretic approach to mitigate viral escape in HIV

A dissertation submitted for the degree of
Doctor of Philosophy

by

Esteban Abelardo Hernandez Vargas

Supervisor: Prof. Richard H. Middleton

Hamilton Institute
National University of Ireland, Maynooth
Ollscoil na hÈireann, Mà Nuad

June 2011

Contents

Abstract

A very important scientific advance was the identification of HIV as a causative agent for AIDS. HIV infection typically involves three main stages: a primary acute infection, a long asymptomatic period and a final increase in viral load with a simultaneous collapse in healthy CD4+T cell count during which AIDS appears. Motivated by the worldwide impact of HIV infection on health and the difficulties to test in vivo or in vitro the different hypothesis which help us to understand the infection, we study the problem from a control theoretic perspective. We present a deterministic ordinary differential equation model that is able to represent the three main stages in HIV infection. The mechanism behind this model suggests that macrophages could be long-term latent reservoirs for HIV and may be important in the progression to AIDS. To avoid or slow this progression to AIDS, antiretroviral drugs were introduce in the late eighties. However, these drugs are not always successful causing a viral rebound in the patient. This rebound is associated with the emergence of resistance mutations resulting in genotypes with reduced susceptibility to one or more of the drugs. To explore antiretroviral effects in HIV, we extend the mathematical model to include the impact of therapy and suggest different mutation models. Under some additional assumptions the model can be seen to be a positive switched dynamic system. Consequently we test clinical treatments and allow preliminary control analysis for switching treatments. After introducing the biological background and models, we formulate the problem of treatment scheduling to mitigate viral escape in HIV. The goal of this therapy schedule is to minimize the total viral load for the period of treatment. Using optimal control theory a general solution in continuous time is presented for a particular case of switched positive systems with a specific symmetry property. In this case the optimal switching rule is on a sliding surface. For the discrete-time version several algorithms based on linear programming are proposed to reduce the computational burden whilst still computing the optimal sequence. Relaxing the demand of optimality, we provide a result on state-feedback stabilization of autonomous positive switched systems through piecewise co-positive Lyapunov functions in continuous and discrete time. The performance might not be optimal but provides a tractable solution which guarantees some level of performance. Model predictive control (MPC) has been considered as an important suboptimal technique for biological applications, therefore we explore this technique to the viral escape mitigation problem.

Acknowledgments

First, thanks to God who gave me the chance to achieve this goal on my life.

I feel truly fortune to have had the opportunity to work under the wise guidance of Prof. Richard H. Middleton, always providing several ideas to this project. I really appreciate his help and his infinite patience.

This project was supported by the vast experience of Prof. Patrizio Colaneri, his close collaboration enriched the present work. I also would like to say thanks to Prof. Franco Blanchini for his expertise provided to this thesis. The comments of the examiners Prof. Alessandro Astolfi and Oliver Mason are really appreciated. Moreover, I acknowledge the discussions and collaborations with Jorge dos Santos, Zhan Shu, Wilhelm Huisinga, Max von Kleist and Diego Oyarzun.

Prof. Peter Wellstead, Dimitris Kalamatianos, Oliver Mason, Rosemary, Kate and Ruth for welcoming me at the Hamilton Institute. The financial support by the Science Foundation Ireland through the awards 07/RPR/I177 and 07/IN/I1838 is truly appreciated.

My friends in Ireland who have made my stay an enjoyable experience; Alessandro, Helga, Fernando, Magdalena, Colm, Stella, David, Emanuele, Andres, Arieh, Buket, Adelaide, Martina, ELMhadi, Daniela, Paul and Hessan. Moreover, a number of people in Mexico who support me despite a big distance; Adriana, Fatima, Alma, Alvaro, Miguel, David, Antonio, Blanca and Ornelas. My relatives which always have been with me; Elfega Vargas, Lourdes Vargas, Miguel Hernandez, and cousins Moreno, Ronaldo, and Mayela. I would like to recognize the teachings and motivation of my previous two advisers Dr. Edgar Sanchez and Dr. Gabriel Segovia.

Dedicado a mis padres
Elia del Carmen Vargas Jaime
y Esteban Hernandez Torres,
a mi hermana
Alejandra Hernandez Vargas,
y a mi abuelita
Ana Maria Jaime

Despues me dijo un arriero,
que no hay que llegar primero,
pero hay que saber llegar

Then an arriero told me,
that you do not have to arrive first,
but you have to know how to arrive

Jose Alfredo Jimenez

Chapter 1

Introduction

The update of UNAIDS in 2009 showed a worldwide increase of people living with HIV (human immunodeficiency virus). Approximately 33.4 million people (adults and children) are living with HIV and the estimated number of people newly infected with HIV was 2.7 million in 2008, 20% higher than the number in 2000. At present, there is no known cure that results in eradication of the virus in an infected person. Antiretroviral therapy may be used and is largely successful in suppressing viral load. However, long term treatment to control the replication often fails, causing patients infected with HIV to progress to AIDS (Acquired Immune Deficiency Syndrome). The estimation of deaths due to AIDS in 2007 was 2 million people [1]. For this reason, much effort has been conducted for the last 30 years to find a possible solution to stop the infection. To understand how HIV infection collapses the immune system numerous theories have been proposed. However, to date, mathematical models of HIV infection do not fully explain all events observed to occur in practice. In the last decade, as a result of the relevant health problems and the difficulty to understand HIV infection process, mathematical modeling has started to be employed. This modeling helps to understand the relation between HIV and the immune system, and how treatments may affect the HIV cycle. These approaches are mainly modeled on the interaction of the HIV with CD4+T cells.

HIV infection can be roughly described in three stages; an early peak in the viral load, a long asymptomatic period and a final increase in viral load with a simultaneous collapse in healthy CD4+T cell count during which AIDS appears. In an untreated patient, the time course of these three stages is approximately 10 years. Models of HIV infection have been able to describe the primary infection and the symptomatic stages. However they are not able to explain the transition to AIDS, which is very important for the patient's health. Typically, to model this transition to AIDS, time-varying parameters (with no detailed mechanistic model) are used [2]. Of course, with appropriately selected time-varying parameters, the full course of the disease can be represented. However, due to the lack of a mechanistic model of the parameter variations, we consider it is not suitable for predicting the results of alternate therapy options or schedules.

Most of the studies of the interaction between HIV and host body cells have been dedicated to CD4+T cells. Macrophages have been known since 1980s to be susceptible to HIV infection. However, they have passed as a "sideshow" relative to the "main attraction" of CD4+T cells [3]. In recent years, there has been a growing suspicion that antigen-presenting cells might be central to AIDS progression.

To the best of our knowledge, [4] proposed the first model able to represent the three stages of infection without time varying parameters during the simulation. Numerical results showed that macrophages might play an important role in the final stages of the infection. Nonetheless, dynamical studies of the model in [4] exhibit high sensitivity to parameter variations. These sensitivities show that for small parameter changes of the order of 3%, the typical time course to AIDS may reduce from 10 years to 2 years or may disappear entirely. Such unusually sensitive behavior shows that the model proposed by [4] requires more effort to robustly obtain the appropriate course of HIV infection. For this purpose, a reduction of [4] is proposed in order to analyze in detail the full course of HIV infection. In contrast to [4] the proposed model in this thesis has a robust behavior to parameter variations, such performance tells us this model can be a good tool to understand AIDS progression. Once we have certain grade of confidence in the model, different studies are performed on it.

The treatment of HIV infected patients is of major importance in today's social medicine. Highly Active Antiretroviral Therapies (HAART) are the most important treatment strategies for HIV infected patients. Antiretroviral therapy for treating HIV-1 has improved steadily since the advent of potent therapy in 1996. New drugs have been approved, they offer new mechanisms of action, improvements in potency and activity (even against multi-drug-resistant viral strains), dosing convenience, and tolerability. These therapies prevent immune deterioration, reduce morbidity and mortality, and prolong the life expectancy of people infected with HIV. Moreover, viral load in the blood is reduced by at least five orders of magnitude.

Nonetheless, HAART is not always successful. Many patients have long-term complications while others experience virological failure. Virological failure is defined as the inability to maintain HIV RNA levels less than 50 copies/ml [5]. In most cases, viral rebound is associated with the emergence of resistance-conferring mutations within the viral genome, resulting in virus with reduced susceptibility to one or more of the drugs. Published guidelines [5] suggest that the primary goal of the initial regimen is to suppress viral replication to the maximum degree possible and sustain this level of suppression as long as possible. Unfortunately, even when the virus is suppressed, ongoing low-level replication still occurs, hence the likelihood of developing resistance is always present. Moreover, virus eradication by HAART does not appear to be achievable in the foreseeable future. In this environment, one key goal day-to-day clinical management is to delay the time until patients exhibit strains resistant to all of existing regimens.

There is therefore a crucial tradeoff between switching drugs too early, which risks poor adherence to a new drug regimen and prematurely exhaust the limited number of remaining salvage therapies,

and switching drugs too late, which allows the accumulation of mutations that leads to multidrug resistance [6]. The guidelines for the use of antiretroviral agents in HIV-1-infected adults and adolescents [5] have not achieved a consensus on the optimal time to change therapy for virologic failure. The most aggressive approach would be to change for any repeated detectable viremia (e.g. two consecutive HIV RNA $>$ 50 copies/ml after suppression). The most acceptable strategy has been to allow detectable viremia up to an arbitrary level (e.g. 1000-500 copies/ml). This later approach is called switch on virologic failure. Using a mathematical approach [7] hypothesized that alternating HAART regimens would further reduce the likelihood of the emergence of resistance. Years after, [8], [9] evaluated this proactive switching in a clinical trial, which they called SWATCH (SWitching Antiretroviral Therapy Combinations against HIV-1). Surprisingly, alternating regimens outperformed the virologic failure based treatment.

However, there are still many links missing with alternating regimens. The most important is how this alternation regimen should be designed in order to minimize the viral load. For this reason we address the problem of HAART scheduling using a control theoretic approach. This is because control systems have been shown to be an effective tool to deal with optimization problems under time constraints. For the sake of simplicity in the control design approach, we make some assumptions on the proposed HIV model. The most important assumption is that healthy CD4+T cell and macrophage concentrations remains approximately constant under treatment. This will allow us to characterize the model as a switched positive linear system, where the switching action will indicate the regimen that is being used. Therefore, the problem will be defined as to find the switching trajectory which minimizes the total viral load and maintains a low level for as long as possible.

Thus, we introduce optimal control for positive switched systems to minimize viral load in a finite horizon. Although the systems are linear, the solution to the optimal control is not trivial as a result of the switching action. The problem of determining optimal switching trajectories in hybrid systems has been widely investigated, both from theoretical and computational point of view. In this work, for a particular case with a certain class of symmetry, we solve analytically for the optimal solution. For this case, the optimal solution belongs to a sliding surface.

For discrete-time systems the problem remains complex and numerical algorithms have been proposed to determine optimal trajectories. On one hand iterative solutions based on Pontryagin's maximum principle have been proposed, but without any guarantee of convergence. On the other hand, dynamic programming is good for problems of reasonable dimension. Here, based on the specific problem considered, we suggest algorithms based on linear programming (LP) to reduce the computational burden and simulation time.

A general solution for the optimal control problem is hard to find even numerically. Consequently, it is necessary to explore other strategies to find solutions which guarantee certain performance. Relaxing the demand of optimality we use linear co–positive Lyapunov functions. Based on these, we examine stability properties and then guaranteed cost controls for switched positive systems

are presented. Simulation results show the effectiveness of these methods. Moreover, we consider the application of Model Predictive Control (MPC) as it appears to be suitable for a suboptimal application in the biomedical area. Based on the switched linear system we applied optimal and suboptimal strategies on a nonlinear mutation model. Simulation results exhibit good performance of these strategies when applied to a high order nonlinear model although they are based on a simplified linear model.

1.1 Overview and Contributions

In **Chapter 2** we review the basic concepts to understand the immune system and the various cell types involved in the immune response. Moreover, we put together many concepts and ideas in HIV, these are the HIV cycle, HIV disease progression and the different mechanisms by which HIV causes the depletion of CD4+T cells. To describe how antiretroviral treatments can tackle HIV, we introduce an up to date list of accepted drugs against HIV and their different guidelines.

In **Chapter 3** we address the modeling problem of HIV infection using differential equations. We start the chapter with a description of different mathematical models in the area and how different mechanisms have been used to explain the progression to AIDS. The contributions of this chapter are the following:

- The derivation of a mathematical model able to represent the three stages of HIV infection is presented. The main difference with other models is that our model exhibits a robust behavior to parameter variations and contemplates the long-term behavior in HIV infection.
- We provide a sensitivity and steady state analysis with the end to understand the reasons of the transition to AIDS.
- By inclusion of cell proliferation terms we can improve the match between the model dynamics with common clinical observations, and still maintain behavior that is robust to parameter variations.
- Under normal treatment circumstances, we assume constant cell concentrations. Then we derive three different positive switched linear mutation models to test clinical treatments and to allow preliminary control analysis for the switching treatment.

In **Chapter 4** we address the optimal control problem for positive switched systems using a finite horizon cost function. The contributions of this chapter are the following:

- A formulation of the optimal control problem for positive switched systems with application to mitigate HIV escape is proposed.

- The main result of the chapter is a general solution for a particular case of switched systems with a certain symmetry property, where the optimal switching rule is on a sliding surface. A more general permutation case is presented.
- Using dynamic programming we formulate the discrete-time optimal control problem. This gives a two point boundary value problem, that is difficult to solve due to the switched system nature. Alternatively, exhaustive search approaches may be used but are computationally prohibitive. To relax these problems we propose several algorithms based on linear programming to reduce the computational burden whilst still computing the optimal sequence.

Relaxing the demand of optimality in **Chapter 5** we address different suboptimal strategies for positive switched systems in finite horizon. The contributions of this chapter are the following:

- We provide a result on state-feedback stabilization of autonomous positive switched systems through piecewise co-positive Lyapunov functions in continuous and discrete time. The performance might not be optimal but provides a solution which guarantees an upper bound on the achieved cost.
- We explore model predictive control application for positive switched systems, which has been used for many biomedical applications.
- The performance of optimal and suboptimal strategies is tested via simulation using three different switched linear systems. To verify if these strategies can be applied to a more realistic scenario, we test them on a nonlinear system. We apply optimal and suboptimal strategies to this nonlinear mutation model where the control is designed using a reduced order linear approximation of the dynamics.

We conclude in **Chapter 6** summarizing the main ideas and results of the thesis and pointing out some open questions for future research. Some of the results of this thesis have led to the following peer-reviewed publications:

- E.A. Hernandez-Vargas, Dhagash Mehta, R. Middleton, Towards Modeling HIV Long Term Behavior, IFAC World Congress, Milan, Italy, 2011
- E.A. Hernandez-Vargas, R. Middleton, P. Colaneri, Optimal and MPC Switching Strategies for Mitigating Viral Mutation Escape, IFAC World Congress, Milan, Italy, 2011
- E.A. Hernandez-Vargas, P. Colaneri, R. Middleton, F. Blanchini, Dynamic Optimization Algorithms to Mitigate HIV escape, IEEE Conference on Decision Control, Atlanta, USA, 2010
- R. Middleton, P. Colaneri, E.A. Hernandez-Vargas, F. Blanchini, Continuous-time Optimal Control for Switched Positive Systems with application to mitigating viral escape, NOLCOS, Bologna, 2010

- E.A. Hernandez-Vargas, P. Colaneri, R. Middleton, F. Blanchini, Discrete-time control for Switched Positive Systems with Application to Mitigating viral escape, International Journal of Robust and Nonlinear Control, 2010.
- J. Ferreira, E.A. Hernandez-Vargas, R. Middleton, Computer Simulation of Structured Treatment Interruption for HIV infection, Computers Methods and Programs in Biomedicine, 2011.

PART I

BIOLOGICAL BACKGROUND

Chapter 2

HIV and the Immune System

In this chapter we briefly describe the immune system and the various cell types involved in an adaptive immune response, as well as their interactions. An introduction to HIV infection, AIDS progression and its possible causes are presented. We conclude the chapter by providing the most recent list of drugs accepted for treatment of HIV infection and their different guidelines for use.

2.1 Immune System

Immunology is the study of the body's defense against infection. Our body's reactions to infection by potential pathogens are known as immune responses. The immune system can be divided into two parts, called innate and adaptive. The innate immune system is composed of physiological barriers that prevent the invasion of foreign agents. Most infectious agents activate the innate immune system and induce an inflammatory response. The adaptive immune response is mediated by a complex network of specialized cells that identify and respond to foreign invaders. It is called adaptive due to the fact that it can respond with great specificity to a very broad class of foreign substances, and exhibits memory, so that subsequent re-challenge results in a powerful, immediate response. The immune system is composed of different types of white blood cells (leukocytes), antibodies and some active chemicals. These cells work together to defend the body against diseases by foreign invaders. All the cellular elements of the blood, including the red blood cells that transport oxygen, the platelets that trigger blood clotting in damaged tissues, and the white blood cells of the immune system arise from the pluripotent hematopoietic stem cells in the bone marrow. White cells then migrate to guard the peripheral tissues- some of them residing within the tissues, other circulating in the bloodstream and in a specialized system of vessels called lymphatic system, which drains extracellular fluid and frees cells from tissues, transports them through the body as lymph, and eventually empties into the blood system [10].

2.1.1 Immune System Components

A major distinguishing feature of some leukocytes is the presence of granules; white blood cells are often characterized as granulocytes or agranulocytes. Granulocytes are leukocytes characterized by the presence of differently staining granules in their cytoplasm when viewed under microscopy. These granules are membrane-bound enzymes which primarily act in the digestion of endocytosed particles. There are three types of granulocytes: neutrophils, basophils, and eosinophils. Agranulocytes are leukocytes characterized by the apparent absence of granules in their cytoplasm, these include lymphocytes and monocytes [10]. The three major types of lymphocyte are T cells, B cells and natural killer (NK) cells. T cells (Thymus cells) and B cells (bone cells) are the major cellular components of the adaptive immune response. The specific roles played by various agranulocytes cells and their interactions are presented below.

Dendritic Cells

Dendritic cells are known as antigen-presenting cells (APCs), which are particularly important to activate T cells. They have long finger-like processes, see Fig.2.1 like dendrites of nerve cells, which gives them their name. There are at least two broad classes of dendritic cells (DCs) that have been recognized; the conventional dendritic cells (cDC) that seem to participate most directly in antigen presentation and activation of naive T cells; and plasmacitoid dendritic cells (pDC), a distinct lineage that generate large amounts of interferons, particularly in response to viral infections, but do not seem to be as important for activating naive T cells.

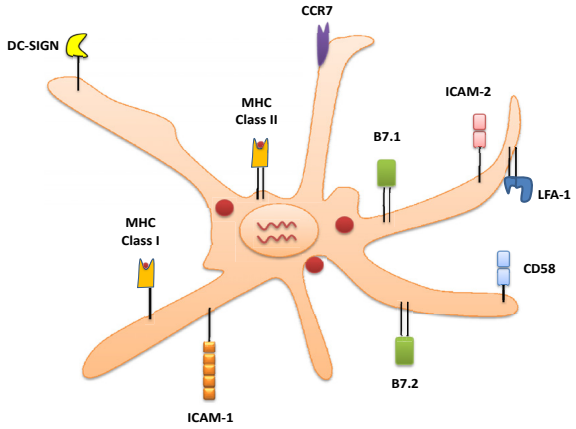

Fig. 2.1: Conventional dendritic cell

Cells detect peptides derived from foreign antigens. Such antigens peptide fragments are captured by Major Histocompatability Complex (MHC) molecules, which are displayed at the cell surface.

There are two main types of MHC molecules, called MHC I and II. The most important differences between the two classes of MHC molecule lie not in their structure but in the source of the peptides that they can trap and carry to the cell surface. MHC class I molecules collect peptides derived from proteins synthesized in the cytosol, therefore they are able to display fragments of viral proteins on the cell surface. MHC class II molecules bind peptides derived from proteins in intracellular vesicles, and thus display peptides derived from pathogens living in macrophage vesicles and B cells. MHC class II receptors are only displayed by APCs.

T Lymphocytes

T lymphocytes or T cells are a subset of lymphocytes defined by their development in the thymus. During T cell arrangement, a number of random rearrangements occur in the portion of the genome responsible for creating the T cell Receptor (TCR) protein. This occurs in every immature T cell expressing a unique TCR surface protein, providing an enormous range of specificity. All cells that express TCR that do not bind with sufficient strength to MHC molecules are killed as well as those express TCR that bind too strongly to MHC molecules. T cells that survive are those whose TCR proteins are capable of recognizing MHC molecules with bound peptide fragments, but do not bind strongly to any peptide fragments occurring naturally in uninfected cells. During this process, the lineage of the T cells is also determined; either they become helper T cells, expressing the surface molecule CD4 and TCR that bind with MHC class II, or they become cytotoxic T cells, expressing the surface molecule CD8 and TCR that bind to MHC class I.

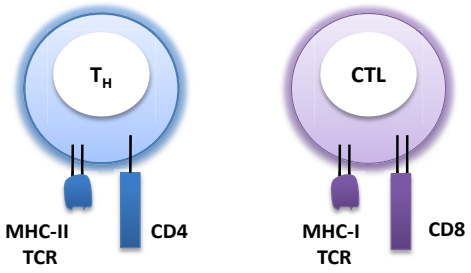

Fig. 2.2: Types of effector T cell

Once T cells are mature, they enter the bloodstream. Naive T cells are those mature recirculating T cells that have not yet encountered their specific antigens. To participate in the adaptive immune response, a naive T cell must meet its specific antigen. Then they are induced to proliferate and differentiate into cells that have acquired new activities that contribute to remove the antigen. CD4+T or Helper T cells do not directly mediate an adaptive immune response; instead, they regulate the development of the humoral (B-cell mediated) or cellular (T cell mediated) immune

responses. CD4+T cells have a more flexible repertoire of effector activities, the most important are: T_H1 cells are able to activate infected macrophages, T_H2 cells provide help to B cells for antibody production, T_H17 cells enhance neutrophil response, and T_{reg} cells suppress T cell responses.

CD8+T cells are T cells that carry the co-receptor CD8, see Fig.2.2. They recognize antigens, for example viral antigens, that are synthesized in the cytoplasm of a cell. Naive CD8 T cells are long-lived, and remain dormant until interacting with an APC displaying the antigen MHC class I complex for which the cells unique TCR is specific. The co-stimulatory molecule B7 is also necessary to activate a CD8+T cell into a cytotoxic-T cell (CTL). CTL can produce as many as 104 daughter cells within one week [11]. During CD4+T cell expansion, signals provided by CD4+T cells condition the expanding clones to be able to revert to a functional memory pool; however, the exact nature of this help is not known [12].

Lymphocytes are in different parts of the human body. They can circulate through the primary lymphoid organs (thymus and bone marrow), the secondary lymphoid organs (spleen, lymph nodes (LN)), tonsils and Peyers patches (PP) as well as non-lymphoid organs, such as blood, lung and liver, see Table 2.1. Lymphocytes numbers in the blood are used to evaluate the immune status because is an accessible organ system, however blood lymphocytes represent only about 2% of the total numbers of lymphocytes in the body. The number of lymphocytes in the blood depend on race and is influenced by various factors [13].

Table 2.1: Lymphocytes Distribution

Organ	**Lymphocytes** (10^9)
Blood	10
Lung	30
Liver	10
Spleen	70
Lymph nodes	190
Gut	50
Bone marrow	50
Thymus	50
Other Tissue	30

B Cells

B cells are lymphocytes that play a large role in the humoral immune response, and are primarily involved in the production of antibodies, proteins that bind with extreme specificity to a variety of extra-cellular antigens. B cells (with co-stimulation) transform into plasma cells which secrete antibodies. The co-stimulation of the B cell can come from another antigen presenting cell, like a dendritic cell. This entire process is aided by T_H2 cells which provide co-stimulation. Antibody

molecules are known as immunoglobulins (Ig), and the antigen receptor of B lymphocytes as membrane immunoglobulin. There are five classes of antibodies that B cells can produce; IgM, IgG, IgA, IgD, and IgE; each of which has different chemical structure in their invariant region (the portion of the molecule that does not affect the antibodies antigen specificity).

Macrophages

Macrophages, large mononuclear phagocytic cells, are resident in almost all tissues and are the mature form of monocytes, which circulate in the blood and continually migrate into tissues, where they differentiate. Macrophages are long-lived cells and perform different functions throughout the innate response and the subsequent adaptive immune response. Their role is to phagocytose (engulf and then digest) cellular debris and pathogens either as stationary or mobile cells, and to stimulate lymphocytes and other immune cells to respond to the pathogen.

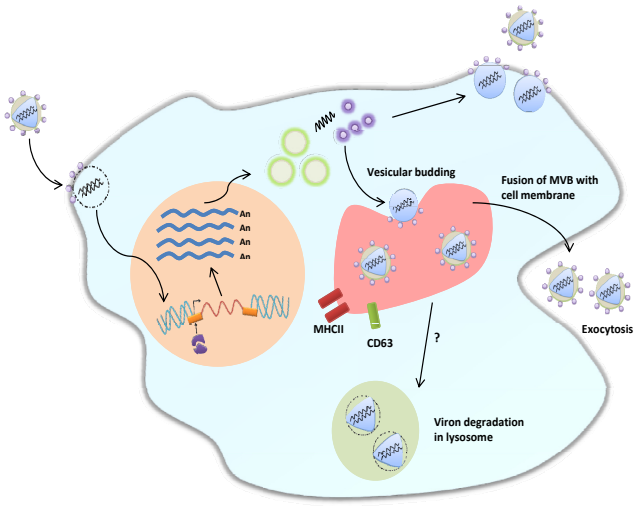

Fig. 2.3: Macrophage scheme

A crucial role of macrophages is to orchestrate immune responses: they help induce inflammation and secrete signaling proteins that activate other immune system cells. These proteins are cytokines and chemokines. Cytokine is a general name for any protein that is secreted by cells and affects the behavior of nearby cells bearing appropriate receptors. Chemokines are secreted proteins that attract cells bearing chemokine receptors out of the blood stream and into the infected tissue.

2.2 HIV Infection

In 1981, reports of a new disease emerged in the USA, which caused tumors, such as Kaposis sarcoma and other opportunistic infections originating from immunologic abnormalities. The new disease was called Acquired Immunodeficiency Syndrome (AIDS) based on the symptoms, infections, and cancers associated with the deficiency of the immune system. In 1983, Sinoussi and Montagnier isolated a new human T-cell leukemia viruses from a patient with AIDS [14], which was later named HIV (Human Immunodeficiency Virus). It is now clear that there are at least two types, HIV-1 and HIV-2 which are closely related. HIV-2 is endemic in west Africa and now spreading in India. Most AIDS worldwide is, however, caused by the most virulent HIV-1, which has been infecting humans in central Africa for far longer than had originally been thought [10].

2.2.1 HIV Components and Cycle

Like most viruses, HIV does not have the ability to reproduce independently. Therefore, it must rely on a host to aid reproduction. Each virus particle whose structure is shown in Fig.2.4 consists of nine genes flanked by long terminal repeat sequences. The three major genes are gag, pol, and env. The gag gene encodes the structural proteins of the viral core, pol encodes the enzymes involved in viral replication and integration, env encodes the viral envelope glycoproteins. The other six genome are smaller, Tat and Rev perform regulatory functions that are essential for viral replication, and the remaining four Nef, Vif, Vpra and Vpu are essential for efficient virus production. HIV expresses 72 glycoprotein projections composed of gp120 and gp41. Gp41 is a transmembrane molecule that crosses the lipid bilayer of the envelope. Gp120 is non-covalently associated with gp41 and serves as the viral receptor for CD4+T cells.

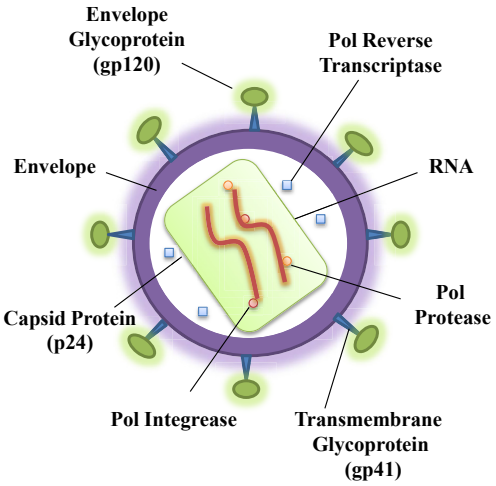

Fig. 2.4: HIV components

The HIV genome consists of two copies of RNA, which are associated with two molecules of reverse transcriptase and nucleoid proteins p10, a protease, and an integrase. During infection the gp120 binds to a CD4 molecule on the surface of the target cell, and also to a co-receptor, see Fig.2.5. This co-receptor can be the molecule CCR5, primarily found on the surface of macrophages and CD4+T cells, or the the molecule CXCR4, primarily found on the surface of CD4+T cells. After the binding of gp120 to the receptor and co-receptor, gp41 causes fusion of the viral envelope with the cell's membrane, allowing the viral genome and associated viral proteins to enter the cytoplasm. HIV is classified as a retrovirus, an RNA virus which can replicate in a host cell via the enzyme reverse transcriptase to produce DNA from its RNA genome. The DNA is then incorporated into the cell nucleus by an integrase enzyme. Once integrated the viral DNA is called a provirus. Then the DNA hijacks the host cell, and directs the cell to produce multiple copies of viral RNA. These viral RNA are translated into viral proteins to be packaged with other enzymes that are necessary for viral replication. An immature viral particle is formed, which undergoes a maturation process. The enzyme protease facilitates maturation by cutting the protein chain into individuals proteins that are required for the production of new viruses. The virus thereafter replicates as part of the host cell's DNA [15].

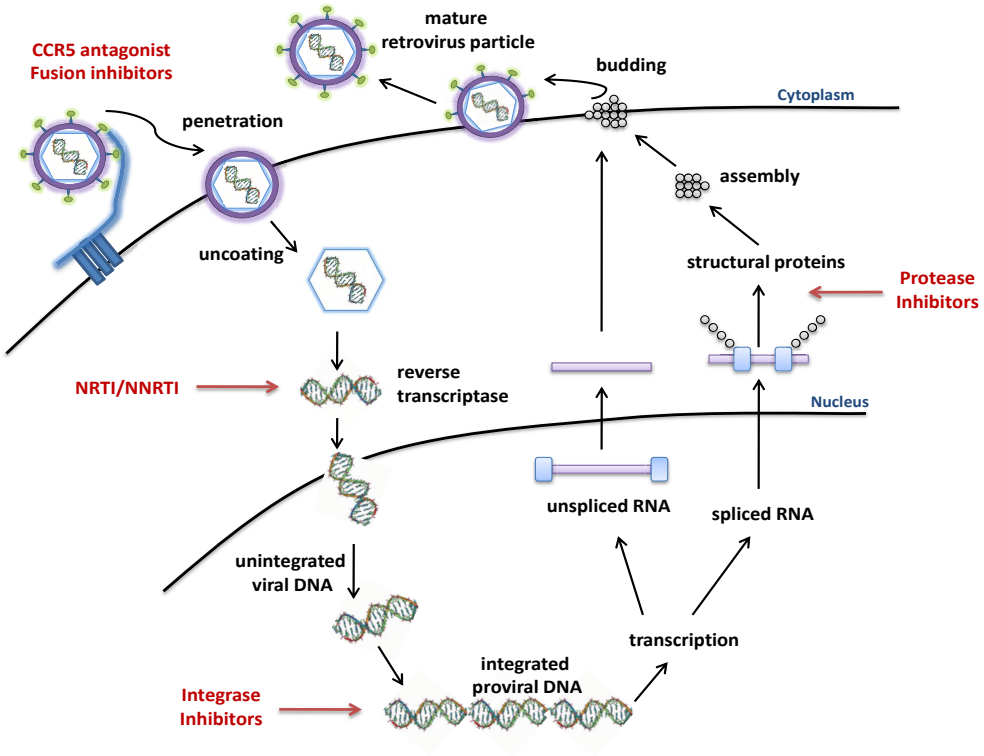

Fig. 2.5: HIV cycle

2.2.2 HIV Disease Progression

The term viral tropism refers to which cell types HIV infects. When a person is infected with HIV, its target are CD4+T cells, macrophages and dendritic cells. Because of the important role of these cells in the immune system, HIV can provoke devastating effects on the patients health. For clinicians, the key markers of the disease progression are CD4+T cell count and viral levels in the plasma. A typical patient's response consists of an early peak in the viral load, a long asymptomatic period and a final increase in viral load with a simultaneous collapse in healthy T cell count during which AIDS appears. This course is shown in Fig.2.6.

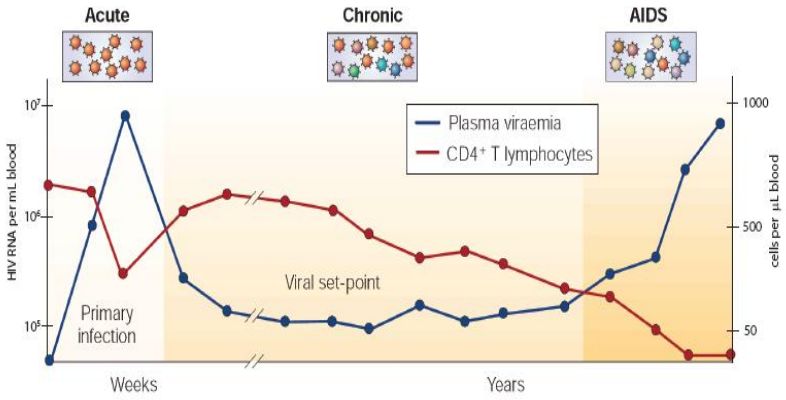

Fig. 2.6: Typical HIV/AIDS course. Picture taken from [36].

During the acute infection period (2-10 weeks) there is a sharp drop in the concentration of circulating CD4+T cells, and a large spike in the level of circulating free virus (to an average of 10^7 copies/ml). In this primary period, patients developed an acute syndrome characterized by flu-like symptoms of fever, malaise, lymphadenopathy, pharyngitis, headache and some rash. Following primary infection, seroconversion occurs, when people develop antibodies to HIV, which can take from 1 week to several months. After this period, the level of circulating CD4+T cells returns to near-normal, and the viral load drops dramatically (to an average of about 50,000/ml). In the asymptomatic or latency period, without symptoms, the patient does not exhibit any evidence of disease, even though HIV is continuously infecting new cells and actively replicating. The latent period varies in length from one individual to another, there are reports of this latent period lasting only 2 years, while other reports more than 15 years [3]. Normally, this period ranges from 7 to 10 years. After the long asymptomatic period, the virus eventually gets out of control and the remaining cells are destroyed. When the CD4+T cell count has dropped lower than 250 cells/mm^3, the individual is said to have AIDS. During this stage the patient starts to succumb to opportunistic infections as the depletion of CD4+T cells leads to severe immune system malfunction.

2.2.3 How Does HIV cause AIDS?

AIDS is characterized by the gradual depletion of CD4+T cells from blood. The mechanism by which HIV causes depletion of CD4+T cells in infected patients remains unknown. Numerous theories have been proposed, but none can fully explain all of the events observed to occur in patients. The most relevant mechanisms are explained below.

Thymic Dysfunction

The thymus is the primary lymphoid organ supplying new lymphocytes to the periphery. Thymopoiesis, the basic production of mature naive T lymphocytes populating the lymphoid system is most active during the earlier parts of life. However, recent advances in characterizing thymic functions suggest that the adult thymus is still actively engaged in thymopoiesis and exports new T cells to the periphery till 60 years of age [16]. Several works [17], [18] have reported that HIV induced thymic dysfunction, which could influence the rate of disease progression to AIDS, suggesting a crucial role of impaired thymopoiesis in HIV pathogenesis. Moreover, thymic epithelial cells can also be infected and this in turn could promote intrathymic spread of HIV [19].

The Homing theory

An important mechanism to explain AIDS is Homing (a precisely controlled process where T cells in blood normally flow into the lymph system). This process occurs when CD4+T cells leave the blood, then abortive infection with HIV induces resting CD4+T cells to home from the blood to the lymph nodes, see [20],[21],[22]. All this homing T cells are abortively infected and do not produce HIV mRNA [21]. The normal lymph-blood circulation process is within one or two days [23], but when they enter in the blood, they exhibit accelerated homing back to the lymph node. Once these abortive cells are in the lymph node, half of them are induced to apoptosis by secondary signals through homing receptors (CD62L, CD44, CD11a) as shown in [21]. The few active infected T cells in lymph nodes, bind to surrounding T cells (98-99% of which are resting) and induces signals through CD4+T and/or chemokine co-receptors.

The Dual role of Dendritic cells

In HIV, DCs play a dual role of promoting immunity while also facilitating infection. C-type lectin receptors on the surface of DCs, such as DC-SIGN can bind HIV-1 envelope gp120 [24]. DCs can internalize and protect viruses, extending the typically short infectious half-life of virus to several days [25]. The progressive alteration of the immune system resulting in the transition to AIDS, could be caused by the dysfunction of DCs. During progression, DCs either fail to prime T cells or are

actively immune-suppressive, resulting in failure of the immune control; however, the reasons for this dysfunction are unknown. [26] proposed that DCs could be directly affected by HIV or indirectly causing dysfunction due to a lack of CD4+T cells.

Persistent Immune Activation

Cytopahic effects alone can not fully account for the massive loss of CD4+ T cells, since productively infected cells occupy a small fraction of total CD4+ T cells (typically of the order of 0.02% to 0.2%). Various clinical studies have linked the massive depletion of CD4+ T cells to the wide and persistent immune activation, which seemed to increase with duration of HIV-1 infection [12], [27]. According to this theory, the thymus produces enough naive T cells during the first years of life to fight a lifelong battle against various pathogens. Thus, long-lasting overconsumption of naive supplies through persistent immune activation, such as observed during HIV-1 infection will lead to accelerated depletion of the CD4+T and CD8+T cells stock. This effect would be more pronounced if thymic output depends only on age and not on homeostatic demand, though this view is debated [17].

Immune Escape

Numerous reasons for lack of immune control have been proposed. The best documented has been immune escape through the generation of mutations in targeted epitopes of the virus. When effective selection pressure is applied, the error-prone reverse transcriptase and high replication rate of HIV-1 allow for a rapid replacement of circulating virus by those carrying resistance mutations as was first observed with administration of potent antiretroviral therapy [28]. Note that escape may occur even through single amino-acid mutation in an epitope (part of an antigen that is recognized by the immune system), at sites essential for MHC binding or T cell receptor recognition.

Reservoirs and Sanctuary Sites

Long-lived reservoirs of HIV-1 are a barrier to effective immune system response and antiretroviral therapy, and an obstacle for strategies aimed at eradicating HIV-1 from the body. Persistent reservoirs may include latently infected cells or sanctuary sites where antiretroviral drug penetrance is compromised. Moreover, the cell type and mechanism of viral latency may be influenced by anatomical location. Some studies [29], [30] have suggested that latently infected resting CD4+T cells could be one of these long-term reservoir while other studies have been conducted to explore the role of macrophages as an HIV sanctuary [31].

2.3 Antiretroviral Drugs for HIV infection

The most important scientific advance after the identification of HIV as the causative agent for AIDS was the development of effective antiretroviral drugs for treating individuals infected with HIV. The first effective drug against HIV was the reverse transcriptase inhibitor azidovudine, which was developed as an anticancer drug but was not effective in that capacity. It was licensed as the first antiretroviral drug in 1987. The use of zidovudine during pregnancy was documented to decrease neonatal transmission of HIV from 25.5% to 8.3% [32]. Subsequently, more drugs have been developed to target specific vulnerable points in the HIV life cycle, see Fig.2.5. Currently, there are 20 drugs approved and their use in combinations of three or more drugs have transformed the treatment of individuals. Morbidity and mortality owing to HIV disease have sharply declined [3].

Highly active antiretroviral therapy (HAART), the combination of three or more antiretrovirals, was used to reduce viral replication and to delay the progression of the infection. Another salutary effect of HAART is the restoration of immune function, which routinely occurs on long-term therapy and leads to the regeneration of robust CD4+T and CD8+T cellular responses to recall antigens [33].

There are more than 20 approved antiretroviral drugs in 6 mechanistic classes with which to design combination regimens, see Table 2.2. These 6 classes include the nucleoside/nucleotide reverse transcriptase inhibitors (NRTIs), non-nucleoside reverse transcriptase inhibitors (NNRTIs), protease inhibitors (PIs), fusion inhibitors (FIs), CCR5 antagonist, and integrase strand transfer inhibitors (INSTI). The most extensively studied combination regimens for treatment-naive patients that provide durable viral suppression generally consist of two NRTIs plus one NNRTI or PI [5].

Fusion Inhibitors and CCR5 Antagonists interfere with the binding, fusion and entry of an HIV virion to a human cell. There are several key proteins involved in the HIV entry process: CD4, gp120, CCR5, CXCR4, gp41. FIs have shown very promising results in clinical trials, with low incidences of relatively mild side-effects, but they are large molecules that must be given through injection or infusion, which limits their usefulness. The CCR5 co-receptor antagonists inhibit fusion of HIV with the host cell by blocking the interaction between the gp-120 viral glycoprotein and the CCR5 chemokine receptor [34]. The adverse events are abdominal pain, cough, dizziness, musculoskeletal symptoms, pyrexia and upper respiratory tract infection.

Nucleoside Reverse Transcriptase Inhibitors mimic natural nucleosides, and are introduced into the DNA copy of the HIV RNA during the reverse transcription event of infection. However, the NRTI are nonfunctional, and their inclusion terminates the formation of the DNA copy. The side effects associated with NRTI use seem to be related to mitochondrial toxicity [21], and can include myelotoxicity, lactic acidosis, neuropathy, pancreatitis, lipodystrophy, fatigue, nausea, vomiting, and diarrhea.

Table 2.2: Antiretroviral Drugs [5]

Class	Generic Name	Trade Name	Intracellular Half-life
NNRTIs	Delavirdine	Rescriptor	5.8 hrs
	Efavirenz	Sustiva	40-55 hrs
	Etravirine	Intelence	41 +/-20 hrs
	Nevirapine	Viramune	25-30 hrs
NRTIs	Abacavir	Ziagen	1.5 hrs/12-26 hrs
	Didanpsine	Videx	1.5 hrs/ 20 hrs
	Emtricitabine	Emtriva	10 hrs/ 20 hrs
	Lamiduvine	Epivir	5-7 hrs
	Stavudine	Zerit	1 hr/ 7.5 hrs
	Tenofovir	Viread	17 hrs/ 60 hrs
	Zidovudine	Retrovir	1.1 hrs/ 7 hrs
PIs	Atazanavir	Reyataz	7 hrs
	Darunavir	Prezista	15 hrs
	Fosamprenavir	Lexiva	7.7 hrs
	Indinavir	Crixivan	1.5-2 hrs
	Lopinavir	Kaletra	5-6 hrs
	Nelfinavir	Viracept	3.5-5 hrs
	Ritonavir	Norvir	3-5 hrs
	Saquinavir	Invirase	1-2 hrs
	Tipranavir	Aptivus	6 hrs
INSTIs	Raltegravir	Isentress	9 hrs
FIs	Enfuvirtide	Fuzeon	3.8 hrs
CCR5 Antagonists	Maraviroc	Selzentry	14-18 hrs

Non-Nucleoside Reverse Transcriptase Inhibitors also block the creation of a DNA copy of the HIV RNA, but work by binding directly to key sites on the reverse transcriptase molecule, blocking its action. These drugs do not work well on their own, but in conjunction with NRTIs, they increase the effectiveness of viral suppression. Side-effects can include hepatoxicity, rash, dizziness, and sleepiness depending on the drug used.

Integrase strand transfer inhibitors are a class of antiretroviral drug designed to block the action of integrase, a viral enzyme that inserts the viral genome into the DNA of the host cell. Sides effects may include nausea, headache, diarrhea and pyrexia.

Protease inhibitors target the viral enzyme protease that cuts the polyproteins into their respective components. With this step of viral replication blocked, the infected cell produces viral particles unable to infect cells. All currently available PIs can cause lipodystrophy, a severe redistribution of body-fat that can drastically change the patients appearance. Other side effects include gastrointestinal disorders, nephrolithiasis, dry skin, severe diarrhea, and hepatoxicity.

2.4 Viral Mutation and Drug Resistance

The process of reverse transcription is extremely error-prone, and the resulting mutations may cause drug resistance or allow the virus to evade the immune system. Drug resistance is a prominent issue in HIV infection, which means the reduction in effectiveness of a drug in curing the disease. HIV differs from many viruses because it has very high genetic variability. This diversity is a result of its fast replication cycle, with the generation of about 10^{10} virions every day, coupled with a high mutation rate of approximately 3×10^{-5} per nucleotide base per cycle of replication [35]. This complex scenario leads to the generation of many variants of HIV in the course of one day.

Genotypic and phenotypic resistance assays are used to assess viral strains and inform selection of treatment strategies. On one hand, the genotype is the genetic makeup of a cell, or an organism usually with reference to a specific characteristic under consideration. Then the genotypic assays detect drug resistance mutations present in relevant genes. On the other hand, a phenotype is any observable characteristic or trait of an organism: such as its morphology, development, biochemical or physiological properties and behavior. Hence phenotypic assays measure the ability of a virus to grow in different concentrations of antiretroviral drugs [5].

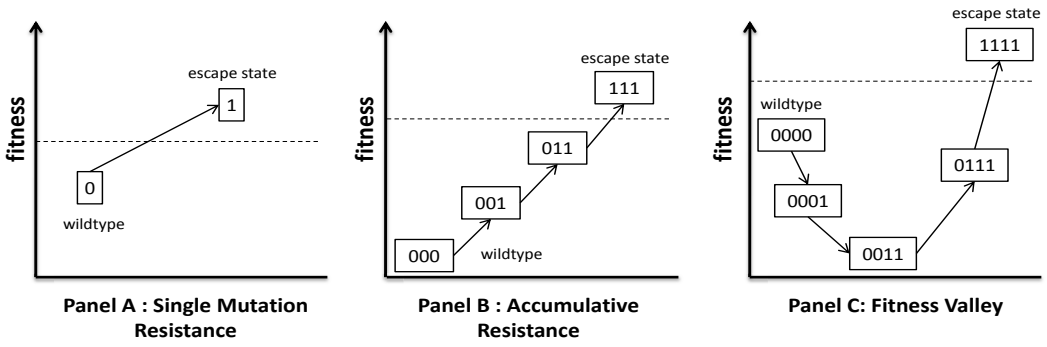

Fig. 2.7: Resistance pathways

The fitness of a viral strain, which can be described as the capability of an individual of a certain genotype to reproduce in a certain environment depends on the genotype. Through adaptation, the frequencies of the genotypes will change over generations and the genotypes with higher fitness become more common. Fig.2.7 shows some resistance pathways which were presented in [36]. Panel A illustrates a resistance pathway with a single point mutation, this has been observed when a single drug is supplied, for example Lamivudine. Resistance can emerge through accumulation of resistance-associated mutations as is shown in Panel B. In other cases, resistance can be developed after multiple steps of fitness loss, see Panel C, which then enable the emergence of mutants that are fit enough to sustain the population.

2.5 Guidelines for HAART Treatment

The use of HAART for suppression of measurable levels of virus in the body has greatly contributed to restore and preserve the immune system in HIV patients. In the 90s, the dogma for HIV therapy was "Hit HIV early and hard" [37]. However, the treatment of HIV is complicated by the existence of tissue compartments and cellular reservoirs. Long-term reservoirs can survive for many years and archive many quasispecies of virus that can re-emerge and propagate after withdrawal of HAART. Moreover, the virus in the central nervous and in semen evolves independently of virus found in blood cells [38], [39]. The initial enthusiasm for initiating therapy early was tempered by the recognition that standard antiretroviral therapy would probably not lead to eradication and, therefore, that therapy would need to be sustained indefinitely. This could be difficult for many patients due to adverse health events, metabolic complications, adherence and costs. These short and long term problems associated with HAART have led to proposals for alternative treatment strategies for controlling HIV infection. Next, the most important treatment guidelines and trials are explained.

2.5.1 Current Clinical Guidelines

Accumulating data showed that immune reconstitution was achievable even in those individuals with very low CD4+T cells count, and the time to diagnosis of AIDS or mortality was not different in those individuals who were treated early. Based on this consideration, the guidelines were changed to recommend that therapy should be initiated in asymptomatic patients when their CD4+T cells count drop between 200 and 350 $cell/mm^3$ [5]. In 2010, [40] presented a new treatment regimen, the recommendations emphasize the importance of starting HAART early and continuing treatment without interruption. HAART can be started at any time, but it is recommended for those asymptomatic individuals with counts at 500 cell/μl or below, and should be considered for asymptomatic individuals with counts above 500 cell/μl. Regardless of CD4+T cells count, HAART is recommended in the following settings; symptomatic patients, rapid disease progression: people older than 60 years old, pregnancy, chronic hepatitis B or hepatitis C and HIV-associated kidney disease.

The DHHS (Department of Health and Human Services) panel recommends initiating antiretroviral therapy in treatment patients with one of the following types of regimen: NNRTIs + 2 NRTIs, PIs + 2 NRTIs, and INSTIs + 2 NRTIs. However, the selection of a regimen should be individualized based on virologic efficacy, toxicity, pill burden, dosing frequency, drug-drug interaction potential, resistance testing results, and comorbid conditions [5].

HIV drug resistance testing should be performed to assist in the selection of active drugs when changing HAART regimens in patients with virologic failure, defined as the inability to sustain suppression of HIV RNA levels to less than 50 copies/ml. The optimal virologic response to treatment

is maximal virologic suppression (e.g., HIV RNA level <400 copies/ml after 24 weeks, <50 copies/ml after 48 weeks). Persistent low-level viremia (e.g. HIV RNA 50-200 copies/ml) does not necessarily indicate virologic failure or a reason to change treatment [5].

Immunologic failure can be defined as a failure to achieve and maintain an adequate CD4+T cell response despite virologic suppression. There is no consensus for when and how to treat immunologic failure. For some patients with high treatment experience, maximal virologic suppression is not possible. In this case, HAART should be continued with regimens designed to minimize toxicity, preserve CD4+T cell counts, and avoid clinical progression. In this scenario, expert advice is essential and should be sought.

Antiretroviral treatment failure is defined as a suboptimal response to therapy. Treatment failure is often associated with virologic failure, immunologic failure, and/or clinical progression. Many factors are associated with an increased risk of treatment failure, including starting therapy in earlier years, presence of drug-resistant virus, prior treatment failure, incomplete medication adherence, drug side effects, toxicities, suboptimal pharmacokinetics, and other unknown reasons.

2.5.2 Structured Treatment Interruptions

Structured treatment interruptions (STIs) consist of therapy withdrawal and re-initiation according to specific criteria. STIs were motivated in part by the clinical success of a patient in Germany, who was treated soon after diagnosis of acute HIV infection [41]. Before initiation of treatment in this patient, HIV RNA levels exceeded $80,000$ copies/ml on two separate occasions, suggesting that a steady state of viremia had already been reached. After viral suppression on HAART, the therapy was temporarily discontinued, which was associated with recurrence of viremia. However, after a second discontinuation of treatment due to concurrent hepatitis A infection, viral rebound was not observed in that patient who decided to stop therapy completely and remained virologically suppressed for the next 19 months. Since the patient's immune response progressively improved despite the absence of treatment, it was hypothesized that, intermittent exposure to HIV antigens may have boosted the HIV-specific immune response in this patient via autoimmunization.

In this context note that those individuals who have been living with HIV for at least 7 to 12 years (different authors use different time spans) and have stable CD4+T counts of 600 or more cells/mm^3 of blood and no HIV-related diseases have been called Long-Term Non-progressors (LNTP). However, the term LTNP is a misnomer, as it must be noted that progression toward AIDS can occur even after 15 years of stable infection [42]. The aim of the STIs mentioned earlier was either or both of: (i) to stimulate the immune system to react to HIV, (ii) to allow re-emergence of wild-type virus and thereby reduce problems of drug resistance. However, a number of clinical trials of STIs [43], [44], [45], [46] have shown adverse outcomes for patients under discontinuous therapy, including serious health risks associated with treatment interruptions. For these reasons, the recent trend in research has been solidly against STIs.

2.5.3 Switching Regimen

There is no consensus on the optimal time to change therapy to avert or compensate for virologic failure. The most aggressive approach would be to change for any repeated, detectable viremia (e.g. two consecutive HIV RNA $>$ 50 copies/ml after suppression). Other approaches allow detectable viremia up to an arbitrary level (e.g. 1000-500 copies/ml). However, ongoing viral replication in the presence of antiretroviral drugs promotes the selection of drug resistance mutations and may limit future treatment options [47].

Antiretroviral drug sequencing provides a strategy to deal with virologic failure and anticipates that therapy will fail in a proportion of patients due to resistant mutations. The primary objectives of therapy sequencing are the avoidance of accumulation of mutations and selection of multi-drug-resistant viruses [9]. Using a mathematical model, [7] hypothesized that alternating HAART regimens, even while plasma HIV RNA levels were lower than 50 copies/ml, would further reduce the likelihood of the emergence of resistance. This concept has preliminary support from a clinical trial [8] called SWATCH (SWitching Antiviral Therapy Combination against HIV). In this study, 161 patients were assigned to receive regimen A (staduvine, didanosine, efavirenz), regimen B (zidovudine, lamivudine, nelfinavir), or regimen C (alternating regimens A and B every 3 months for 12 months). Regimen A and B had the same performance, with only 20% failure rate at the end of 48 week observation. The alternating regimen outperformed both regimens A and B with only three failure events. In addition, virologic failure was noted in regimens A and B, while in regimen C no resistance was documented [7]. These results, suggest that proactive switching and alternation of antiretroviral regimens with drugs that have different resistance profiles might extend the overall long-term effectiveness.

Chapter 3

Mathematical Modeling

A description of several mathematical models of HIV infection is presented. Using the latent reservoir theory, a deterministic model is proposed in order to explain the long-term behavior of HIV infection and the progression to AIDS. A parameter variation study exhibits the robust behavior of the model. We conclude the chapter by proposing different linear mutation models that will be used to test clinical treatment strategies and to allow preliminary control analysis for the therapy alternation.

3.1 Modeling Background

Since 1990 a large number of mathematical models have been proposed to describe the interaction between the adaptive immune system and HIV. These present a basic relation between CD4+T cells, infected CD4+T cells and virus [48], [49], [50], [51], [52], [53]. A significant effort has been made in understanding the interaction of the immune response with HIV [54], [55], [56]. These studies confirm that activated CD8+T cells or cytotoxic T cells (CTL) have an important function during HIV infection, however this function is thought to be compromised during the progression to AIDS. Single compartment models are able to describe the primary infection and the asymptomatic stage of infection. However, they are not able to describe the transition to AIDS. Most of them use ordinary or partial differential equations, while other authors proposed random variations because of the stochastic nature of HIV infection [57], [58]. A few studies characterize the problem as a cellular automata model to study the evolution of HIV [59], [60]. These models have the ability to reflect the clinical timing of the evolution of the virus. To obtain a more widely applicable model, some authors have tried to introduce other variables, taking into consideration other mechanisms by which HIV causes depletion of CD4+T cells. Numerous theories [12], [17], [20], [24], [28], [29] have been proposed, but none can fully explain all events observed to occur in practice.

Recent laboratory studies [20], [21], [22] have shown that HIV infection promotes apoptosis in resting CD4+T cells by the homing process. Basically, abortive infection of resting CD4+T cells induces those CD4+T cells to home from the blood to the lymph nodes. This mechanism was modeled in two compartments by [61], simulation results showed that therapeutic approaches involving inhibition of viral-induced homing and homing-induced apoptosis may prove beneficial for HIV patients. Several other investigators have reported that HIV induces thymic dysfunction, which could influence the rate of the disease progression to AIDS. In [62], authors found that infection of the thymus can act as a source of both infectious virus and infected CD4+T cells.

Dendritic cell interactions were analysed and described in a mathematical model in [63]. The authors gave two main hypotheses for the role of DC dysfunction in progression to AIDS. The first hypothesis suggests that as CD4+T cells become depleted by HIV infection, they are presented in insufficient numbers to license DC, which in turn reduces the ability of DC to prime CD8+T cells. The second hypothesis suggests that DC dysfunction is the result of a direct viral effect on DC intracellular processes.

3.2 HIV Long-Term Model: The latent reservoir

A reservoir is a long-lived cell, which can have viral replication even after many years of drug treatment. Studies [29], [30] have suggested that CD4+T cells could be one of the major viral reservoirs. HIV-1 replicates well in activated CD4+T cells, and latent infection is thought to occur only in resting CD4+T cells. Latently infected resting CD4+T cells provide a mechanism for life-long persistence of replication-competent forms of HIV-1, rendering hopes of virus eradication with current antiretroviral regimens unrealistic. However, recent observations [64] reveal that the virus reappearing in the plasma of patients undergoing interruption of a successful antiviral therapy is genetically different from that harbored in latently infected CD4+T cells by HIV-1. These data strongly suggest that other reservoirs may also be involved in the rebound of HIV-1 replication.

A number of clinical studies have been conducted to explore the role of macrophages in HIV infection [31]. Macrophages play a key role in HIV disease, they appear to be the first cells infected by HIV; have been proposed to spread infection to the brain, and to form a long-lived virus reservoir. A mathematical model which describes the complete HIV/AIDS trajectory was proposed in [4]. Simulation results for that model emphasize the importance of macrophages in HIV infection and progression to AIDS. We believe [4] is a good model to describe the whole HIV infection course, however, further work is needed since the model is very sensitive to parameter variations.

A simplification of [4] is proposed with the the following populations; T represents the uninfected CD4+T cells, T^* represents the infected CD4+T cells, M represents uninfected macrophages, M^* represents the infected macrophages, and V represents the HIV population. The mechanisms considered for this model are described by the following reactions:

Cell production. The source of new CD4+T cells and macrophages from thymus, bone marrow, and other cell sources is assumed to be constant by many authors [51], [52].

$$\varnothing \xrightarrow{s_T} T \tag{3.1}$$

$$\varnothing \xrightarrow{s_M} M \tag{3.2}$$

s_T and s_M are the source terms and represent the generation rate of new CD4+T cells and macrophages, which were estimated as 10 cells/$mm^3 day$, and 0.15 cells/$mm^3 day$ respectively by [51].

Infection process. HIV can infect a number of different cells: activated CD4+T cell, resting CD4+T cell, quiescent CD4+T cell, macrophages and dendritic cells. Dendritic cells play a pivotal role in linking cells and invading pathogens. For simplicity, just activated CD4+T cells and macrophages are considered in the infection process.

$$T + V \xrightarrow{k_T} T^* \tag{3.3}$$

$$M + V \xrightarrow{k_M} M^* \tag{3.4}$$

The parameter k_T is the rate at which free virus V infects CD4+T cells, this has been estimated by different authors, and the range for this parameter is from 10^{-8} to 10^{-2} ml/day copies [4]. The macrophage infection rate, k_M, is fitted as 2.4667×10^{-7} ml/ day copies. Parameter fitting was realized by an iterative trial-and-error process to match clinical data in [65], [66].

Virus proliferation. HIV may be separated into their source, either CD4+T cells or macrophages by the host proteins contained within their coat [67]. Viral proliferation is considered as occurring in activated CD4+T cells and macrophages.

$$T^* \xrightarrow{p_T} V + T^* \tag{3.5}$$

$$M^* \xrightarrow{p_M} V + M^* \tag{3.6}$$

The amount of virus produced from infected CD4+T cells and macrophages is given by $p_T T^*$ and $p_M M^*$ respectively, where p_T and p_M are the rates of production per unit time in CD4+T cells and macrophages. The values for these parameters are in a very broad range depending on the model, cells and mechanisms. We take values from [4], where p_T ranges from 0.24 to 500 copies mm^3/cells ml and from 0.05 to 300 copies/cells day for p_M. Notice that not all virus particles are infectious, only a limited fraction ($\approx 0.1\%$) of circulating virions are demonstrably infectious [68]. Some virus particles have defective proviral RNA, and therefore they are not capable of infecting cells. In mathematical models, generally, V describes the population dynamics of free infectious virus particles.

Natural death. Cells and virus have a finite lifespan. This loss is represented by the following reactions

$$T \xrightarrow{\delta_T} \emptyset \tag{3.7}$$
$$T^* \xrightarrow{\delta_{T^*}} \emptyset \tag{3.8}$$
$$M \xrightarrow{\delta_M} \emptyset \tag{3.9}$$
$$M^* \xrightarrow{\delta_{M^*}} \emptyset \tag{3.10}$$
$$V \xrightarrow{\delta_V} \emptyset \tag{3.11}$$

The death rate of CD4+T cells in humans is not well characterized, this parameter has been chosen in a number of works as $\delta_T = 0.01\ day^{-1}$, a value derived from BrdU labeling macaques [51]. The infected cells were taken from [51] with values of δ_{T^*} ranging from 0.26 to 0.68 day^{-1}, this value is bigger than uninfected CD4+T cells because infected CD4+T cells can be cleared by CTL cells and other natural responses.

In contrast to CD4+T cells, HIV infection is not cytopathic for macrophages and the half-life of infected macrophages may be of the order of months to years depending on the type of macrophage. These long lives which could facilitate the ability of the virus to persist [69]. Moreover, studies of macrophages infected in vitro with HIV showed that they may form multinucleated cells that could reach large sizes before degeneration and necrosis ensued [31]. The current consensus is that the principal cellular target for HIV in the CNS (Central Nervous System) is the macrophage or microglial cell. A large study in clinical well-characterized adults found no convincing evidence for HIV DNA in neurons [70]. Thus macrophages and infected macrophages could last for very long periods, we estimated δ_M and δ_{M^*} as $1 \times 10^{-3}\ day^{-1}$ using clinical data for the CD4+T cells [65], [66]. Clearance of free virions is the most rapid process, occurring on a time scale of hours. The values of δ_V ranged from 2.06 to 3.81 day^{-1} [51], [52], [53].

First, let us consider mechanisms 3.1-3.11 as the most relevant. Then the following model may be obtained

$$\begin{aligned} \dot{T} &= s_T - k_T T V - \delta_T T \\ \dot{T^*} &= k_T T V - \delta_{T^*} T^* \\ \dot{M} &= s_M - k_M M V - \delta_M M \\ \dot{M^*} &= k_M M V - \delta_{M^*} M^* \\ \dot{V} &= p_T T^* + p_M M^* - \delta_V V \end{aligned} \tag{3.12}$$

In the next section, we shall show that even given the simplicity in the system 3.12, compared with other macrophages models [4], [51], [52], we can still obtain some of the main features of the long-term dynamics in HIV infection with a behavior that is suitably robust to parameter variations.

3.2.1 Model Simulation

There are approximately $6000/mm^{-3}$ white blood cells in a healthy human according to [71]. For initial condition values, previous works are considered [4], [51]: CD4+T cells are taken as 1000 cells/mm^3 and 150 cells/mm^3 for macrophages. Infected cells are considered as zero and initial viral concentration as 10^{-3} copies/ml. The model implementation outlined in last section is conducted in MATLAB, using parameter values presented in Table 3.1.

Table 3.1: Parameters values for (3.12)

Parameter	Nominal Value	Taken from:	Parameter Variation
s_T	10	[51]	7 - 20
s_M	0.15	[51]	0.1 - 0.3
k_T	3.5714×10^{-5}	[4]	3.2×10^{-5} - 1.0×10^{-4}
k_M	4.3333×10^{-7}	Fitted	3.03×10^{-7} - 1.30×10^{-6}
p_T	38	[4]	30.4 - 114
p_M	44	[4]	22 - 132
δ_T	0.01	[4]	0.001-0.017
δ_T^*	0.4	[51]	0.1-0.45
δ_M	1×10^{-3}	Fitted	1×10^{-4} - 1.4×10^{-3}
δ_M^*	1×10^{-3}	Fitted	1×10^{-4} - 1.2×10^{-3}
δ_V	2.4	[4]	0.96- 2.64

Numerical results given in Fig.3.1 show a fast drop in healthy CD4+T cells, while there is a rapid increase in viral load. It might be expected that the immune system responds to the infection, proliferating more CD4+T cells, which gives rise to the increment in CD4+T cells. However, in (3.12) there is no term for proliferation, therefore the observed increase in CD4+T cell count is due to a saturation of infection in CD4+T cells and a consequent sharp drop in the viral load experienced. For approximately, 4 to 5 years an untreated patient experiences an asymptomatic phase where in CD4+T cell counts levels are over 300 cells/mm^3. On one hand CD4+T cells experience a slow but constant depletion, on the other hand the virus continues infecting healthy cells and therefore a slow increase in viral load take place as can be seen in Fig.3.2b. At the end of the asymptomatic period, constitutional symptoms appear when CD4+T cell counts are below 300 cells/mm^3. The last stage and the most dangerous for the patient is when the depletion in CD4+T cells crosses 250 cells/mm^3, which is considered as AIDS. This is usually accompanied by a rapid growth in viral load, and the severe immuno-deficiency frequently leads to potentially fatal opportunistic diseases. Fig.3.1 reveals how the model is able to represent the three stages in HIV infection and corresponds reasonably well to clinical data.

Infected CD4+T cell dynamics are qualitatively similar to the viral load dynamics in the first years of infection, as can be seen in Fig.3.2a. There is an initial peak of infected CD4+T cells, followed by a small increment but constant population during the asymptomatic stage.

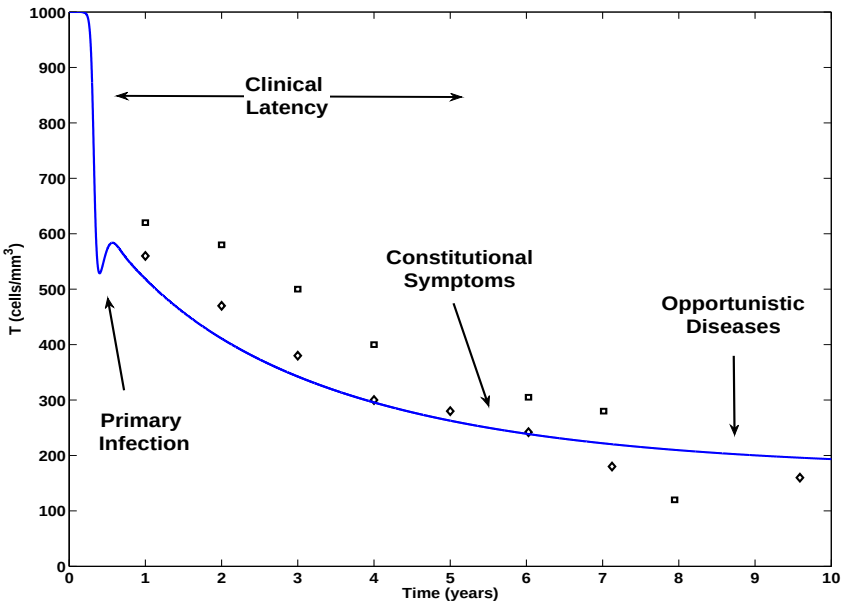

Fig. 3.1: CD4+T cells dynamic over a period of ten years. □ is clinical data taken from [65] and ◊ is data from [66]

Macrophages are considered one of the first points of infection, therefore infected macrophages may become long-lived virus reservoirs as is stated in [31]. Fig.3.2c shows healthy macrophage dynamics with a slow depletion in counts, this depletion is because of their change to infected status. The number of infected macrophages increases slowly during the asymptomatic period, but when constitutional symptoms appear, infected macrophages increase in population faster than before, see Fig.3.2d. These results suggest that in the last stages of HIV the major viral replication comes from infected macrophages. This is consistent with the work of [72], which states that in the early infection the virus replication rate in macrophages is slower than the replication rate in CD4+T cells. Over the years, the viral replication rate in macrophages grows.

Simulations results help to elucidate various HIV mechanism, see Fig.3.3, which can be considered as two feedback systems. One provides the fast dynamics presented in the early stages of infection as a result of an strong inhibition to CD4+T cells. The second feedback sustains a constant slow infection process in macrophages over the years due to a weak inhibition accompanied by the long time survival conditions of macrophages.

Whilst the model [4] reproduces known long term behavior, bifurcation analysis gives an unusually high sensitivity to parameter variations. For instance, small relative changes in infection rates for macrophages give bifurcation to a qualitatively different behavior. Therefore, it is necessary to check the sensitivity to parameter variation in the proposed model (3.12).

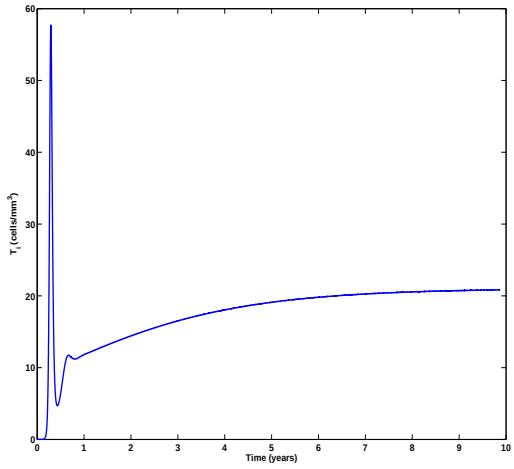

(a) T^* (infected CD4+T cells)

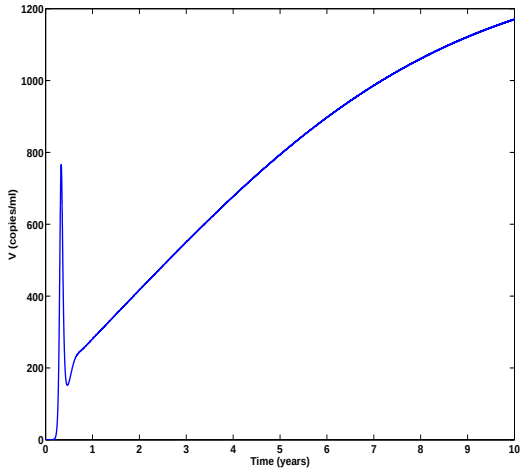

(b) Virus

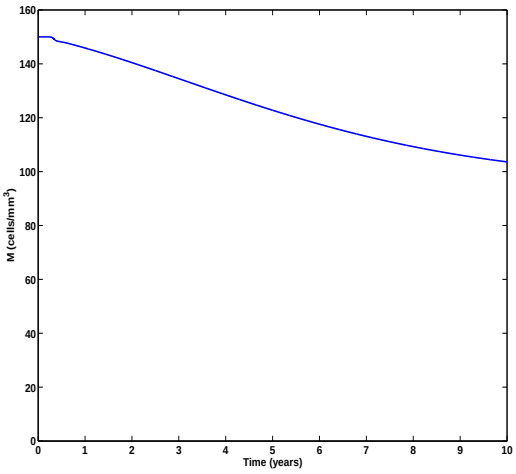

(c) M (healthy macrophages)

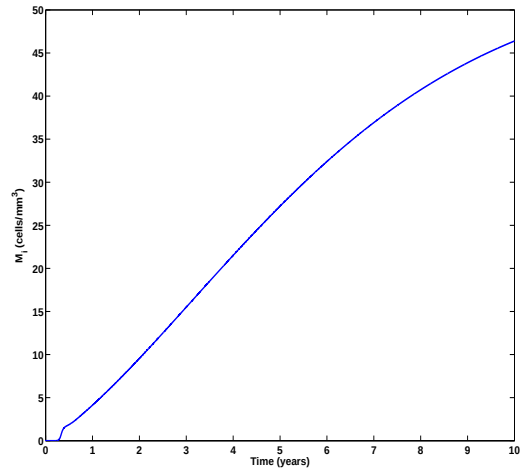

(d) M^* (infected macrophages)

Fig. 3.2: Dynamics of cells and virus over a period of ten years

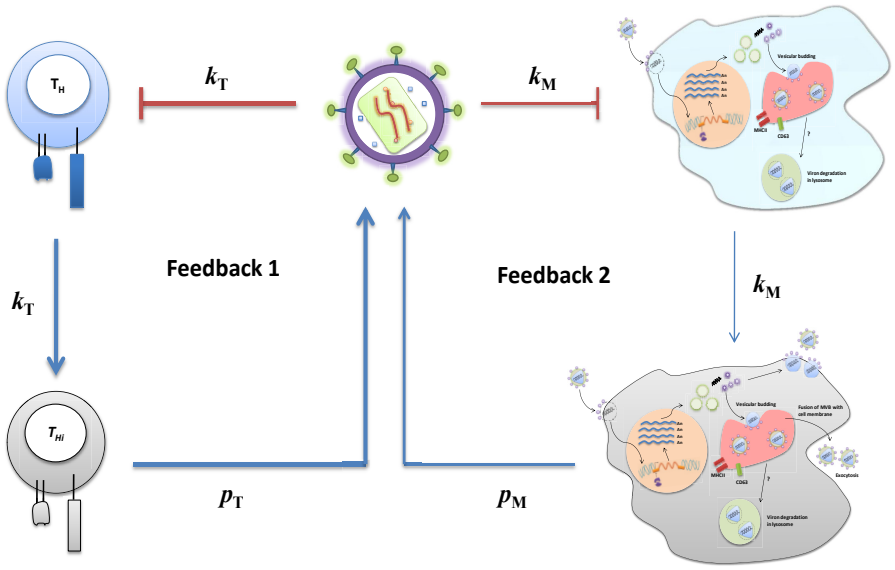

Fig. 3.3: HIV infection scheme

Accordingly, we can vary the parameters to observe the range for which the model (3.12) shows the whole HIV infection trajectory with reasonable different time scales. For instance, Fig.3.4a reveals that the model may reproduce long term behavior despite high variations of the parameter k_T, which may range from 10% below nominal values and 220% above. It can be noticed that higher infection of CD4+T cells speeds up the progression to AIDS. The ranges for other parameters are shown in Table 3.1, this reveals that parameters can be varied in a wide range whilst still showing the three stages in HIV infection with reasonable time scales. In this case we define reasonable time scales as progression to AIDS in between 1 and 20 years. We consider (3.12) might be a useful model to represent the whole HIV infection for different patients as a result of its robustness to represent the three stages of HIV infection.

Interesting conclusions can be obtained if we analyse other parameters. Consider for instance the death rate of healthy CD4+T cells d_T. Initial thoughts might be that increasing the death rate of CD4+T cells will hasten the progression to AIDS. Nonetheless, Fig.3.4b provides interesting insights of the progression to AIDS. On one hand Fig.3.4b shows if the death rate of CD4+T cells is small, then the progression to AIDS is faster since CD4+T cells live for longer periods and become infected, then more virus are produced. Moreover more infection of long term reservoirs takes place. On the other hand, if the death rate of CD4+T cells is high, then the viral load explosion might be inhibited. Indubitably, CD4+T cells levels will be low with a high d_T value, but Fig.3.4b exposed that there is a range for d_T which CD4+T cells could be maintained in safety levels (> 350 cells). Clinical evidence has shown that HIV affects the life cycle of CD4+T cells [21]. For simplicity we considered in (3.12) one compartment of activated CD4+T cells, which are directly infected by HIV. Let us consider d_T as a regulation between two pools of cells, naive and activated cells, consequently

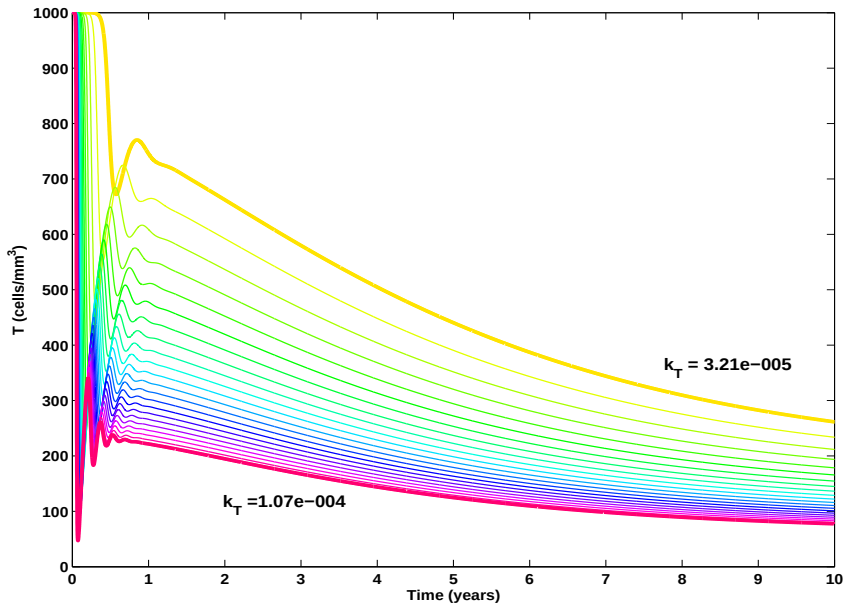

(a) Variation of k_T

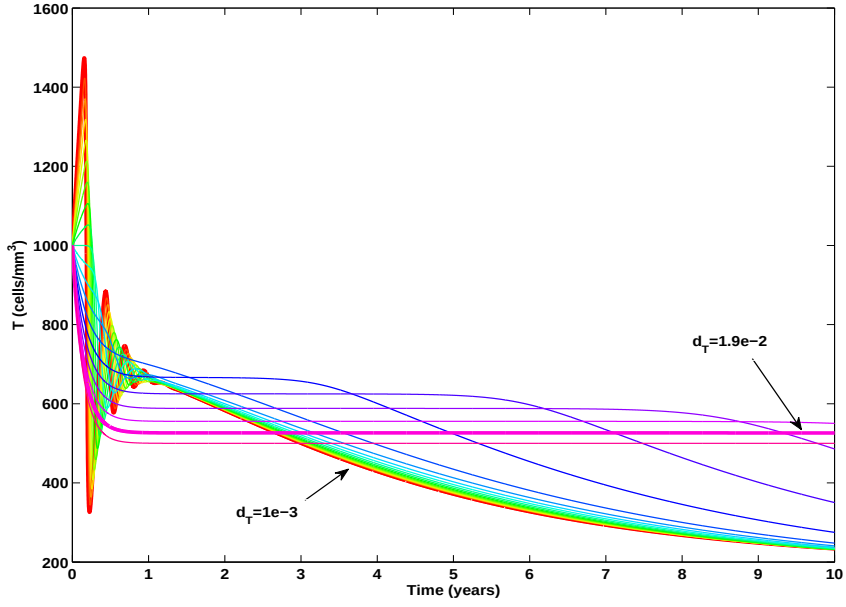

(b) Variation of d_T

Fig. 3.4: CD4+T cell dynamics under parameter variation

we could infer that for a stronger activation of CD4+T cells, the progression to AIDS would be faster. Clinical observations [12] have supported the hypothesis that persistent hyperactivation of the immune system may lead to erosion of the naive CD4+T cells pool and CD4+T cell depletion. Numerical results yield the idea that macrophages need the first stage of viral explosion in order to attain large numbers of long lived reservoirs and cause the progression to AIDS. Thus, a regulation in the activation of CD4+T cells in the early stages of HIV infection might be important to control the infection and its progression to AIDS.

3.2.2 Steady State Analysis

Using the system (3.12), the equilibria may be obtained analytically in the next form

$$T = \frac{s_T}{k_T V + \delta_T}, \quad T^* = \frac{k_T s_T}{\delta_{T^*}} \frac{V}{k_T V + \delta_T}$$
$$M = \frac{s_M}{k_M V + \delta_M}, \quad M^* = \frac{k_M s_M}{\delta_{M^*}} \frac{V}{k_M V + \delta_M}$$

where V is the solution of the polynomial

$$aV^3 + bV^2 + cV = 0 \tag{3.13}$$

The equation (3.13) has three solutions, which are

$$V^{(A)} = 0, \; V^{(B)} = \frac{-b + \sqrt{b^2 - 4ac}}{2a}, \; V^{(C)} = \frac{-b - \sqrt{b^2 - 4ac}}{2a} \tag{3.14}$$

where;
$a = k_T k_M \delta_{T^*} \delta_{M^*} \delta_V$
$b = k_T \delta_{T^*} \delta_M \delta M^* \delta_V + k_M \delta_T \delta_{T^*} \delta_{M^*} \delta_V - s_T k_T k_M p_T \delta_{M^*} - s_2 k_T k_M p_M \delta_{T^*}$
$c = \delta_T \delta_{T^*} \delta_M \delta_{M^*} \delta_V - s_T k_T p_T \delta_M \delta_{M^*} - s_M k_M p_M \delta_T \delta_{T^*}$

Equilibrium A

$$T^{(A)} = \frac{s_T}{\delta_T}, \; T^{*(A)} = 0, \; M^{(A)} = \frac{s_M}{\delta_M}, \; M^{*(A)} = 0, \; V^{(A)} = 0$$

Equilibrium B,C

$$T^{(B,C)} = \frac{s_T}{k_T V^{(B,C)} + \delta_T}, \quad T^{*(B,C)} = \frac{k_T s_T}{\delta_{T^*}} \frac{V^{(B,C)}}{k_T V^{(B,C)} + \delta_T}$$
$$M^{(B,C)} = \frac{s_M}{k_M V^{(B,C)} + \delta_M}, \quad M^{*(B,C)} = \frac{k_M s_M}{\delta_{M^*}} \frac{V^{(B,C)}}{k_M V^{(B,C)} + \delta_M}$$

Proposition 3.1 *The compact set* $\Gamma = \{\{T, T_i, M, M_i, V\} \in R^5_+ : T(t) \leq s_T/\delta_T, M(t) \leq s_M/\delta_M\}$ *, is a positive invariant set.*

Proof The proof can be found in [74].

Remark 3.1 *If c is a negative real number, then* (3.12) *has a unique infected equilibrium in the first orthant.*

Proof This can be seen directly from $b^2 - 4ac > 0$ in (3.14). ∎

Remark 3.2 *It is possible to have two infected equilibria in the first orthant, if b is a negative real number and c is a positive real number. It can be easily shown that using values from Table 3.1 b and c are negative.*

Proposition 3.2 *The uninfected equilibrium is locally unstable if there exists a unique infected equilibrium in the first orthant.*

Proof If we compute the characteristic polynomial for the equilibrium A (uninfected status), we obtain a polynomial of fifth order, where one of the coefficients is equal to c. Applying the Routh Hurwitz criterion yields that the equilibrium is stable if and only if every coefficient of the characteristic polynomial is positive. However, it was previously shown that c must be negative in order to have a unique equilibrium point. Therefore the uninfected equilibrium is unstable. ∎

Equilibrium A represents an uninfected status. Using numerical values, the uninfected equilibrium is unstable, which is consistent with previous works [48], [51], [52], [73]. This might be the reason why it is impossible to revert a patient once infected, back to an HIV-free state.

3.2.3 Cell Proliferation Terms

The macrophage dynamics modeled in this work present a very different scenario from [4]. In [4], the authors presented a model with an explosion in macrophage populations (both infected and healthy over 1000 $cells/mm^3$). In our model, simulation results reveal slightly depletion in macrophages and increment in infected macrophages as can be seen in Fig.3.2c, but the total population remains almost constant. This is consistent with the observation that macrophages have a long life span [51]. This difference in macrophage dynamics is because we do not consider cell

proliferation terms. In order to adjust the fast depletion in CD4+T cells and explosion in viral load, we include cell proliferation terms

$$T + V \xrightarrow{\rho_T} T + (T + V) \tag{3.15}$$

$$M + V \xrightarrow{\rho_M} M + (M + V) \tag{3.16}$$

Using the proliferation rates (3.15) and (3.16) in the proposed model (3.12), the dynamics match better in the final depletion of CD4+T cells as can be noticed in Fig.3.5. The collapsing in CD4+T cells is obvious using the proliferation rates ρ_T and ρ_M. Moreover, after the primary infection stage takes place [3], the recovering in CD4+T cell counts over 500 $cells/mm^3$ is more evident using cell proliferations terms. The authors of [4] emphasized the importance of macrophages in the progression of HIV, however they had not provided any mathematical evidence of the HIV/AIDS transition. Since the model is difficult to analyze, we suggest some simplifying assumptions to allow mathematical analysis.

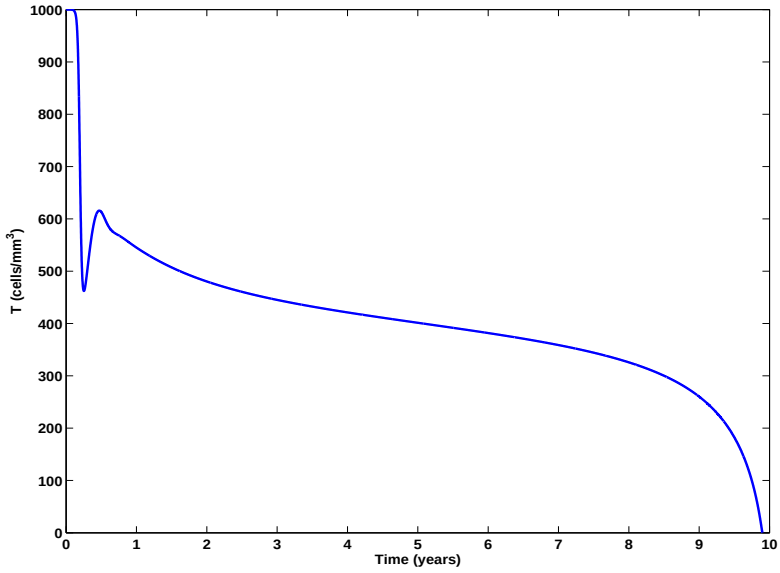

Fig. 3.5: CD4+T cells dynamic using bilinear proliferation rates (3.15) and (3.16)

Assumption 3.1 *Fast Viral Dynamics.*
Using parameter values in Table 3.1, we notice that $\delta_V >> 1$. *This corresponds to viral dynamics with a time constant much less than one day. In this case, the differential equation for the virus can be approximated by the following algebraic equation as suggested in [75]:*

$$V = \frac{p_T}{\delta_V} T^* + \frac{p_M}{\delta_V} M^* \tag{3.17}$$

Assumption 3.2 *T^* is approximately constant during the asymptomatic phase.*
We note that in the asymptomatic period of infection (that is, after the initial transient, and before the final divergence associated with development of AIDS), the concentration of infected CD4+T cells is relatively constant. This assumption is also proposed in [73]. Therefore the following approximation for infected CD4+T cells can be considered:

$$T^*(t) \approx \overline{T}^*, \forall t \geq t_0 \tag{3.18}$$

Using equations (3.17) and (3.18) we obtain

$$V(t) := c_1 M^* + V_{T^*} \tag{3.19}$$

where $V_{T^*} = \frac{p_T}{\delta_V}\overline{T}^*$ and $c_1 = \frac{p_M}{\delta_V}$. Note that if $\bar{T}^*$ is selected as an upper bound on T^*, then (3.19) *represents an upper bound on $V(t)$. Therefore (3.19) describes the long asymptomatic period in the viral load dynamic.*

Using Assumptions 3.1 and 3.2 in (3.12), we have the following system

$$\dot{M} \approx s_M - c_2 M + c_3 M M^* \tag{3.20}$$
$$\dot{M}^* \approx c_4 M + c_5 M M^* - \delta_4 M^* \tag{3.21}$$

where $c_2 = \delta_M - (\rho_M - k_M)V_{T^*}$, $c_3 = (\rho_M - k_M)c_1$, $c_4 = k_M V_{\overline{T}^*}$ and $c_5 = k_M c_1$.

Assumption 3.3 *M and M^* have an affine relation.*
Note that from (3.20) and (3.21), we expect that the bilinear terms are predominant for large M and M^*, then we may assume $\dot{M} \approx \frac{c_3}{c_5}\dot{M}^*$, which can be rearranged in the linear form

$$M^* \approx c_6 M - c_7 \tag{3.22}$$

where $c_6 = \frac{c_2 c_5 + c_3 c_4}{c_3 \delta_{M^*}}$ and $c_7 = \frac{c_5 s_M}{c_3 \delta_{M^*}}$.

Remark 3.3 *Under Assumptions 3.1-3.3 and the parameter condition $4\alpha s_M \geq \beta^2$, the macrophage dynamics in an infected HIV patient are unstable with a finite escape time.*

Substituting (3.22) in equation (3.20), we have a numerically verified approximation for the macrophage equation which is only valid for large amounts of M and M_i

$$\dot{M} \quad = \quad s_M + \alpha M^2 + \beta M \tag{3.23}$$

where
$\alpha = \frac{c_6 p_M (\rho_M - k_M)}{\delta_V}$

$\beta = \frac{(\rho_M - k_M)(p_T \overline{T}^* - c_7 p_M)}{\delta_V} - \delta_M$

The solution of the differential equation (3.23) is given by

$$M = \frac{\beta}{2\alpha} + \frac{\sqrt{4\alpha s_M - \beta^2}}{2\alpha} tan\left(\frac{\sqrt{4\alpha s_M - \beta^2}}{2} t + \eta\right) \tag{3.24}$$

where η is a constant related to the initial condition of the macrophages given by

$$\eta = tan^{-1}\left(\frac{2\alpha M_0 - \beta}{\sqrt{4\alpha s_2 - \beta^2}}\right) \tag{3.25}$$

In (3.24) there is a tangent function if $4\alpha s_M \geq \beta^2$, which tends to ∞ when the argument tends to $\pi/2$, that is when

$$t = T_\infty := \frac{\pi - 2\eta}{\sqrt{4\alpha s_M - \beta^2}} \tag{3.26}$$

which implies that there is a finite escape time.

Whilst the incorporation of proliferations rates (3.15) and (3.16) in the model (3.12) reproduces the observed long term behavior more accurately, any small change in parameters (i.e., 1% nominal value) evidences an unusually high sensitivity. In particular, small relative changes in k_T, ρ_T, ρ_M, δ_T, δ_{T^*}, δ_M, or δ_V give bifurcation to a qualitatively different behavior. This sensitivity to parameter variation is caused by the unstable behavior of the system (3.12) that was shown in Remark 3.3. This finite time escape is because the macrophage proliferation rate is faster than the infection rate of macrophages, that is $\rho_M > k_M$. In order to have the same trajectory presented in Fig.3.5 and robustness to parameter variation, we modify the proliferation terms (3.15) and (3.16) using Michaelis-Menten kinetics in the following form

$$T + V \xrightarrow{\frac{\rho_T}{C_{T+V}}} T + (T + V) \tag{3.27}$$

$$M + V \xrightarrow{\frac{\rho_M}{C_{M+V}}} M + (M + V) \tag{3.28}$$

the new parameters were adjusted to obtain the appropriate HIV trajectory with respect to clinical observations. These parameter values are $\rho_T = 0.01$, $\rho_M = 0.004$, $C_T = 300$ and $C_M = 500$. Adding cell proliferation rates (3.27) and (3.28) in the model (3.12), we can observe in Fig.3.6a how in the symptomatic period CD4+T cell counts drop dramatically lower than 250 cell/mm^3. In addition, the primary infection dynamics are adapted better to clinical observations, that is when CD4+T cells drops below 400 (cells/mm^3) and then returns to near-normal values [3]. Viral load trajectories agree with clinical observations; a large spike in the level of circulating virus, follow by a fast drop in viral concentration. In the latent period the viral load remains almost constant, and finally the explosion in viral load takes place in the symptomatic stage. The relevance of these cell proliferation rates incorporated in the model (3.12) is that robust properties to parameter variation are preserved and can be varied as is shown in Table 3.1.

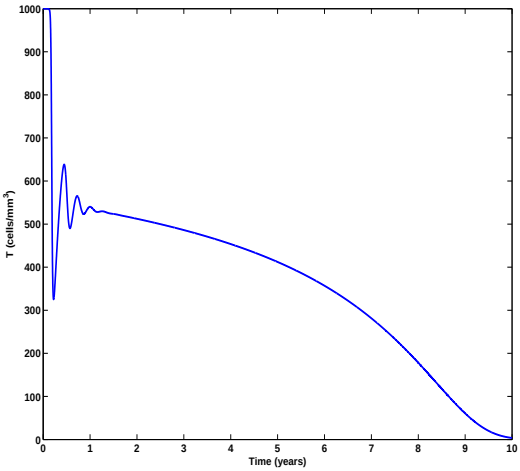

(a) CD4+T cells

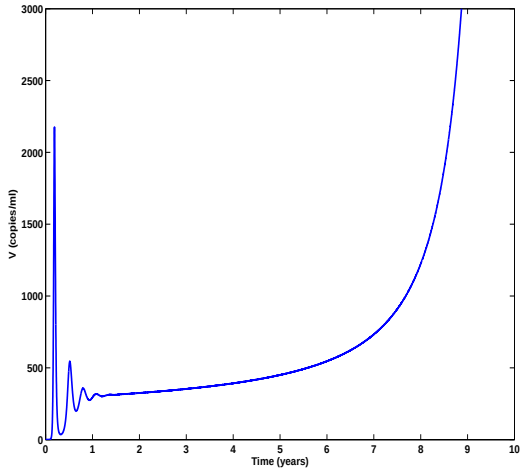

(b) Virus

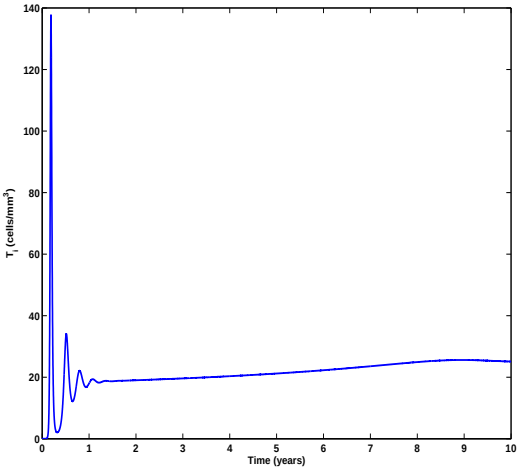

(c) T^* (infected CD4+T cells)

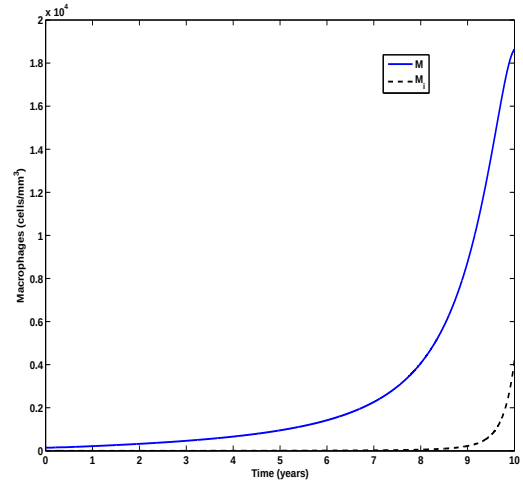

(d) Macrophages

Fig. 3.6: CD4+T cell, macrophage and viral dynamic using proliferation rates (3.27) and (3.28)

Viral explosion promotes more infection of long-term cells, which will replicate virus during long periods. This is consistent with simulation results in [4], which found that infected macrophages increase slowly in number during the asymptomatic period and exponentially in the later stage of the disease.

There is lack of information regarding infected cells in HIV. Simulation results show that infected macrophages experience an explosion in population as can be seen in Fig.3.6d. This is consistent with studies in rhesus macaques [72], using the highly pathogenic simian immunodeficiency virus/HIV type 1 (SHIV) infection in monkeys. This is an exaggerated model of HIV infection in humans that allows scientist to address certain clinical aspects of retrovirus that are difficult to study in people. Lymphoid organs such as lymph nodes and spleen for the source of the remaining virus were examined in [72]. They found that 95% of the virus-producing cells were macrophages and only 1 to 2% were CD4+T cells. Moreover, macrophages contain and continue to produce large amounts of HIV-like virus in monkeys even after the virus depletes CD4+T cells.

3.2.4 Drug Therapy Model

Antiretrovirals may interfere with different parts of the HIV cycle. There are 20 approved antiretroviral drugs in 6 mechanistic classes to design combination regimens. The most extensive study for combination regimens provides durable viral suppression and generally consists of 2 NRTIs plus one NNRTI or a PI [5]. In that event, we modify (3.12) to include the effect of these drugs:

$$\begin{aligned} \dot{T} &= s_T - (1-\eta_{RT})k_T TV - \delta_T T \\ \dot{T^*} &= (1-\eta_{RT})k_T TV - \delta_{T^*} T^* \\ \dot{M} &= s_M - (1-f\eta_{RT})k_M MV - \delta_M M \\ \dot{M^*} &= (1-f\eta_{RT})k_M MV - \delta_{M^*} M^* \\ \dot{V} &= (1-\eta_{PI})p_T T^* + (1-f\eta_{PI})p_M M^* - \delta_V V \end{aligned} \tag{3.29}$$

On one hand RTIs can block infection and hence reduce the infection rate of CD4+T cells and macrophages. This can be represented including the term $(1-\eta_{RT})$ into the cell infection rates. RTIs like other drugs are not perfect, thus η_{RT} is the "effectiveness" of the reverse transcriptase inhibitors [52]. Inhibitor efficient is in the range $0 \leq a_{RT} \leq \eta_{RT} \leq b_{RT} \leq 1$, where a_{RT} and b_{RT} represent minimal and maximal drug efficacy. On the other hand PIs inhibit the protease of HIV, resulting in a decrease of the viral proliferation, this is represented including $(1-\eta_{PI})$ in the viral proliferation rate of infected cells. Because macrophages are long-lived cells [31], inhibitors are more effective in CD4+T cells than in macrophages, this is contemplated using $f \in [0,1]$ [55].

The primary goal of antiretroviral therapy is to reduce HIV-associated morbidity and mortality.

Over the last 20 years, several changes have been made to the recommendations on when to start therapy. The standard procedure for the panel of antiretroviral guidelines for adults and adolescents with HIV in USA [5] is to only make recommendations in agreement with two-thirds of the panel members. This has not been possible for ***When to Start*** recommendations in its last updated version [5]. However, there is a general consensus that antiretroviral therapy should be initiated in all patients with a history of an AIDS-defining illness or when CD4+T counts are less than 350 cells/mm^3 [5].

Using the model (3.29), we notice in Fig.3.7 that HAART treatment would be initiated approximately around the third year after infection. Fig.3.7a shows how CD4+T cells experience a rapid depletion in counts. When treatment is introduced, CD4+T cells counts recover and maintain normal counts. One of the most important goals of therapy is to achieve maximal virologic suppression, that is HIV RNA level less than 400 copies/ml after 24 weeks, and less than 50 copies/ml after 48 weeks, this fact can be seen in Fig.3.7b.

Infected cells play an important role in HIV infection. On one hand, infected CD4+T cells show a rapid depletion when HAART is introduced, and this is maintained at a very low level for several years, see Fig.3.7c. On the other hand, infected macrophages have a very slow depletion as is shown in Fig.3.7d. Therefore they can still contribute to the viral load population for a long period of time. This is consistent with many works on the area, which propose that macrophages are responsible for the second phase in the decay of plasma virus level [52].

Remark 3.4 *Under the assumption of perfect effectiveness in the treatment, CD4+T cells and macrophages dynamics become uncoupled from viral dynamic equation. Therefore we can solve the equations for the infected cells*

$$T^* = T_0^* exp(-\delta_{T^*} t)$$

$$M^* = M_0^* exp(-\delta_{M^*} t)$$

Using these equations is easy to see that for this model, the longer the delay to initiate HAART, the more new infections of cells and reservoirs will take place, consequently a longer period is necessary to clear the virus.

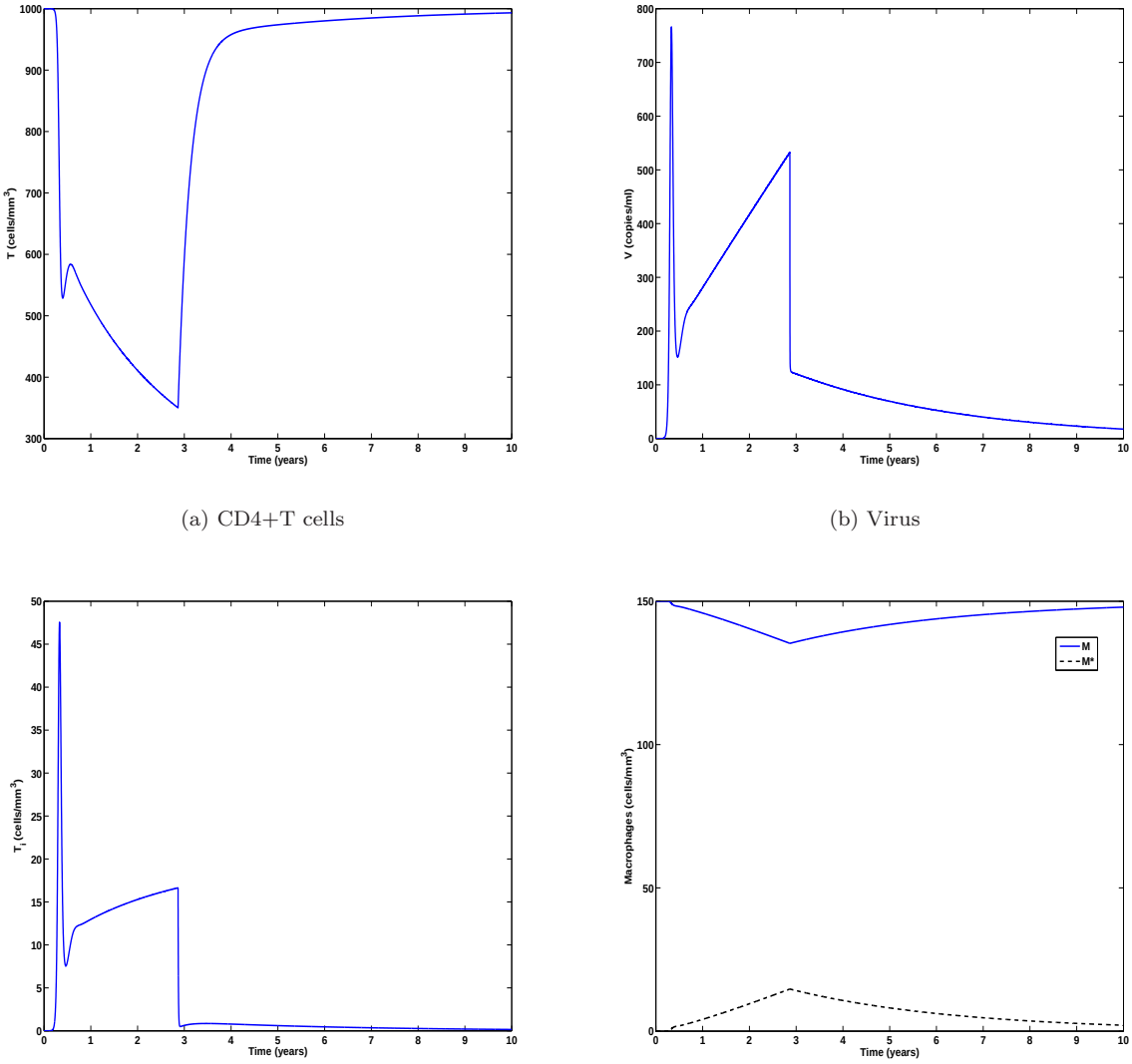

(a) CD4+T cells

(b) Virus

(c) T^* (infected CD4+T cells)

(d) Macrophages

Fig. 3.7: CD4+T cell, macrophage and viral dynamic under HAART treatment

3.3 Basic Viral Mutation Treatment Model

Numerical results suggest that the mathematical model (3.12) is able to represent the complete trajectory of HIV infection. Furthermore, the inclusion of treatment effects expose the fast recover in CD4+T cells and reduction of viral load. According to simulation results, HIV infection progression could be delayed for an undetermined period of time. Notwithstanding, HIV may mutate, this is problematic since it gives rise to drug resistance if a single drug or single drug combination is given. Consequently, it is necessary to consider different genetic strains. For the sake of simplicity, we propose a model for mutation dynamics that is simple enough to allow control analysis and optimisation of treatment switching. Based on (3.12), we make the following assumptions in designing our control strategies.

Assumption 3.4 *Constant macrophage and CD4+T cell counts. The main non-linearities in the more general model are bilinear, and all involve either the macrophage or healthy CD4+T cell count. Under normal treatment circumstances (that is after the initial infection stage, and until full progression to a dominant highly resistant mutant) typical simulations and/or clinical data suggest that the macrophage and CD4+T cell counts are approximately constant [52]. This assumption allows to simplify the dynamics to being essentially linear.*

Assumption 3.5 *Scalar dynamics for each mutant. A more extensive model for HIV dynamics would include a set of states for each possible genotype such as: $V_i(t)$ (viral concentration); $T_i^*(t)$ (CD4+T cells infected by mutant i); $M_i^*(t)$ (macrophages infected by mutant i) etc. To simplify the model we focus on the viral load $V_i(t)$ only.*

Assumption 3.6 *Viral clearance rate independent of treatment and mutant. In some cases, particularly in view of the earlier assumption of representing the dynamics as scalar, viral clearance rate might well depend on one or more of the treatment regimes, or the viral genetics. For simplicity, we take this as a constant.*

Assumption 3.7 *Mutation rate independent of treatment and mutant. In a similar vein, we assume that the mutation rate, between species with the same genetic distance, is constant. In practice, there is some dependence of mutation rate on the replication rate, and therefore there is some relationship between mutant, treatment and mutation rate.*

Assumption 3.8 *Deterministic model. We are interested in deriving control strategies with either optimal or "verifiable" performance. To simplify the control design we rely on a deterministic model.*

3.3.1 A 4 variant, 2 drug combination model

Assumptions 3.4-3.8 the model includes n different viral genotypes, with viral populations, $x_i : i = 1, ...n$; and N possible drug therapies that can be administered, represented by $\sigma(t) \in \{1, ...N\}$, where σ is permitted to change with time, t. The viral dynamics are represented by the equation:

$$\dot{x}_i(t) = \rho_{i,\sigma(t)} x_i(t) - \delta_V x_i(t) + \sum_{j \neq i} \mu m_{i,j} x_j(t) \tag{3.30}$$

where μ is a small parameter representing the mutation rate, δ_V is the death or decay rate and $m_{i,j} \in \{0, 1\}$ represents the genetic connections between genotypes, that is, $m_{i,j} = 1$ if and only if it is possible for genotype j to mutate into genotype i. Equation (3.30) may be rewritten in vector form as

$$\dot{x}(t) = \left(R_{\sigma(t)} - \delta_V I\right) x(t) + \mu M_u x(t) \tag{3.31}$$

where $M_u := [m_{ij}]$ and $R_{\sigma(t)} := diag\{\rho_{i,\sigma(t)}\}$.

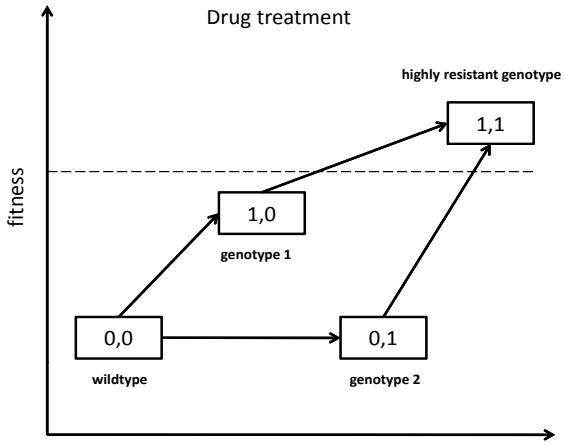

Fig. 3.8: Drug treatment

As a simple motivating example, we take a model with 4 genetic variants, that is $n = 4$, and 2 drug therapies, $N = 2$. The viral variants (also called 'genotypes' or 'strains') are described as follow.

- Wild Type(WT): In the absence of any drugs, this is the most prolific variant. It is also the variant that both drug combinations have been designed to combat, and therefore is susceptible to both therapies.
- Genotype 1 (G1): A genotype that is resistant to therapy 1, but is susceptible to therapy 2.
- Genotype 2 (G2): A genotype that is resistant to therapy 2, but is susceptible to therapy 1.

- Highly Resistant Genotype (HRG): A genotype, with low proliferation rate, but that is resistant to all drug therapies.

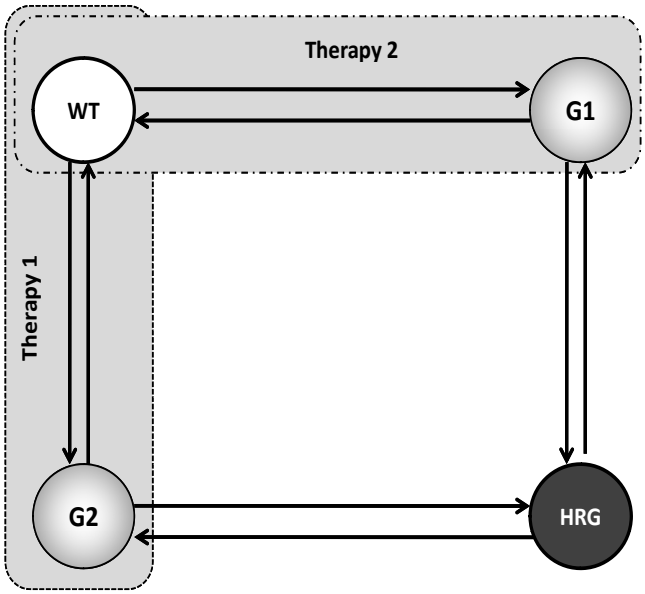

Fig. 3.9: Mutation tree for a 4 variant, 2 drug combination model

We take the viral clearance rate as $\delta_V = 0.24\ day^{-1}$ which corresponds to a half life of slightly less than 3 days [51]. Typical viral mutation rates are of the order of $\mu = 10^{-4}$. We consider a mutation graph that is symmetric and circular, see Fig.3.9. That is, we allow only the connections: $WT \leftrightarrow G1$, $G1 \leftrightarrow HRG$, $HRG \leftrightarrow G2$ and $G2 \leftrightarrow WT$. Other connections would require double mutations and for simplicity, we consider these to be of negligible probability. This leads to the mutation matrix:

$$M_u = \begin{bmatrix} 0 & 1 & 1 & 0 \\ 1 & 0 & 0 & 1 \\ 1 & 0 & 0 & 1 \\ 0 & 1 & 1 & 0 \end{bmatrix} \tag{3.32}$$

We propose three different scenarios for viral replication as can be found in the Table 3.2. The first scenario, the most ideal case, describes a complete symmetry between $G1$ and $G2$, in the sense that therapy 1 inhibits $G2$ with the same intensity that therapy 2 inhibits $G1$. In practice, we might expect a small difference in relative proliferation ability. Furthermore, a more detailed model would also include asymmetry in the genetic tree, which would usually have a much more complex structure than a simple cycle. The second scenario shows an asymmetry for replication rates in $G1$ and $G2$, although both therapies induce the same replication in the WTP and HRG. The more realistic case is when all genotypes experience different dynamics to the new treatment, this is represented in the Scenario 3.

Scenario	Therapy	WT(x_1) 1	G1 (x_2)	G2(x_3)	HRG (x_4)
1	1	$\rho_{1,1} = 0.05$	$\rho_{2,1} = 0.27$	$\rho_{3,1} = 0.05$	$\rho_{4,1} = 0.27$
	2	$\rho_{2,1} = 0.05$	$\rho_{2,2} = 0.05$	$\rho_{3,2} = 0.27$	$\rho_{4,2} = 0.27$
2	1	$\rho_{1,1} = 0.05$	$\rho_{2,1} = 0.28$	$\rho_{3,1} = 0.01$	$\rho_{4,1} = 0.27$
	2	$\rho_{2,1} = 0.05$	$\rho_{2,2} = 0.20$	$\rho_{3,2} = 0.25$	$\rho_{4,2} = 0.27$
3	1	$\rho_{1,1} = 0.05$	$\rho_{2,1} = 0.26$	$\rho_{3,1} = 0.01$	$\rho_{4,1} = 0.29$
	2	$\rho_{2,1} = 0.01$	$\rho_{2,2} = 0.15$	$\rho_{3,2} = 0.25$	$\rho_{4,2} = 0.27$

Table 3.2: Replication rates for viral variants and therapy combinations

Remark 3.5 *Notice that the system* (3.30) *is not stabilizable under the switching action. The biological reason is because that the highly resistant genotype will escape the effects of treatments and immune system.*

These numbers are of course idealized, however, the general principles are based on:

- Genetic distance from wild type reduces fitness: In the absence of effective drug treatments, we might expect that fitness (that is, reproduction rate) decreases with genetic distance from the wild type, which we expect to be the most fit.
- Therapy at best 90% effective: In the absence of drugs, from typical data, we might expect an overall viral proliferation rate (with high, constant CD4+T cell count) of approximately $\rho = 0.5\ day^{-1}$.

3.3.2 Clinical Treatments using the Basic Viral Mutation Model

"When does the patient need to change therapy?" has been a question of discussion in [5]. There are very clear factors when the patient needs to change therapy: drug side effects, prior treatment failure, comorbidities, lower CD4+T cell counts, presence of drug-resistant virus or other reasons. Nonetheless, there is no consensus on the optimal time to change therapy for virologic failure. Guidelines for the use of antiretroviral agents [5] recommends change for any detectable viremia up to an arbitrary level (e.g. 1000 copies/ml). Antiretroviral sequencing, called SWATCH, was proposed in order to deal with virologic failure and anticipates therapy failure in a proportion of patients [8]. In this trial, patients were alternating between two treatments every 3 months for 12 months.

Encouraged by the optimal time to change therapy, the model (3.30) is used to test these two treatments. For numerical analysis, we propose that the patient has a complete medical history, physical examination, laboratory evaluation once a month for one year period. Fig.3.10 reveals how the total viral load initially drops rapidly for the three different scenarios. However the appearance of resistant genotypes will drive a virologic failure (viral load $>$ 1000 copies/ml) after 8 months, then a new therapy is needed. Scenarios 1 and 2 exhibit a second drop in viral population, not as

Table 3.3: Total viral load at the end of treatment using model (3.30)

Scenario	Monotherapy	Switched on failure	SWATCH
Scenario 1	1.3692×10^4	344.25	45.35
Scenario 2	3.7116×10^4	919.29	60.59
Scenario 3	3.8725×10^4	1.2437×10^4	1045.27

pronounce as it was for therapy 1. For scenario 3, the viral load explosion is almost not affected by the new therapy, this is because the HRG is directing the dynamics of the system. Using the SWATCH treatment, a lower concentration in the total viral load over the year is shown in Fig.3.11.

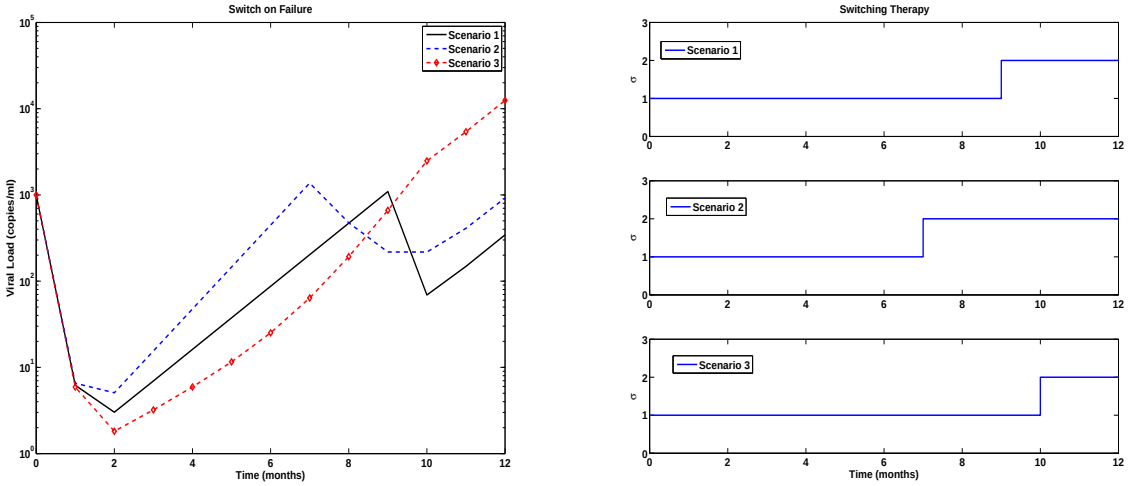

(a) Total Viral Load

(b) Switching Rule

Fig. 3.10: Switching on failure treatment for model (3.30)

Some clinicians recommend to wait as long as possible to switch a therapy, to have more choices for future treatments. However, it can be noticed in Table 3.3 if we wait for a long period, the total viral load will have very high concentration levels for the three scenarios. This is because we just inhibit one intermediate genotype, and we allow proliferation of the other genotype. Then, it is more likely to encounter highly resistant mutants. Even when we introduce the other therapy, it would not be enough to decrease the total viral load. This basic model gives the insight that prior treatment may be important to maximally suppress HIV levels and prevent further selection of resistant mutants.

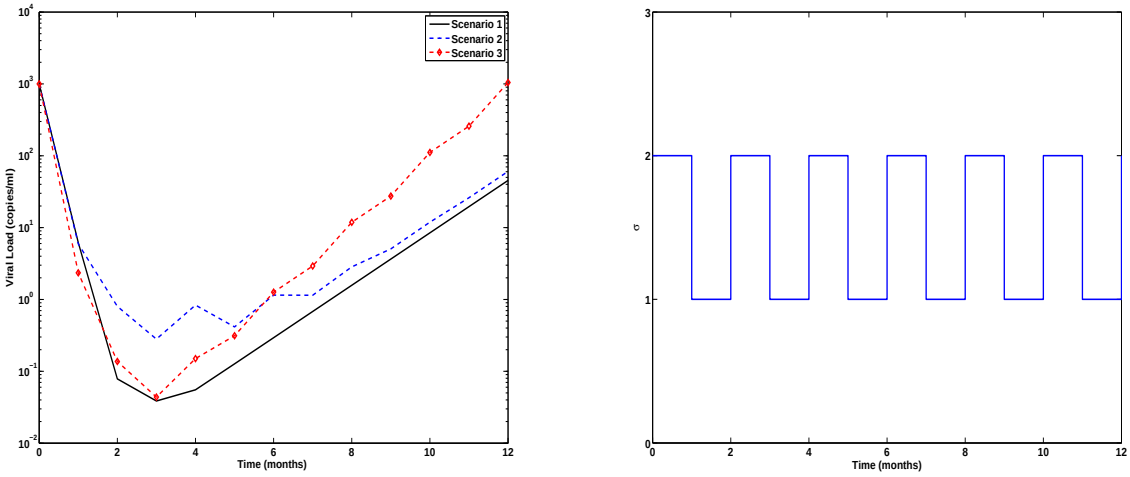

(a) Total Viral Load

(b) Switching Rule

Fig. 3.11: SWATCH treatment for model (3.30)

3.4 Macrophage Mutation Model

In Section 3.3 we showed a model with a single state variable representing each genotype. The simulation results exhibit virologic failure before a year of treatment. This is not consistent with clinical evidence, for instance [76] observed that the median time to failure was 68.4 months for patients with persistence low-viremia (51-1000 copies/ml for at least 3 months) and more than 72 months for patients without persistence low-viremia (PLV). [76] suggests that PLV is associated with virological failure. That is, patients with a PLV>400 copies/ml and a history of HAART experience are more likely to experience virological failure, moreover they recommend that patients with PLV should be considered for treatment optimization and interventional studies.

Accordingly, it is important to study models with more species to better match clinical observations of disease time-scales. In fact, the significance of considering such models is due to the observation of Perelson et al, [52], that after the first rapid phase of decay during the initial 1-2 weeks of antiretroviral treatment, plasma virus declined at a considerably slower rate. This second phase of viral decay was attributed to the turnover of a longer-lived virus reservoir. Hence, the two target cell models are more accurate than one target cell models [52]. Therefore we relax Assumption 3.6, and consider other species for a more realistic model. However, the design of switching strategies for the nonlinear model (3.12) can be very demanding. For the sake of simplicity, we use

Assumption 3.4 to obtain a linear switched system of the form:

$$\begin{aligned} \dot{T}_i^* &= k_{T,\sigma} T V_i - \delta_{T^*} T_i^* + \sum_{j=1}^{n} \mu m_{i,j} V_j T \\ \dot{M}_i^* &= k_{M,\sigma} M V_i - \delta_{M^*} M_i^* + \sum_{j=1}^{n} \mu m_{i,j} V_j M \\ \dot{V}_i &= p_{T,\sigma} T_i^* + p_{M,\sigma} M_i^* - \delta_V V_i \end{aligned} \tag{3.33}$$

where T and M are treated as constant. The infection rate is expressed as $k_{T,\sigma}$ for CD4+T cells and a $k_{M,\sigma}$ for macrophages. Viral proliferation is achieved in infected activated CD4+T cells and infected macrophages, this is represented by $p_{T,\sigma}$ and $p_{M,\sigma}$ respectively. These parameters depend on the fitness of the genotype and the therapy. The mutation rate is expressed by μ, and $m_{i,j} \in \{0, 1\}$ represents the genetic connections between genotypes. The death rates are δ_{T^*}, δ_{M^*}, δ_V respectively. For simulation purposes, we shall use the parameters shown in Table 3.4. The system (3.33) can be

Table 3.4: Parameters values for (3.33)

Parameter	Value	Value taken from:
k_T	3.4714×10^{-5}	Fitted
k_M	4.533×10^{-7}	Fitted
p_T	44	Fitted
p_M	44	Fitted
δ_{T^*}	0.4	[4]
δ_{M^*}	0.001	[4]
δ_V	2.4	[4]

rewritten as follows

$$\dot{x} = \begin{bmatrix} \Lambda_{1,\sigma} & 0 & \dots & 0 \\ 0 & \Lambda_{2,\sigma} & \dots & 0 \\ \vdots & & \ddots & \vdots \\ 0 & 0 & \dots & \Lambda_{n,\sigma} \end{bmatrix} x + \mu M_u x \tag{3.34}$$

where $x' = [T_1^*, M_1^*, V_1, \dots, T_n^*, M_n^*, V_n]$, $\Lambda_{j,\sigma}$ is given by

$$\Lambda_{j,\sigma} = \begin{bmatrix} -\delta_{T^*} & 0 & k_{T,\sigma} T \\ 0 & -\delta_{M^*} & k_{M,\sigma} M \\ p_{T,\sigma} & p_{M,\sigma} & -\delta_V \end{bmatrix}$$

and the mutation matrix is

$$M_u = \begin{bmatrix} \begin{bmatrix} 0 & 0 & T \\ 0 & 0 & M \\ 0 & 0 & 0 \end{bmatrix} & \dots & m_{1,j} \begin{bmatrix} 0 & 0 & T \\ 0 & 0 & M \\ 0 & 0 & 0 \end{bmatrix} \\ \vdots & \ddots & \vdots \\ m_{i,1} \begin{bmatrix} 0 & 0 & T \\ 0 & 0 & M \\ 0 & 0 & 0 \end{bmatrix} & \dots & m_{i,j} \begin{bmatrix} 0 & 0 & T \\ 0 & 0 & M \\ 0 & 0 & 0 \end{bmatrix} \end{bmatrix}$$

3.4.1 A 9 variant, 2 drug combination model

To accommodate a more complicated scenario we suggest 9 genetic variants, that is $n = 9$, and 2 possible drug therapies, $N = 2$. The viral variants are organized in a square grid as shown in Fig.3.12. The wild type genotype (g_1) would be the most prolific variant in the absence of any drugs, however, it is also the variant that all drug combinations have been designed to combat, and therefore is susceptible to all therapies. After several mutations the highly resistant (g_9) is a genotype with low proliferation rate, but resistant to all drug therapies.

In this model, therapies are composed of reverse transcriptase inhibitors and protease inhibitors, that are represented by

$$k^i_{T,\sigma} = k_T f_i \eta^T_{\sigma,i} \tag{3.35}$$

$$k^i_{M,\sigma} = k_M f_i \eta^M_{\sigma,i} \tag{3.36}$$

$$p^i_{T,\sigma} = p_T f_i \theta^T_{\sigma,i} \tag{3.37}$$

$$p^i_{M,\sigma} = p_M f_i \theta^M_{\sigma,i} \tag{3.38}$$

where $\eta_{\sigma,i}$ represents the infection efficiency for genotype i under treatment σ, and $\theta_{\sigma,i}$ expresses the production efficiency for the genotype i under treatment.

We assume that in the absence of treatment, mutation reduces the fitness of the genotype. Thus we use linear decreasing factors f_i, which represents the fitness of the genotype i. Drugs effects can be seen in Fig.3.12, where the arrows indicate the efficiency of the drug. Moreover, based on clinical evidence [31], inhibitors are more effective in CD4+T cells than in macrophages, this is modeled using $\eta^T_{\sigma,i} > \eta^M_{\sigma,i}$ and $\theta^T_{\sigma,i} > \theta^M_{\sigma,i}$.

For simulation purposes, we suggest the linear decreasing factors on the same axis in Fig.3.12 as $f_i = [1, 0.95, 0.95]$ and the treatment efficiencies are as follow: $\eta^T_{\sigma,1} = \theta^T_{\sigma,1} = [0.2, 0.9, 1]$, $\eta^T_{\sigma,2} = \theta^T_{\sigma,2} = [0.2, 0.5, 1]$, $\eta^M_{\sigma,1} = \theta^M_{\sigma,1} = [0.25, 0.5, 1]$, and $\eta^M_{\sigma,2} = \theta^M_{\sigma,2} = [0.1, 0.8, 1]$.

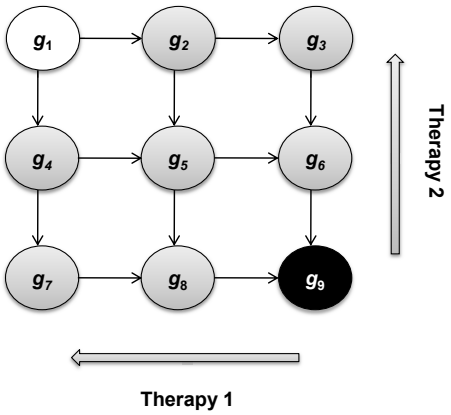

Fig. 3.12: 9 genotypes mutation tree

3.4.2 Clinical Treatments using the Macrophage Mutation Model

To evaluate extended time-scales in the model (3.33) we consider longer treatment periods, and propose that the patient has full clinical examination, once every three months as stated in [8]. Fig.3.13a exhibits the first virologic failure after 6 years of treatment, which is consistent with clinical observations [76]. Numerical results reveal two observations. One is that infected CD4+T cells show very similar dynamics to the viral load because viral replication is rapid in infected CD4+T cells. Secondly, infected macrophages show a more robust behavior against treatments, which reveals strong evidence that macrophages can persist even during long periods of HAART treatment. Therefore, maintaining therapy in patients is important to avoid the formation of latent reservoirs, which will continue to experience viral replication. Simulation results suggest that both therapies will last for approximately 14 years before virological failure is occurred.

In contrast to virologic failure treatment, the SWATCH treatment can maintain the total viral load under virologic failure levels for roughly 16 years, see Fig.3.13b. This gives an extension of nearly 2 years compared with virological failure treatment. These simulation results support the recycling therapies to extend HAART treatments. Similar evidence was found in [8], where significantly more patients in the alternating therapy group than in the virological failure treatment group had plasma HIV-1 RNA levels less than 400 copies/ml while receiving treatment.

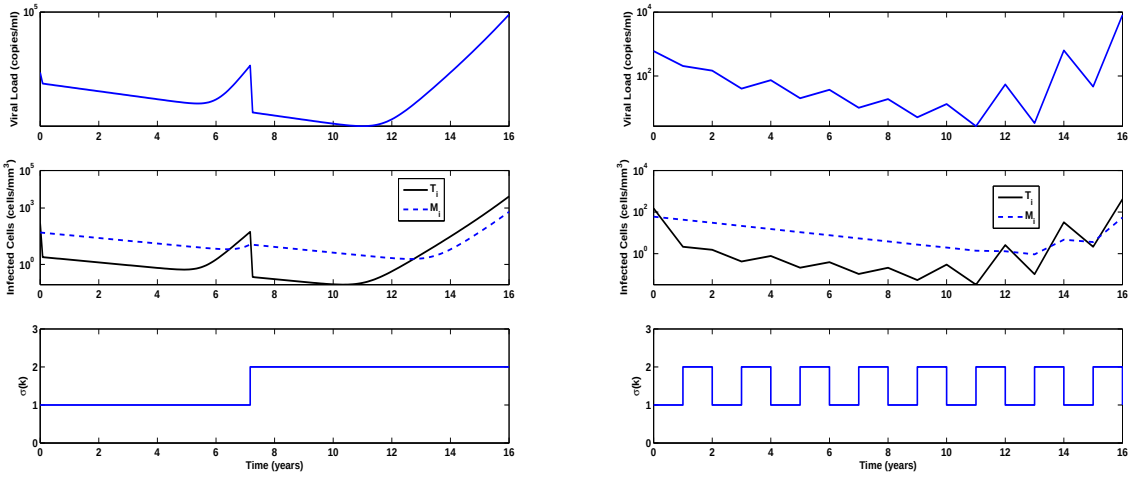

(a) Virologic Failure Treatment

(b) SWATCH

Fig. 3.13: Clinical treatments evaluation for a 9 genotypes model

3.5 Latently infected CD4+T cells Model

Simulation results reveal that the model (3.33) exhibits time-scales consistent with clinical observations. Now, we explore whether another mechanism can match clinical evidence. Using the homing theory and the fact that latently infected CD4+T cells might have an important role in the late HIV infection stage, we adopt the model proposed by [52]. Using Assumption 3.4 we obtain the model

$$\begin{aligned} \dot{T}_i^* &= \psi k_{T,\sigma} T V_i + a_L L_i - \delta_{T^*} T_i^* + \sum_{j=1}^{n} \mu m_{i,j} V_j T \\ \dot{L}_i &= (1-\psi) k_{T,\sigma} T V_i - a_L L_i - \delta_L L_i \\ \dot{V}_i &= p_{T,\sigma} T_i^* - \delta_V V_i \end{aligned} \tag{3.39}$$

where $L_{i,}$ represents the latently infected CD4+T cells. The infection rate is expressed by $k_{T,\sigma}$. This parameter depends on the genotype and the therapy that is used. Once CD4+T cells are infected, a proportion of cells ψ passes into the infected cells population, whereas a proportion $(1-\psi)$ passes into the latently-infected cell population. These latently-infected cells might be activated later and start the virus replication, which is represented by the term a_L. Viral proliferation is achieved in infected activated CD4+T cells, this is represented by $p_{T,\sigma}$, which depends on the fitness of the genotype and the therapy. The mutation rate is represented by μ, the death rates are represented by δ_{T^*}, δ_L, δ_V for T^*, L, V respectively. $m_{i,j} \in \{0,1\}$ represents the genetic connections between genotypes. For simulation purposes, we use the parameters shown in Table 3.5.

Table 3.5: Parameters values for (3.39)

Parameter	Value	Value taken from:
k_T	3.8×10^{-3}	Fitted
p_T	6.45×10^{-1}	Fitted
δ_{T^*}	0.4	[4]
δ_V	2.4	[4]
δ_L	0.005	[4]
a_L	3×10^{-4}	[4]
ψ	0.97	[4]

Assumption 3.4 allows to simplify the dynamics to a linear system. Therefore the system (3.39) can be rewritten as (3.34), where $x' = [T_1^*, L_1, V_1, \ldots, T_n^*, L_n, V_n]$, $\Lambda_{j,\sigma}$ is given by

$$\Lambda_{j,\sigma} = \begin{bmatrix} -\delta_{T^*} & a_L & \psi k_{T,\sigma} T \\ 0 & -(a_L + \delta_L) & (1-\psi) k_{T,\sigma} T \\ p_{T,\sigma} & 0 & -(c_T T + \delta_V) \end{bmatrix}$$

and the mutation matrix is

$$M_u = \begin{bmatrix} m_{1,1} \begin{bmatrix} 0 & 0 & T \\ 0 & 0 & 0 \\ 0 & 0 & 0 \end{bmatrix} & \cdots & m_{1,j} \begin{bmatrix} 0 & 0 & T \\ 0 & 0 & 0 \\ 0 & 0 & 0 \end{bmatrix} \\ \vdots & \ddots & \vdots \\ m_{i,1} \begin{bmatrix} 0 & 0 & T \\ 0 & 0 & 0 \\ 0 & 0 & 0 \end{bmatrix} & \cdots & m_{i,j} \begin{bmatrix} 0 & 0 & T \\ 0 & 0 & 0 \\ 0 & 0 & 0 \end{bmatrix} \end{bmatrix}$$

3.5.1 A 64 variant, 3 drug combination model

We propose 64 genetic variants, that is $n = 64$, and 3 possible drug therapies, $N = 3$. The viral variants are organized in a three-dimensional lattice as shown in Fig.3.14. This lattice is based on the simplifying assumption that multiple independent mutations are required to achieve resistance to all therapies.

As with the previous models the wild type genotype (g_1) would be the most prolific variant in the absence of any drugs, however, it is also the variant that is susceptible to all therapies. After several mutations the highly resistant genotype (g_{64}) is a genotype with low proliferation rate, but that is resistant to all drug therapies. In a similar vein to other models, therapies are composed of

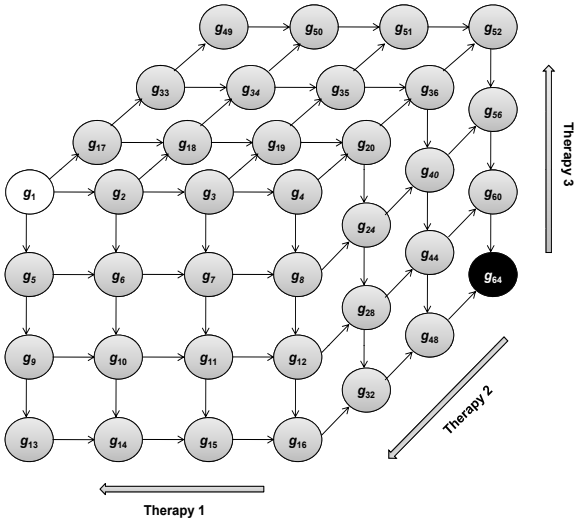

Fig. 3.14: Three lattice mutation tree

reverse transcriptase inhibitors and protease inhibitors, that is

$$k_{T,\sigma} = k_T f_j \eta_{\sigma,j} \tag{3.40}$$

$$p_{T,\sigma} = p_T f_j \theta_{\sigma,j} \tag{3.41}$$

where $\eta_{\sigma,j}$ represents the infection efficiency for genotype j under treatment σ, and $\theta_{\sigma,j}$ expresses the production efficiency for the genotype j under treatment. Similarly, we assume that in the absence of treatment mutation reduces the fitness of the genotype, thus we use linear decreasing factors for f_j, which represent the fitness of the genotype j.

The drug efficiency gradients are illustrated in Fig. 3.14, where the arrows indicate the efficiency of the drug. For instance, the genotypes $g_1, g_5, ..., g_{61}$ are all on one face of the lattice, and are fully susceptible to therapy 1. The opposite face, $g_4, g_8, ..., g_{64}$ describes all genotypes highly resistant to therapy 1. For simulation purposes, we suggest the linear decreasing factors on the same axis in the three lattice Fig.3.14 as $f_i = [1, 0.98, 0.96, 0.94]$ and the treatment efficiencies are as follow: $\eta^T_{\sigma,1} = \theta^T_{\sigma,1} = [0.5, 0.6, 0.75, 1]$, $\eta^T_{\sigma,2} = \theta^T_{\sigma,2} = [0.2, 0.5, 0.7, 1]$, and $\eta^T_{\sigma,3} = \theta^T_{\sigma,3} = [0.3, 0.6, 0.85, 1]$.

3.5.2 Clinical Treatments using Latently infected CD4+T cells Mutation Model

We use a more complex mutation tree model to evaluate the switch on failure treatment and the SWATCH treatment. Using 64 genotypes and three therapies, we consider longer treatment periods, and propose that the patient has full clinical examination, once every three months. Fig.3.15a shows how the first virologic failure occurs around the first year of treatment. Active infected CD4+T cells

have a very similar dynamic to the viral load, this is because in activated CD4+T cells, viral replication is rapid and efficient. On the other hand, latently infected cells shows a more robust behavior against treatments, where patients under HAART provided the first real evidence that HIV-1 can persist in a latent form and then it can be rescued from cells ex vivo after their activation [3].

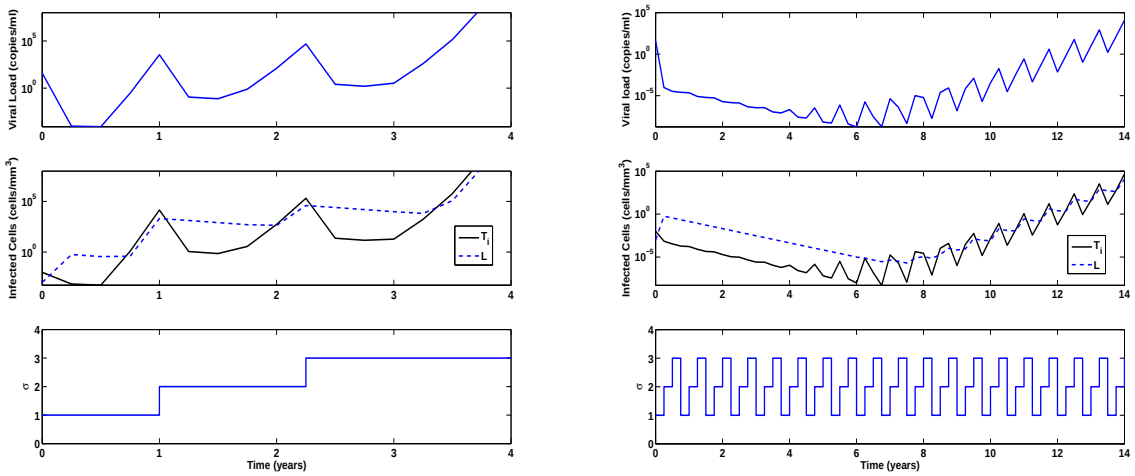

(a) Virologic Failure Treatment

(b) SWATCH

Fig. 3.15: Clinical treatments evaluation for a 64 genotypes model

In contrast to virological failure treatment, the SWATCH treatment (switching between regimens every three months) can maintain the total viral load under detectable level for approximately 10 years, and the virologic failure appears after 14 years. Qualitatively similar evidence was found in [8], where significantly more patients in the alternating therapy group than in the virologic failure treatment group had plasma HIV-1 RNA levels less than 400 copies/ml while receiving treatment. It can be inferred that switching regimens affect stronger latently infected cells, as a result low viral load is prolonged for a longer period than the period of the virologic failure treatment.

Simulation results expose that even with the complexity of the mutation tree presented in Fig.3.14, time scales for virologic dynamics under treatment match better in the macrophages linear model (3.33). We presume that long-term behavior of macrophages is necessary to obtain the appropriate responses.

3.6 Concluding Remarks

In this chapter we have described different mathematical models for HIV infection in order to explore two very important issues: understand HIV progression to AIDS and how to avoid or delay the appearance of highly resistant genotypes using HAART treatments. These questions are still points of discussion in clinical circles, but using mathematical models we offer new insights into HIV infection. The major contributions in this chapter are as follows;

- We provided a review of the most relevant mathematical models in literature. Using different mechanisms these models explain distinct parts in the infection and how drugs may help to control it.
- Using the latent reservoir theory, we proposed a mathematical model which is able to represent the three stages of HIV infection. Simulation results show how infected macrophages lead to symptomatic infection provoking viral explosion. This model provides important insights on how latent reservoirs play a very important role in the last stages of HIV infection.
- A dynamic study is realized for the model. Steady state analysis provides with three equilibrium points: the first equilibrium represents the uninfected status which is unstable, this reveals the difficulty to return to this status once a person is infected by HIV. Using nominal parameters values, we found just one equilibrium in the positive orthant, which is stable and represents the infected status.
- A robustness analysis demonstrates that the model retains its ability to describe the three stages in HIV infection even for moderately large parameter variation. Incorporating cell proliferation terms, dynamics in CD4+T cells and virus can match better clinical observations and preserve the property of robustness in the model.
- Treatment terms are included in the model. Simulation results suggest the importance of starting HAART treatment in early stages of the infection in order to avoid new cell infections, especially for macrophages which will take a long time to clear.
- When the patient is under treatment, we suggest three different models to explore how the switch on regimens should be provided. We compare two clinical treatments, the switched on failure which is commonly used in clinical practice and SWATCH. Simulations exposed the importance of proactive switching to decrease viral load maximally.
- The long-term behavior of macrophages or similar long lived reservoirs appears to be necessary to obtain the appropriate time scales and treatment responses for HIV infection.

PART II

THEORETICAL APPROACH

Chapter 4

Optimal Control Strategies

In this chapter we provide a background on positive switched linear systems. We shall discuss the optimal control problem applied to a certain class of positive switched linear systems. Using dynamic programming, we propose different algorithms to numerically solve the discrete-time optimal control problem. For the sake of simplicity, optimal strategies will be discussed just for the basic mutation model. We conclude the chapter by testing via simulations the robustness of the optimal control.

4.1 Positive Switched Linear Systems - definitions

Dynamical systems that are described by an interaction between continuous and discrete dynamics are usually called hybrid systems [83]. Continuous-time systems with (isolated) discrete switching events are referred as switched systems. A switched system may be obtained from the hybrid system neglecting the details of the discrete behavior and instead considering all possible switchings from a certain class. In this work, we are interested in those systems which belong to the positive orthant called positive systems. These systems have the important property that any nonnegative input and nonnegative initial state generates a nonnegative state trajectory and output for all future times. Common examples of positive systems include, chemical processes (reactors, heat exchangers, distillation columns, storage systems), stochastic models where states represent probabilities, and many other models used in biology, economics and sociology [84].

We consider the following positive switched linear system on a finite time interval,

$$\Sigma_A : \dot{x}(t) = A_{\sigma(t)}x(t), \quad x(0) = x_0, \tag{4.1}$$

where $A_{\sigma(t)}$ switches between some given finite collection of matrices A_1,...,A_N, $t \geq 0$, $x(t) \in R_+^n$ is the state variable vector, $x_0 \in R_n^+$, $\sigma(t)$ is the switching signal. This is a piecewise constant function

σ, which has a finite number of discontinuities, which we call the switching times - on every bounded time interval and takes a constant value on every interval between two consecutive switching times. We now introduce the mathematical definition of continuous time positive systems.

Theorem 4.1 *The system* (4.1) *is said to be positive if and only if the matrices A_i are Metzler, that is, their nondiagonal elements are nonnegative. Then, for every nonnegative initial state and every nonnegative input its state and output are nonnegative.*

Throughout this chapter the following notation is adopted:

i. for $x \in R^n$, $x \succ 0$ ($x \succeq 0$) means that $x_i > 0$ ($x_i \geq 0$) for $1 \leq i \leq n$

ii. for $A \in R^{n \times n}$, $A \succ 0$ ($A \succeq 0$) means that $a_{ij} > 0$ ($a_{ij} \geq 0$) for $1 \leq i, j \leq n$

iii. for $x, y \in R^n$, $x \succ y$ ($x \succeq y$) means that $x - y \succeq 0$ ($x - y \succeq 0$)

A matrix is said to be *Hurwitz* if all its eigenvalues have negative real part. We write A' for the transpose of A, and e^A for the exponential matrix of A. The symbol $\mathcal{S}_{gn}$ denotes the sign function, that takes value 1 when its argument is positive, -1 when its argument is negative and 0 when its argument is 0. A convex hull for a set of points X in a real vector space is the minimal convex set containing X. Finally $co(X_1, X_2, \cdots, X_N)$ denotes a convex hull of the matrices X_i.

4.2 Optimal control for Positive Switched Systems

Beginning in the late 1950s and continuing today, the issues concerning dynamic optimization have received a lot of attention within the framework of control theory [77]. Optimal control's goal is to determine the control signals that will cause a process to satisfy the physical constraints and at the same time minimize (or maximize) some performance criterion.

The solution for the optimal control problem is mainly based in two techniques; the so-called Hamilton-Jacobi theory supplies sufficient conditions for the global optimality together with its most significant achievement, namely the solution of the Linear Quadratic (LQ) problem. The second technique is called the Maximum Principle, which exploits a first order variational approach and provides powerful necessary conditions suited to encompass a wide class of fairly complex problems. A complete background in optimal control can be found in [77], [78], [79],[80], [81] and [82].

The problem of determining optimal switching trajectories in hybrid systems has been widely investigated, both from the theoretical and from the computational points of view [85], [86], [87] and [88]. For continuous-time switched systems, several works present necessary and/or sufficient

conditions for a trajectory to be optimal using the minimum principle [89] and [90]. However, there is no general solution for the problem.

In this work, we are concerned with a specific class of autonomous switched systems, where the continuous control is absent and only the switching signal must be determined [88]. The switched system may be embedded into a larger family of nonlinear systems. Sufficient conditions for optimality on a finite horizon are developed using [80]. No constraints are imposed on the switching and the performance index contains no penalty on the switching.

The cost functional to be minimized over all admissible switching sequences is given by

$$J(x_0, x, \sigma) = \int_0^{t_f} q'_{\sigma(\tau)} x(t) dt + c' x(t_f) \tag{4.2}$$

where $x(t)$ is a solution of (4.1) with the switching signal $\sigma(t)$. The vectors q_i are assumed to have nonnegative entries and c is assumed to have all positive entries. The optimal switching signal, the corresponding trajectory and the optimal cost functional are denoted as $\sigma^o(t, x_0)$, $x^o(t)$ and $J(x_0, x^o, \sigma^o)$ respectively. The Hamiltonian function relative to the system (4.1) and the cost functional (4.2) is given by

$$H(x, \sigma, \pi) = q'_\sigma x(t) + \pi' A_\sigma x(t) \tag{4.3}$$

Theorem 4.2 *Continuous-time Optimal Control for Positive Switched Systems*
Let $\sigma^o(t, x_0) : [0, t_f] \times R^n_+ \to \mathcal{I} = \{1, \ldots, N\}$ be a switching signal relative to x_0 and let $x^o(t)$ be the corresponding trajectory. Let $\pi^o(t)$ denote a positive vector solution of the system of differential equations

$$\begin{aligned} \dot{x}^o(t) &= A_{\sigma^o(t,x_0)} x^o(t) && (4.4)\\ -\dot{\pi}^o(t) &= A'_{\sigma^o(t,x_0)} \pi^o(t) + q_{\sigma^o(t,x_0)} && (4.5)\\ \sigma^o(t, x_0) &= \arg\min_{i \in \mathcal{I}} \{\pi^{o\prime}(t) A_i x^o(t) + q'_i x^o(t)\} && (4.6) \end{aligned}$$

with the boundary conditions $x^o(0) = x_0$ and $\pi^o(t_f) = c$. Then $\sigma^o(t, x_0)$ is an optimal switching signal relative to x_0 and the value of the optimal cost functional is

$$J(x_0, x^o, \sigma^o) = \pi'^o(0) x_0 \tag{4.7}$$

Proof The scalar function

$$v(x, t) = \pi^o(t)' x(t) \tag{4.8}$$

is a generalized solution of the HJE

$$0 = \tfrac{\partial v}{\partial t}(x, t) + H\left(x(t), \sigma^o(t, x_0), \tfrac{\partial v}{\partial x}(x, t)'\right) \tag{4.9}$$

where

$$H(x, \sigma, \pi) = q'_\sigma x(t) + \pi'(t) A_\sigma x(t) \tag{4.10}$$

Notice that the triple (x^o, π^o, σ^o) satisfies the necessary conditions of the Pontryagin principle, since

$$H(x^o, \sigma^o, \pi^o) \leq H(x, \sigma, \pi), \quad \sigma = 1, 2$$

Moreover,

$$\frac{\partial v}{\partial x}(x, t) = \pi^o(t)' \tag{4.11}$$

$$\frac{\partial v}{\partial t}(x, t) = \dot{\pi}^o(t)' x(t) \tag{4.12}$$

so that, for almost all $t \in [0, t_f]$

$$\dot{\pi}^o(t)' x^o(t) + q'_{\sigma^o(t,x_0)} x^o(t) + \pi^o(t)' A_{\sigma^o(t,x_0)} x^o(t) = 0 \tag{4.13}$$

Moreover it satisfies the boundary condition

$$v(x^o(t_f), t_f) = \pi^o(t_f)' x^o(t_f) = c' x^o(t_f) \tag{4.14}$$

This completes the proof. ∎

The HJE partial differential equation is reduced to a set of ordinary differential equations (4.5). Notice that these equations are inherently nonlinear. The state equations must be integrated forward whereas the co-state equations must be integrated backward, both according to the coupling condition given by the switching rule. As a result, the problem is a two point boundary value problem, and can not be solved using regular integration techniques. Next, we shall discuss how the system (4.5) can be solved analytically under certain assumptions on the matrix A_σ.

4.3 Optimal control to Mitigate HIV Escape

The CD4+T cell count is a key factor in deciding whether to initiate antiretroviral therapy and is the strongest predictor of subsequent disease progression [5]. However, viral load is the most important indicator of response to antiretroviral therapy. Analysis of 18 trials with viral load monitoring showed significant association between a decrease in plasma viremia and improved clinical outcome [91]. Therefore we can infer that viral load and CD4+T cells matter. But mostly during treatments and numerical simulations, viral load is low and CD4+T cell count is good (over 350 cells/mm^3) until the final escape in viral load appears. Moreover, the final escape of the virus is at some almost uncontrollable exponential rate and final viral load is a surrogate for time to escape.

Consequently it is reasonable to think that if the total viral load is small enough during a finite time of treatment, new cell infections would be less likely. Therefore there is a significant probability that the total virus load becomes zero.

Notice that in a more accurate stochastic model of viral dynamics, $x_i(t)$ is the expected value of the number of virus V_i. Hence, from Markov's inequality, it can be shown that small $E[x]$ guarantees a high probability of viral extinction ($P(\sum_i v_i = 0) \geq 1 - E[\sum_i v_i] = 1 - \sum_i x_i$). It is therefore logical to propose a cost

$$J := c'x(t_f) \tag{4.15}$$

where c is the column vector with all ones, and t_f is the final time for the treatment. This cost is minimized under the action of the switching rule.

Remark 4.1 *Another interesting interpretation of the cost relies on the theory of Markov jump linear systems. Indeed, notice that the state, equation* (3.30) *can be written as follows:*

$$\dot{x}_i(t) = \eta_{i,\sigma(t)} x_i(t) + \mu \sum_{j \neq i} \lambda_{ij} x_j(t) \tag{4.16}$$

where $\eta_{i,\sigma(t)} = \rho_{i,\sigma(t)} + 2\mu - \delta$ *and* $\lambda_{i,j} = m_{i,j}$, $i \neq j$, $\lambda_{i,i} = -2$. *Notice that matrix:* $\mu\Lambda$, *where* $\Lambda = \{\lambda_{i,j}\}$ *is a stochastic matrix, that can be considered as the infinitesimal transition matrix of the Markov jump linear system*

$$\dot{\xi} = 0.5\eta_{i,\sigma(t)}\xi \tag{4.17}$$

Moreover $\sum_{i=1}^{n} x_i(t) = E[\xi^2(t)]$. *Minimizing* $\sum_{i=1}^{n} x_i(t)$ *is then equivalent to minimizing the variance of the stochastic process* $\xi(t)$. *Notice that if* $lim_{t\to\infty} E[\xi^2(t)] = 0$ *then the system (4.17) is stable in the mean-square sense.*

It was explained that there is no general consensus amongst clinicians on the optimal time to change therapy to avoid virologic failure. The clinical trial in [9] suggested that proactive switching and alternation of antiretroviral regimens could extend the overall long-term effectiveness of the available therapies. Then, we define the optimal problem to mitigate viral escape as follows.

Problem 4.1 *Given the 4 variant model* (3.30), *find for a fixed period of treatment* t_f *the optimal switching signal between two HAART regimens to minimize the total viral load, represented by the performance criterion* (4.15).

4.3.1 General Solution for a Symmetric Case

In this section, we shall solve analytically the Problem 4.1 for a specific case of mutation, that is when there is a symmetry in replication rates as it was shown in Chapter 3 for Scenario 1. Then,

for the system Σ_A the matrix A_σ has the following form

$$A_\sigma = \begin{bmatrix} \lambda_1 & 0 & 0 & 0 \\ 0 & \lambda_{2\sigma} & 0 & 0 \\ 0 & 0 & \lambda_{3\sigma} & 0 \\ 0 & 0 & 0 & \lambda_4 \end{bmatrix} + \mu \begin{bmatrix} 0 & 1 & 1 & 0 \\ 1 & 0 & 0 & 1 \\ 1 & 0 & 0 & 1 \\ 0 & 1 & 1 & 0 \end{bmatrix}$$

Using symmetric replications rates, we can assume that

Assumption 4.1

$$\lambda_{21} > 0, \quad \lambda_{22} < 0, \quad \lambda_{31} < 0, \quad \lambda_{32} > 0$$

Assumption 4.2

$$\lambda_{21} - \lambda_{22} + \lambda_{31} - \lambda_{32} = 0$$

Using Assumption 4.1 and 4.2 note that

$$\Delta A = A_1 - A_2 = (\lambda_{21} - \lambda_{22}) \begin{bmatrix} 0 & 0 & 0 & 0 \\ 0 & 1 & 0 & 0 \\ 0 & 0 & -1 & 0 \\ 0 & 0 & 0 & 0 \end{bmatrix} = (\lambda_{21} - \lambda_{22})\bar{J}$$

Since $\lambda_{21} - \lambda_{22} > 0$, we can define the decision function $\gamma(t) = \pi(t)'\bar{J}x(t)$ that takes the form

$$\gamma(t) = \pi_2(t)[x_2(t) - x_3(t)] + x_3(t)[\pi_2(t) - \pi_3(t)] \tag{4.18}$$

Moreover, from the structure of A_1 and A_2 it is possible to conclude that

$$\dot{\gamma}(t) = [\pi_2(t) - \pi_3(t)][x_1(t) + x_4(t)] - [x_2(t) - x_3(t)][\pi_1(t) + \pi_4(t)] \tag{4.19}$$

The following lemma, which can be proven directly from (4.18) and Assumption 4.1 is useful to characterize the optimal solution.

Lemma 4.1 *Under Assumption 4.1 the following conditions hold:*

$$\begin{aligned}
|\mathcal{S}_{gn}[x_2(t) - x_3(t)] + \mathcal{S}_{gn}[\pi_2(t) - \pi_3(t)]| = 2 \\
\implies \mathcal{S}_{gn}[\gamma(t)] = \mathcal{S}_{gn}[x_2(t) - x_3(t)] \\
\mathcal{S}_{gn}[x_2(t) - x_3(t)] + \mathcal{S}_{gn}[\pi_2(t) - \pi_3(t)] = 0, \\
\implies \mathcal{S}_{gn}[\dot{\gamma}(t)] = \mathcal{S}_{gn}[\pi_2(t) - \pi_3(t)] \\
\mathcal{S}_{gn}[\dot{x}_2(t) - \dot{x}_3(t)] = \mathcal{S}_{gn}[1.5 - \sigma(t)] \\
\mathcal{S}_{gn}[\dot{\pi}_2(t) - \dot{\pi}_3(t)] = \mathcal{S}_{gn}[\sigma(t) - 1.5]
\end{aligned}$$

Remark 4.2 *Theorem 4.2 does not consider the possible existence of sliding modes, i.e. infinite frequency switching of $\sigma(t)$. However, the optimal state and costate variables x^o, π^o can lie on a sliding surface, and this corresponds to a chattering switching law. This leads to the notion of extended (Filippov) trajectories satisfying a differential inclusion. To be precise, the optimal control is characterized by:*

$$\dot{x}^o(t) \in co\{A_1 x^o(t), A_2 x^o(t), \cdots, A_N x^o(t)\} \tag{4.20}$$

$$-\dot{\pi}^o(t) \in co\{A_1' \pi^o(t) + q_1, \cdots, A_N' \pi^o(t) + q_N\} \tag{4.21}$$

$$\pi'^o(t) A_i x^o(t) = constant, \forall i \tag{4.22}$$

In order to characterize the sliding modes, we look for a convex combination of the matrices.

$$A_\alpha = \alpha A_1 + (1 - \alpha) A_2$$

with $\alpha \in [0, 1]$.

Lemma 4.2 *Under Assumption 4.2 the Filippov solution corresponding to*

$$\alpha = \frac{\lambda_{32} - \lambda_{22}}{\lambda_{32} - \lambda_{22} + \lambda_{21} - \lambda_{31}}$$

satisfy

$$\dot{x}(t) = (\alpha A_1 + (1 - \alpha) A_2) x(t),$$

$$\dot{\pi}(t) = -(\alpha A_1 + (1 - \alpha) A_2) \pi(t)$$

then the sliding surface is

$$x_2(t) = x_3(t), \quad \pi_2(t) = \pi_3(t)$$

such that

$$\gamma(t) \equiv 0$$

Proof It is enough to show that the variables $x_2(t) - x_3(t)$ and $\pi_2(t) - \pi_3(t)$ obey autonomous differential equations. Indeed,

$$\dot{x}_2(t) - \dot{x}_3(t) = \alpha(\lambda_{21} - \lambda_{31})x_2(t) + (1-\alpha)(\lambda_{22} - \lambda_{32})x_3(t)$$

where

$$\alpha(\lambda_{21} - \lambda_{31}) = (1-\alpha)(\lambda_{22} - \lambda_{32})$$

so that

$$\dot{x}_2(t) - \dot{x}_3(t) = r(x_2(t) - x_3(t))$$

Analogously

$$\dot{\pi}_2(t) - \dot{\pi}_3(t) = -r(\pi_2(t) - \pi_3(t))$$

where

$$r = \frac{\lambda_{21}\lambda_{32} - \lambda_{22}\lambda_{31}}{\lambda_{32} - \lambda_{22} + \lambda_{21} - \lambda_{31}}$$

∎

Now, let

$$\begin{aligned} k_1 &= \text{argmin}\{x_2(0), x_3(0)\} \\ k_2 &= \text{argmin}\{c_2, c_3\} \end{aligned}$$

and

$$\begin{aligned} T_1^\star &= \min_{t\geq 0} : [0\ 1\ -1\ 0]e^{A_{k_1}t}x(0) = 0, \\ T_2^\star &= \min_{t\leq t_f} : [0\ 1\ -1\ 0]e^{-A_{k_2}(t-t_f)}c = 0. \end{aligned}$$

Notice that, thanks to the definition of k_1, k_2 and the monotonicity conditions of $x_2(t) - x_3(t)$, $\pi_2(t) - \pi_3(t)$, the time instants $T_1^\star$ and $T_2^\star$ are well defined and unique. Clearly, by definition $x_2(T_1^\star) = x_3(T_1^\star)$ and $\pi(T_2^\star) = \pi_3(T_2^\star)$. We are now in the position to provide the main result of this section.

Theorem 4.3 *Long Horizon Case*
Let Assumptions 4.1, 4.2 be met with and assume that $T_1^\star \leq T_2^\star$. Then, the optimal control associated with the initial state $x(0)$ and cost $c'x(t_f)$ is given by $\sigma(t) = k_1, \quad t \in [0, T_1^\star]$ and $\sigma(t) = k_2, \quad t \in [T_2^\star, t_f]$. For $t \in [T_1^\star, T_2^\star]$, the optimal control is given by the Filippov trajectory along the plane $x_2 = x_3$, with dynamical matrix $A = \alpha A_1 + (1-\alpha)A_2$.

Proof We shall verify that the control law satisfies the conditions given by the Hamilton-Jacobi equations in the intervals $[0, T_1^\star]$ and $[T_2^\star, t_f]$. Moreover, in the interval $[T_1^\star, T_2^\star]$ the optimal control

state and costate variables slide along the trajectories $x_2(t) = x_3(t)$ and $\pi_2(t) = \pi_3(t)$. To this end, let $\sigma(t) = k_1$ for $t \in [0, T_1^\star]$, $\sigma(t) = k_2$ for $t \in [T_2^\star, t_f]$ and

$$\begin{aligned}
\pi(t) &= e^{A_{k_1}(T_1^\star - t)}\pi(T_1^\star), \quad t \in [0, T_1^\star] \\
\pi(t) &= e^{A(T_2^\star - t)}\pi(T_2^\star), \quad t \in [T_1^\star, T_2^\star] \\
\pi(t) &= e^{A_{k_2}(t_f - t)}c, \quad t \in [T_2^\star, t_f] \\
x(t) &= e^{A_{k_1}t}x(0), \quad t \in [0, T_1^\star] \\
x(t) &= e^{A(t - T_1^\star)}x(T_1^\star), \quad t \in [T_1^\star, T_2^\star] \\
x(t) &= e^{A_{k_2}(t - T_2^\star)}x(T_2^\star), \quad t \in [T_2^\star, t_f]
\end{aligned}$$

First of all notice that, by definition, $x_2(T_1^\star) = x_3(T_1^\star)$ and $\pi_2(T_2^\star) = \pi_3(T_2^\star)$. Thanks to Lemma 4.2, in the interval $[T_1^\star, T_2^\star]$ we have $x_2(t) = x_3(t)$ and $\pi_2(t) = \pi_3(t)$. In the intervals $[0, T_1^\star]$ and $[T_2^\star, t_f]$, consider the decision function and its derivative, given by (4.18), (4.19), respectively. Now, we have $\gamma(T_1^\star) = \gamma(T_2^\star) = 0$ and, for $t \in [0, T_1^\star]$, $t \in [T_2^\star, t_f]$:

$$\dot{x}_2(t) - \dot{x}_3(t) = \lambda_{2k_i}x_2(t) - \lambda_{3k_i}x_3(t) = \begin{cases} > 0 & k_i = 1 \\ < 0 & k_i = 2 \end{cases}$$

$$\dot{\pi}_2(t) - \dot{\pi}_3(t) = -\lambda_{2k_i}\pi_2(t) + \lambda_{3k_i}\pi_3(t) = \begin{cases} < 0 & k_i = 1 \\ > 0 & k_i = 2 \end{cases}$$

This means that, for $t \in [0, T_1^\star]$, $t \in [T_2^\star, t_f]$:

$$\begin{aligned}
x_2(t) - x_3(t) &= \begin{cases} < 0 & k_i = 1 \\ > 0 & k_i = 2 \end{cases} \\
\pi_2(t) - \pi_3(t) &= \begin{cases} > 0 & k_i = 1 \\ < 0 & k_i = 2 \end{cases} \\
\dot{\gamma}(t) &= \begin{cases} > 0 & k_i = 1 \\ < 0 & k_i = 2 \end{cases}
\end{aligned}$$

Since $\gamma(T_i^\star) = 0$ it follows

$$\gamma(0) = \pi(0)'\bar{J}x(0) = \begin{cases} < 0 & k_1 = 1 \\ > 0 & k_1 = 2 \end{cases}$$

$$\gamma(t_f) = \pi(t_f)'\bar{J}x(t_f) = \begin{cases} < 0 & k_2 = 1 \\ > 0 & k_2 = 2 \end{cases}$$

which confirms $\sigma(t) = \text{argmin}_i\ \pi(t)'A_ix(t) = k_1$, for $t \in [0, T_1^\star]$ and $\sigma(t) = \text{argmin}_i\ \pi(t)'A_ix(t) = k_2$, for $t \in [T_2^\star, t_f]$. ∎

Even though in practice the horizon length t_f may often be large enough to guarantee that $T_1^\star \leq T_2^\star$, for completeness, we shall consider the *small horizon* case.

Theorem 4.4 *Small Horizon Case*
Let Assumption (4.1) be met and $0 < T_2^\star \leq T_1^\star < t_f$. *Then, the optimal control associated with the initial state* $x(0)$ *and cost* $c'x(t_f)$ *is given as follows:*

If $k_1 = k_2$, *then*

$$\sigma(t) = k_1, \quad t \in [0, t_f]$$

otherwise, if $k_1 \neq k_2$, *then*

$$\sigma(t) = \left\{ \begin{array}{ll} k_1: & t \in [0, T_3^\star] \\ k_2: & t \in [T_3^\star, t_f] \end{array} \right\}$$

where $T_3^\star \in [T_2^\star, T_1^\star]$ *is such that for* $t = T_3^\star$

$$x(T_2^\star)' e^{A_{k_1}(t-T_2^\star)} \bar{J} e^{-A_{k_2}(t-T_1^\star)} \pi(T_1^\star) = 0$$

Proof Let first consider the case $k_1 = k_2$. Then, we will verify that the constant control law $\sigma(t) = k_1$ satisfies the sufficient condition given by the Hamilton-Jacobi equations, i.e.

$$\sigma(t) = \text{argmin}_i \ \pi(t)' A_i x(t),$$

$$\dot{\pi}(t) = -A_{\sigma(t)} \pi(t), \quad \pi(t_f) = c$$

To this end, consider again the decision function $\gamma(t)$ and its derivative, given by (4.18) and (4.19), respectively. Consider

$$\begin{array}{rcl} \pi(t) & = & e^{A_{k_1}(t_f - t)} c, \quad t \in [0, t_f] \\ x(t) & = & e^{A_{k_1} t} x(0), \quad t \in [0, t_f] \end{array}$$

Moreover let $\bar{k}_1 = 1$ if $k_1 = 2$ and viceversa. Since $T_2^\star \leq T_1^\star$, we conclude that

$$\mathcal{S}_{gn}[x_2(t) - x_3(t)] = \mathcal{S}_{gn}[\pi_2(t) - \pi_3(t)] = k_1 - \bar{k}_1,$$

in the interval $(T_2^\star, T_1^\star)$. This implies that $\mathcal{S}_{gn}[\gamma(t)] = k_1 - \bar{k}_1$ in the same interval. Moreover,

$$\mathcal{S}_{gn}[\dot{\gamma}(t)] = \mathcal{S}_{gn}[\pi_2(t) - \pi_3(t)]$$

in $t \in [0, T_2^\star)$ and $t \in (T_1^\star, t_f]$. This means that the sign of $\gamma(t)$ is constant in $[0, t_f]$ and equals $k_1 - \bar{k}_1$. The proof of the first part is concluded.

Consider now the case $k_1 \neq k_2$. By assumption,

$$\mathcal{S}_{gn}[x_2(t) - x_3(t)] = k_1 - \bar{k}_1, \quad t \in [0, T_2^\star)$$

and

$$\mathcal{S}_{gn}[\pi_2(t) - \pi_3(t)] = k_2 - \bar{k}_2, \quad t \in (T_1^\star, t_f]$$

Notice that, in any possible switching point in the interval $[T_2^\star, T_1^\star]$, the derivatives of $x_2(t) - x_3(t)$ and $\pi_2(t) - \pi_3(t)$ change sign at $t = T_3^\star$, so that $\mathcal{S}_{gn}[\dot{\gamma}(t)]$ is constant in $[0, t_f]$, and consequently, $\mathcal{S}_{gn}[x_2(t) - x_3(t)] = k_1 - \bar{k}_1$, $\mathcal{S}_{gn}[\pi_2(t) - \pi_3(t)] = k_2 - \bar{k}_2$ in $[0, t_f]$. We now have to prove that indeed there exists a $T_3^\star$. To this end, notice that

$$\mathcal{S}_{gn}[\gamma(T_2^\star)] = k_1 - \bar{k}_1, \quad \mathcal{S}_{gn}[\gamma(T_1^\star)] = k_2 - \bar{k}_2$$

This, together with $\mathcal{S}_{gn}[\dot{\gamma}(t)] = \mathcal{S}_{gn}[x_2(t) - x_3(t)]$ implies that there exists $T_3^\star \in (T_2^\star, T_1^\star)$ for which $\gamma(T_3^\star) = 0$. This value is the only point $t \in [T_2^\star, T_1^\star]$ satisfying $x(T_2^\star)' e^{A_{k_1}(t - T_2^\star)} \bar{J} e^{-A_{k_2}(t - T_1^\star)} \pi(T_1^\star) = 0$. ∎

To illustrate these last results, we consider Scenario 1 portrayed in Table 3.2, the initial condition $x_0 = [10^3, 10^2, 0, 10^{-5}]$ and the cost function weighting as $c = [1, 1, 1, 1]'$ (that means we want to minimize the total viral load equally). Firstly, we need to compute the initial time $T_1^\star$ during which the system will not switch. For this example $T_1^\star = 24.64$ days. Then the control will be on the sliding surface $x_2 = x_3$ for the remaining time as can be observed in Fig.4.1. From the clinical point

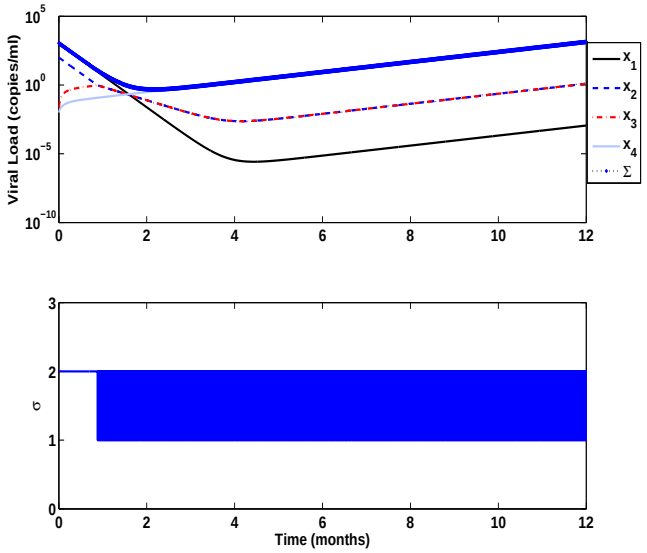

Fig. 4.1: Optimal switching rule

of view, this strategy is unrealistic because of the high frequency switching. Nonetheless, we may

speculate that when there are two intermediate resistants genotypes as presented in the Scenario 1, it would be recommended to switch treatment as soon as clinicians consider the patient's health is not under any risk.

4.4 General Permutation Case

In last section we explored a general solution for a four genotype mutation tree, with certain symmetry in the proliferation rates under switching, using Pontryagin principle we obtained necessary conditions for optimality. In this section we want to establish which conditions are necessary for a more complicated structure model to satisfy optimality conditions. For example, we might start

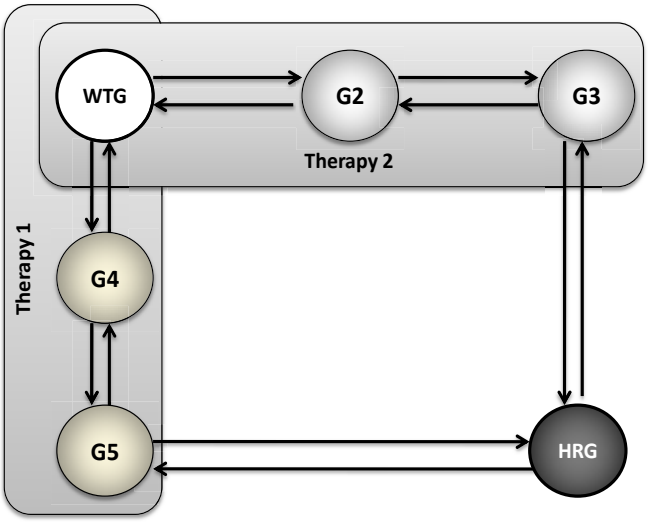

Fig. 4.2: Example 6 genotype symmetric case

introducing two intermediate genotypes to the 4 genotype mutation tree presented before. This new mutation arrangement, as can be seen in Fig.4.2, has the wild type genotype that need to mutate three times in order to be resistant to therapy. The mathematical model is the same as (3.30), then for this problem the matrix A_σ has the form

$$A_\sigma = \begin{bmatrix} \lambda_1 & 0 & 0 & 0 & 0 & 0 \\ 0 & \lambda_{2\sigma} & 0 & 0 & 0 & 0 \\ 0 & 0 & \lambda_{3\sigma} & 0 & 0 & 0 \\ 0 & 0 & 0 & \lambda_{4\sigma} & 0 & 0 \\ 0 & 0 & 0 & 0 & \lambda_{5\sigma} & 0 \\ 0 & 0 & 0 & 0 & 0 & \lambda_6 \end{bmatrix} + \mu \begin{bmatrix} 0 & 1 & 0 & 1 & 0 & 0 \\ 1 & 0 & 1 & 0 & 0 & 0 \\ 0 & 1 & 0 & 0 & 0 & 1 \\ 1 & 0 & 0 & 0 & 1 & 0 \\ 0 & 0 & 0 & 1 & 0 & 1 \\ 0 & 0 & 1 & 0 & 1 & 0 \end{bmatrix}$$

Extending the number of genotypes, the next assumptions need to be satisfied.

Assumption 4.3 *The matrix A_1 may be linked to A_2 by permuting some elements in it, this is expressed by*

$$A_2 = PA_1P \tag{4.23}$$

where P is a symmetric matrix.

Assumption 4.4 *The permutation matrix P can be written as a function of a matrix v in the form*

$$P = I - vv' \tag{4.24}$$

Assumption 4.5 *The matrix v has the property*

$$v'v = 2I \tag{4.25}$$

In order to satisfy optimality conditions for the 4 genotype symmetric case, it was necessary to consider the existence of sliding modes. To follow this objective, a linear combination of matrices was established;

$$A_\alpha = \alpha A_1 + (1-\alpha)A_2$$

with $\alpha = \frac{1}{2}$. For a more general case, we shall need to find a left invariant set subspace to A_α, hence we need to introduce the following lemma.

Lemma 4.3 *Let Assumptions 4.3-4.5 be satisfied, then v' is a basis for a left invariant subspace of $A_{\frac{1}{2}}$; that is $v'A_{\frac{1}{2}} = \frac{1}{2}(v'A_1v)v'$*

Proof Using (4.23) we may rewrite $A_{\frac{1}{2}}$ as

$$A_{\frac{1}{2}} = \frac{1}{2}(A_1 + PA_1P)$$

Using (4.24) in $A_{\frac{1}{2}}$ we obtain

$$A_{\frac{1}{2}} = \frac{1}{2}(2A_1 - vv'A_1 - A_1vv' + vv'A_1vv')$$

then

$$v'A_{\frac{1}{2}} = \frac{1}{2}(2v'A_1 - v'vv'A_1 - v'A_1vv' + v'vv'A_1vv')$$

therefore

$$v'A_{\frac{1}{2}} = \frac{1}{2}(v'A_1v)v'$$

∎

The last lemma is applied to any mutation tree model which satisfies Assumptions 4.3-4.5. For the proposed example in Fig.4.2 the vector v has the following form;

$$v' = \begin{bmatrix} 0 & 1 & 0 & -1 & 0 & 0 \\ 0 & 0 & 1 & 0 & -1 & 0 \end{bmatrix} \tag{4.26}$$

Theorem 4.5 *Let Assumption 4.3 be met and assume that initial conditions are such that* $v'x(t_1) = 0$ *and* $v'\pi(t_1) = 0$. *Then the optimal control is given by the Filippov trajectory along the plane* $v'x(t) = 0$ *with dynamical matrix* $A_\alpha = \frac{1}{2}(A_1 + A_2)$.

Proof If we consider the system (4.1) as an embedded system [85], the optimal control law can be rewritten as

$$\gamma(t) = \pi(t)'\Delta A x(t)$$

In order to prove that the optimal trajectory is along the plane $v'x(t) = 0$, it is necessary to show that the plane is invariant. Accordingly, we have

$$\Delta A = A_1 - A_2 = A_1 - PA_1P$$

Using Lemma 4.3 we may achieve the expression

$$\Delta A = v(v'A_1 - \frac{1}{2}v'A_1vv') + (A_1v - \frac{1}{2}vv'A_1v)v'$$

we can rewrite as

$$\Delta A := vw' + wv'$$

where

$$w = A_1v - \frac{1}{2}vv'A_1v$$

Therefore, if we start on the sliding surface, this means with $x(t_1)$ such that $v'x(t_1) = 0$ and $\pi(t_1)$ such that $v'\pi(t_1) = 0$, then the next conditions are satisfied;

(i) $v'\dot{x}(t_1) = v'A_\alpha x(t_1) = \frac{1}{2}(v'A_1v)v'x(t_1) = 0$
(ii) $v'\dot{\pi}(t_1) = v'A_\alpha x(t_1) = \frac{1}{2}(v'A_1v)v'\pi(t_1) = 0$
(iii) $\gamma(t_1) = \pi(t_1)'\Delta A x(t) = \pi(t)'(vw' + wv')x(t_1) = 0$
(iv) Similarly, $\dot{\gamma}(t_1) = 0$
Thus, the trajectories will remain on the sliding surface for all future time. ∎

Under the same assumptions the Theorem 4.5 may be applied to a broad number of mutation trees, for instance as is portrayed in Fig.4.3. Therefore, independently of the number of intermediate genotypes, if Assumptions 4.3, 4.4 and 4.5 are satisfied, a fast proactive switching treatment provides the best solution to mitigate the highly resistant genotype.

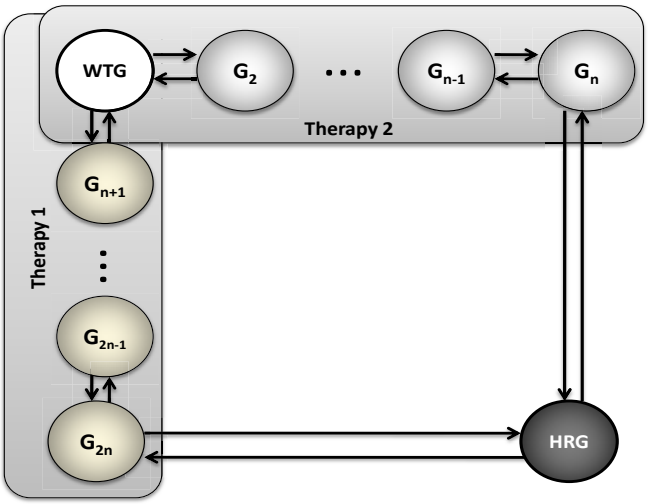

Fig. 4.3: General permutation case

4.5 Restatement as an optimization problem

It was previously exposed that the optimal control solution is difficult even for simple cases. In some situations, the optimal control problem may be restated as a nonlinear optimization problem, which could be considered as an easier choice than the solution of the HJE. For this purpose, instead of finding when the system will switch, it may be considered that the system will switch, but now we shall find the optimal length of the switches. Using the system Σ_A, we consider a constant number of switches for the period t_f. We know the state at every moment using the exponential matrix and obtain

$$x(\tau_1) = e^{A_1 \Delta\tau_1} x(0) \tag{4.27}$$

We can express the problem in time t_f as

$$x(t_f) = \prod_{i=1}^{N_f} e^{A_j \Delta\tau_i} x(0) \tag{4.28}$$

where N_f is the number of switches on the interval $[t_0, t_f]$, and $j = 1$ when i is odd, otherwise is 2. In addition, the next restriction must be satisfied.

$$t_f = \sum_{i}^{N_f} \Delta\tau_i \tag{4.29}$$

Now, if we take the cost function (4.15), this problem could be rewritten in a form that the cost

function depends just of $\Delta\tau_i$.

$$J(t_f) = c' \prod_{i=1}^{N_f} e^{A_j \Delta\tau_i} x(0) \tag{4.30}$$

Lemma 4.4 *Let $\mu = 0$ for the system (3.30), then the optimal switching signal is described by a single switch with duration*

$$T_2 = \frac{1}{2(\lambda_{21} - \lambda_{22})} \ln \frac{x_3(t_f)^{\sigma=1}}{x_2(t_f)^{\sigma=1}} \tag{4.31}$$

Proof Assuming the mutation rate μ is 0 then, the matrices A_i are diagonal. Since diagonal matrices commute $A_1 A_2 = A_2 A_1$, the equation (4.30) is reduced to;

$$J(t_f) = c' e^{A_1 \sum_{i=1}^{N_f} \Delta\tau_i + A_2 \sum_{j=2}^{N_f} \Delta\tau_j} x(0) \tag{4.32}$$

where $i \in$ even numbers and $j \in$ odd numbers. If we use the topology of the system $\Delta A = A_1 - A_2$, then, we rearrange (4.32) as

$$J(t_f) \quad = \quad c' e^{A_1(\sum_{i=1}^{N_f} \Delta\tau_i + \sum_{j=2}^{N_f} \Delta\tau_j) + \Delta A \sum_{j=1}^{N_f} \Delta\tau_j} x(0) = c' e^{\Delta A \sum_{j=2}^{N_f} \Delta\tau_j} x(t_f)^{\sigma=1}$$

where $x(t_f)^{(\sigma=1)} = [x_1(t_f)^{\sigma=1}, x_2(t_f)^{\sigma=1}, x_3(t_f)^{\sigma=1}, x_4(t_f)^{\sigma=1}]'$ is the state vector at time t_f under the only effect of $\sigma = 1$. As a result of the commutation property, the order of the switches is not important for this case, what is really important is how long $\sigma = 2$ will be used independently of the order. For this purpose, we consider in (4.33) that $T_2 = \sum_{j=2}^{N_f} \Delta\tau_j$ as a variable with the only restriction that $T_2 \geq 0$. Computing the first derivative with respect to T_2;

$$\frac{dJ(t_f)}{dT_2} = c' \Delta A e^{\Delta A T_2} x_1(t_f) \tag{4.33}$$

To find the minimum, we solve for T_2

$$T_2 = \frac{1}{2(\lambda_{21} - \lambda_{22})} \ln \frac{x_3(t_f)^{\sigma=1}}{x_2(t_f)^{\sigma=1}}$$

In order to minimize the cost function $J(t_f)$ in the system (3.30), we need to use $\sigma = 2$ for a period T_2. ∎

Remark 4.3 *For the case when $\mu \neq 0$, we have to solve the problem numerically using nonlinear optimization. However, because the problem is non-convex, numerical solution may be very complex.*

4.6 Dynamic Programming for Positive Switched Systems

The model for the treatment of viral mutation given in (3.30) is described in continuous time. In practice, measurements can only reasonably be made infrequently. For simplicity, we consider a regular treatment interval τ, during which the treatment is fixed. If we use $k \in \mathbb{N}$ to denote the number of intervals since $t = 0$, then

$$x(k+1) = A_{\sigma(k)}x(k) \tag{4.34}$$

defined for all $k \in \mathbb{N}$ where $x \in R^n$ is the state, $\sigma(k)$ is the switching sequence, and $x(0) = x_0$ is the initial condition. For (4.34) to be a positive system for any switching sequence, A_i, $i = 1, ..., N$ must be nonnegative matrices, that is, its entries are $a^i_{lj} \geq 0$, $\forall(l, j)$, $l \neq j$, $i = 1, 2, ..., N$. For each $k \in \mathbb{N}$,

$$\sigma(k) \in \{1, 2, ..., N\} \tag{4.35}$$

Consider the following discrete-time cost function to be minimized over all admissible switching:

$$J = c'x(t_f) + \sum_{k=0}^{t_f-1} q'_{\sigma(k)}x(k) \tag{4.36}$$

where $x(k)$ is a solution of (4.34) with the switching signal $\sigma(k)$. The vectors c and q_i, $i = 1, 2, \cdots, N$, are assumed to be positive.

Theorem 4.6 *Discrete-time Optimal Control for Positive Switched Systems*
Let $\sigma^o(k, x_0) : [0, t_f] \times R^n_+ \to \mathcal{I} = \{1, \ldots, N\}$ be an admissible switching signal relative to x_0 and $x^o(k)$ be the corresponding trajectory. Let $\pi^o(k)$ denote a positive vector solution of the system of difference equations

$$\begin{aligned} x^o(k+1) &= A_{\sigma^o(k)}x^o(k)\ ,\ x(0) = x_0 \\ \pi^o(k) &= A'_{\sigma^o(k)}\pi^o(k+1) + q_{\sigma^o(k)}\ ,\ \pi(t_f) = c \\ \sigma^o(k) &= \underset{s}{\operatorname{argmin}}\{\pi^o(k+1)'A_s x^o(k) + q_s x^o(k)\} \end{aligned} \tag{4.37}$$

with the boundary conditions $x^o(0) = x_0$ and $\pi^o(t_f) = c$. Then $\sigma^o(k, x_0)$ is an optimal switching signal relative to x_0.

Proof The optimal switching signal, the corresponding trajectory and the optimal cost functional is denoted as $\sigma^o(k)$, $x^o(k)$ and $J(x_0, x^0, \sigma^0)$ respectively. Letting $u = \sigma(k)$, $q(k, x, u) = q_{\sigma(k)}$, and using the Hamilton-Jacobi-Bellman equation for the discrete case, we have;

$$\bar{V}(x, k) = \min_{u \in U}\{q(k, x, u) + \bar{V}(x(k+1), k+1)\} \tag{4.38}$$

where, denoting the costate vector by $\pi(k)$, the general solution for this system is

$$\bar{V}(x(k),k) = \pi(k)'x(k) \tag{4.39}$$

Using equations (4.34), (4.38), (4.36) and (4.39), we obtain the following system

$$\begin{aligned} x^o(k+1) &= A_{\sigma^o(k)}x^o(k)\ ,\ x(0) = x_0 \\ \pi^o(k) &= A'_{\sigma^o(k)}\pi^o(k+1) + q_{\sigma^o(k)}\ ,\ \pi(t_f) = c \\ \sigma^o(k) &= \underset{s}{\operatorname{argmin}}\{\pi^o(k+1)'A_s x^o(k) + q_s x^o(k)\} \end{aligned} \tag{4.40}$$

∎

Notice that the discrete-time version has the same problem as its continuous version. The state equations must be iterated forward whereas the co-state equation must be iterated backward, both according to the coupling condition given by the switching rule. In addition, σ depends on $\pi(k+1)$ which makes the solution more difficult. As a result, the problem is a two point boundary value problem, and can not be solved using regular techniques. For this case, we shall use dynamic programming techniques to solve numerically [80]. The discrete-time version results in a recursive equation, easily programmed for optimization. To this end, given the initial condition $x(0)$ the optimal control problem turns out to be

$$\min_{i_{t_f}, i_{t_f-1}, \ldots, i_1} \ c'\ A_{i_{t_f}}\ A_{i_{t_f-1}}\ \ldots\ A_{i_1}x(0)$$

Let us recursively define the sequence of matrices

$$\begin{aligned} \Omega_0 &= c \\ \Omega_1 &= [A'_1\Omega_0\ A'_2\Omega_0\ \ldots\ A'_N\Omega_0] = [A'_1c\ A'_2c\ \ldots\ A'_Nc] \\ &\vdots \\ \Omega_{k+1} &= [A'_1\Omega_k\ A'_2\Omega_k\ \ldots\ A'_N\Omega_k] \end{aligned}$$

Then we have that $\bar{V}(x,0) = \min_i \Omega'_{t_f,i}x$, where $\Omega_{t_f,i}$ is the ith column of Ω_{t_f} and, in general

$$\bar{V}(x,k) = \min_i \Omega'_{t_f-k,i}x(k) \tag{4.41}$$

At each step of the evolution the feedback strategy can be computed as

$$u(x(k)) = \underset{i}{\operatorname{argmin}}\, \Omega'_{t_f-k,i}x(k)$$

namely selecting the smallest component of the vector $\Omega'_{t_f-k}x(k)$.

The implementation of the strategy requires storing the columns of $\Omega'_{T-k}x(k)$. These number columns would be $1+N+N^2+N^3+\cdots+N^{t_f}$. This exponential growth could be too computationally demanding. Bellman called this difficulty as "curse of dimensionality", for high-dimensional systems the number of high speed storage locations become prohibitive. In general, many of the columns of the matrices Ω_k may be redundant and can be removed. This can be done by applying established dynamic programming methods as follows, see [92] for details.

4.6.1 Algorithm 1: Reverse Time Solution

Given $\Omega_{k,i}$ solve the Linear Programming (LP) problem

$$\mu_{k,i} = \min_{x:\ \Omega'_{k,\bar{i}}\ x\ \geq \bar{1}} \Omega'_{k,i}x \tag{4.42}$$

where $\bar{1} = [1\ 1\ \ldots\ 1]'$ and $\Omega_{k,\bar{i}}$ the matrix obtained from Ω_k by deleting the $i-th$ column. Then if $\mu_{k,i} \geq 1$ the column $\Omega_{k,i}$ is redundant (and it should be eliminated from Ω_k). This means that for each Ω_k we can generate a "cleaned" version $\widehat{\Omega}_k$ of Ω_k in which all the redundant columns are removed. We point out that this elimination can be done while constructing the matrices Ω_k. Indeed any redundant column of Ω_k necessarily produces only redundant columns in Ω_{k-1}. Then the procedure for the generation of a reduced representation $\Omega_k^{(1)}$ is achieved by performing the procedure described above as follows

Algorithm

i. For a finite step number t_f, suppose we know the initial condition for the state x_0 and the final costate condition $\pi(t_f) = c$

ii. Define $\Omega_{t_f}^{(1)} = c$ and set $k = t_f$

iii. Compute the matrix

$$\widehat{\Omega}_k = [A'_1\Omega_{k-1}^{(1)}\ A'_2\Omega_{k-1}^{(1)}\ \ldots\ A'_N\Omega_{k-1}^{(1)}]$$

iv. For each column i of $\widehat{\Omega}_k$
   i) Solve the LP (4.42) with Ω_k set to $\widehat{\Omega}_k$
   ii) If $\mu_{k,i} \geq 1$ then delete column i from $\widehat{\Omega}_k$

v. After examining all the columns, we have a reduced $\widehat{\Omega}_k$, set $\Omega_k^{(1)} = \widehat{\Omega}_k$, set $k = k-1$.

vi. If $k \geq 0$ return to (iii), otherwise continue

vii. The optimal sequence will be given by,

$$\sigma(k) = \text{argmin}_i \, \Omega'^{(1)}_{k,i} x_0$$

■

Therefore, although the exact solution in general is of exponential complexity, it may be computationally tractable for problems of reasonable dimension in terms of horizon and number of matrices. One way to further reduce the computational burden is to accompany the above algorithm (backward iteration) with its dual version (forward iteration).

Remark 4.4 *A dual version of the above algorithm, may be constructed by taking the forward iterations*

$$\begin{aligned} \Theta^{(1)}_0 &= x(0) \\ \widehat{\Theta}^{(1)}_{k+1} &= [A_1\Theta^{(1)}_k \; A_2\Theta^{(1)}_k \; \ldots \; A_N\Theta^{(1)}_k] \end{aligned}$$

Then we have that the optimal feedback strategy can be computed as

$$\sigma(k) = \underset{i}{\text{argmin}} \, \Theta'_{N-k,i} c$$

so that one can solve the LP problem

$$\nu_{k,i} = \min_{\pi:\ \Theta'_{k,\bar{i}}\ \pi\ \geq \bar{1}} \Theta'_{k,i}\pi$$

where $\Theta_{k,\bar{i}}$ is the matrix obtained from Θ_k by deleting the $i-th$ column. In this case, if $\nu_{k,i} \geq 1$, then column i of Θ_k is redundant and may be removed.

Remark 4.5 *For a given initial state x_0 and final cost vector c, we can combine both the reverse and forward time solutions to, a midpoint (e.g. $t_f/2$) and finding $\min_{i,j} \Omega'^{(1)}_{t_f/2,i}\Theta^{(1)}_{t_f/2,j}$.*

4.6.2 Algorithm 2: Box Constraint Algorithm

The Algorithm 1 removes columns that are redundant for any x in R^n_+. This can be improved if we derive tighter bounds on $x(k)$ which apply independent of the switching sequence. If $A_{LB} \preceq A_i \preceq A_{UB}$ for all i, where bounds can be chosen as $A_{LB} = \min A_i$ and $A_{UB} = \max A_i$, then it must be true that

$$A^k_{LB}x_0 \leq x(k) \leq A^k_{UB}x_0 \tag{4.43}$$

We can therefore replace (4.42) with the test:

$$\mu_{k,i} = \min_{x,\alpha:\ \alpha\geq 0,\ \Omega_{k,\bar{i}}\ x\geq\alpha\bar{1},\ \beta_k} \Omega'_{k,i}x - \alpha \tag{4.44}$$

where β_k represents the inequality (4.43). If $\mu_{k,i} \geq 0$ then $\Omega_{k,i}$ is redundant.

4.6.3 Algorithm 3: Joint Forward/Backward Box Constraint Algorithm

Using a box constraint the search space for Algorithm 1 is reduced. We can apply Remark 4.5 in order to further improve the last algorithm. Instead of solving $t_f/2$ steps forwards and then $t_f/2$ steps backwards and then combining sequences to get the optimal, we can solve backwards-forwards step by step in order to make a tighter box constraint as follows:

Algorithm

i. Initialize $\Omega^{(3)}_{t_f} = c$ and $\Theta^{(3)}_0 = x_0$, $s = 1$
one step backward

ii. Find

$$\widehat{\Omega}^{(3)}_{t_f-s} = [A'_1\Omega^{(3)}_{t_f-s+1}\ A'_2\Omega^{(3)}_{t_f-s+1}\ \ldots\ A'_N\Omega^{(3)}_{t_f-s+1}]$$

iii. For every ℓ solve the LP given in (4.44) using the next tighter box constrained:

$$A^{t_f-2s+1}_{LB}x_{LB,s-1} \leq x_{t_f-2s+1} \leq A^{t_f-2s+1}_{UB}x_{UB,s-1}$$

where $x_{LB,s-1} = \min_\ell \Theta_{s-1,\ell}$ and $x_{UB,s-1} = \max_\ell \Theta_{s-1,\ell}$

iv. Delete column $\widehat{\Omega}_{t_f-s,\ell}$ if $\mu_{t_f-s,\ell} \geq \alpha$

v. After examining all the columns, set $\Omega^{(3)}_{t_f-s} = \widehat{\Omega}^{(3)}_{t_f-s}$
one step forward

vi. Find

$$\widehat{\Theta}^{(3)}_s = [A_1\Theta^{(3)}_{s-1}\ A_2\Theta^{(3)}_{s-1}\ \ldots\ A_N\Theta^{(3)}_{s-1}]$$

vii. For every ℓ, remove the column $\Theta'_{s,\ell}$ and solve the LP given in (4.44) using the tighter box constrained:

$$A'^{t_f-2s}_{LB}\pi_{LB,t_f-s} \leq \pi_s \leq A'^{t_f-2s}_{UB}\pi_{UB,t_f-s}$$

where $\pi_{LB,t_f-s} = \min_\ell \Omega_{t_f-s,\ell}$ and $\pi_{UB,t_f-s} = \max_\ell \Omega_{t_f-s,\ell}$.

viii. Delete column $\Theta_{s,\ell}$ if $\mu_{s,\ell} \geq \alpha$

ix. After examining all the columns, set $\Theta_s^{(3)} = \widehat{\Theta}_s^{(3)}$

x. Increment s. If $s \leq t_f/2$ return to (ii). Otherwise continue

xi. Find the optimal sequence from $\min_{i,j} \Omega'^{(3)}_{t_f/2,i} \Theta^{(3)}_{t_f/2,j}$

■

4.6.4 Numerical results for discrete-time optimal control

Using the parameter values presented in Table 3.2, we compute the optimal switching rule in order to minimize the total viral load concentration at the end of the treatment for the three different scenarios.

Table 4.1: Total viral load at the end of treatment using model (3.30)

Scenario	Monotherapy	Switched on failure	SWATCH	Optimal
1	1.3692×10^4	344.25	45.35	45.35
2	3.7116×10^4	919.29	60.59	57.55
3	3.8725×10^4	1.2437×10^4	1045.27	55.56

Notice in Table 4.1, that there is a significant difference in clinical recommendation treatments and the proactive switching. The SWATCH strategy shows very low levels in viral load compare with the usual recommendation switch on failure, this is because we constantly affect the two intermediate genotypes. However, the SWATCH treatment could fail when the regimens do not affect the highly resistant genotype with the same intensity. Then, it would be important to use the treatment that impacts the most the highly resistant genotype for a longer period of time. Using an optimal control approach, the viral load is decreased to undetectable levels (≤ 50 copies/ml) for the three scenarios, and it can be seen that periodic switching might not be optimal as shown in Fig.4.4.

Computational Resources

Simulation results exhibit the importance of proactive switching at the right moment in order to maintain viral load under detectable values. Nonetheless, computational time is a serious drawback to obtain optimal switching trajectories. One possible numerical solution is a "brute force" approach which analyzes all possible combinations for therapy 1 and 2 with decision time $\tau = t_d$ for a time period $t_f = 336$ days, that is, we evaluate $2^{\frac{t_f}{\tau_d}} = 2^{12}$ possible treatment combinations. To examine long period simulations, it is necessary to find faster algorithms. In Table 4.2 we test different

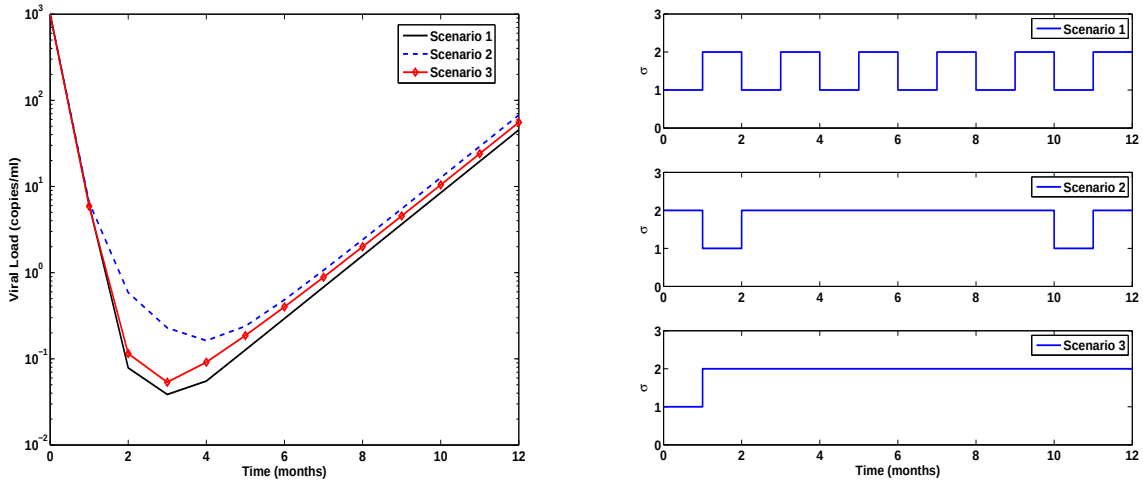

(a) Total viral load

(b) Switching rule

Fig. 4.4: Optimal switching treatment for model (3.30)

algorithms for 12 decisions; it can be seen that "brute force" is extremely slow for this period of simulation, this is because we analyze 4096 columns. Using algorithm 1 we may get a faster simulation, removing redundant columns. At the end of the optimization 11 columns remain with a reduction of 99.7% columns with respect to "brute force", and computational time is reduced dramatically. Using the box constrained algorithm this problem can be solved in less time.

Table 4.2: Computational resources

Method	Brute Force	Algorithm 1	Box Constraint
Time (sec)	555	4.44	3.88
Columns	4096	11	1

Starting from initial and end points, Remark 4.5 suggests a reduction of computational time compared to the previous algorithms, that is for every step in both directions we keep less columns than in a single direction algorithm. Table 4.3 shows that the box constraint algorithm using Remark 4.5 has a lower computation time than algorithm 1. Moreover, we acquire further improvements using algorithm 3; the process of removing columns is more effective than other algorithms due to the tighter box constraint.

These numerical examples reveal that we could compute long treatment sequences in short periods of time. For instance, using algorithm 3 the optimal trajectory for a treatment with 60 decisions is solved in 5 minutes, where 9 cleaned columns are kept at the end of examination. Using "brute force" we would evaluate 2^{60}, something that is not possible using a standard computer. However, there is no guarantee that the proposed algorithms avoid exponential explosion in CPU time. Moreover,

Table 4.3: Computational resources using Remark 4.5

Method	Algorithm 1	Box Constraint	Algorithm 3
Time (sec)	3.3	2.3	1.74
Forward Columns	7	3	1
Backward Columns	10	6	2

for a small number of decisions "brute force" algorithm can overperform computational times of the proposed algorithms.

In the proposed algorithms, we solve a LP problem to delete redundant columns, for implementation we use the MATLAB toolbox "linprog". For long simulation periods "linprog" tool alerted us to some numerical issues. These warnings can arise to different reasons, two of which are explained next.

Firstly, the unstable nature of the high resistant genotype in HIV problem cause an explosion in some states of the system. That is, if we consider long period simulations, the columns of the matrix Ω start to grow exponentially, for example 10^{28}. Then, when the constraint (4.42) is checked, "linprog" algorithm is searching for very small values i.e. 10^{-24}. The default tolerance for "linprog" is 10^{-6}. Therefore, this can cause numerical difficulties in the algorithm. This problem might be solved normalizing the matrix Ω in every step. However, this solution not always works, because one of the states is always stable while other is always unstable, then in one column different time scales can be presented. Therefore, matrix normalization might not be helpful for some problems.

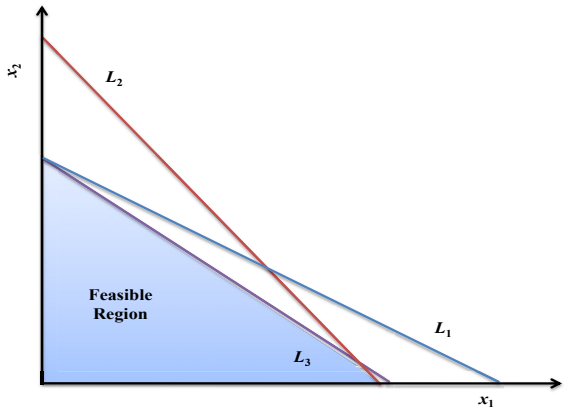

Fig. 4.5: Feasible region in the shape of a simple polygon.

Secondly, linear programming problems are solved by constructing a feasible solution at a vertex of the polytope and then walking along a path on the edges of the polytope to vertices with non-decreasing values of the objective function until an optimum is reached. However, constraints can

be overly stringent and cause difficulties to the solution. If we consider an optimization problem between two variables, it is observed in Fig.4.5 the feasible region of the problem. But we may notice that the intersection between L_1 and L_3 is not obvious. These problems are presented in the proposed algorithms, where for some examples the intersection between lines was difficult to observe because time scales were very small (i.e., 10^{-12}). Moreover, "linprog" could have difficulties when constraints are tight, for instance if lines L_1 and L_2 are almost parallel. An easy way to clean columns is examining element by element of the columns, if all elements of one column are bigger than other column, then it can be deleted. This might help in some examples to reduced the number of warnings and can be combined with the proposed algorithms to make them faster.

Control Robustness

In order to check the robustness of the suggested treatments, we perform several simulations. Considering the symmetric case, we propose perturbations in the proliferation rates using a Gaussian distribution. Then we compute the optimal switching considering we would have the real model and measurements.

Table 4.4: Optimal control robustness

Case	Optimal	Feedback with estimated π	Non exact model
1	45.35	45.35	45.35
2	7101.28	7116.53	7430.21
3	1.22	2.13	3.43
4	3514.61	3514.61	12704.38
5	533.85	840.75	2555.53
6	5.39×10^{-5}	6.085×10^{-4}	$2.30\text{e}\times10^{-3}$
7	0.24	0.29	0.58
8	1.24×10^{7}	1.24×10^{7}	4.9×10^{9}
9	52.31	84.66	283.92
10	0.11	0.13	0.64
11	0.12	0.19	2.68
12	1.84	2.30	217.40
13	4.78	8.81	16.21
14	0.51	1.79	16.22
15	0.41	0.64	37.66
16	2075.24	2075.24	9315.32
17	0.0043	0.0049	0.0061
18	6.63	19.73	2605.47
19	191.40	208.74	5537.86
20	0.0022	0.0052	0.0049

Table 4.4 presents 20 different perturbed systems, the second column displays the optimal control applied to the perturbed system, which around 65% of the cases mantain the viral load under

undetectable values. There are two cases with very high viral level, this is because the perturbations reduce the treatment efficiency for the highly resistant genotype. In the third column, we used a feedback controller using as a estimation of π the computed one for the case 1. It can be unveiled that almost all cases, the performance is very similar or equal to the optimal performance, then this reveals us the insight that optimal trajectories are robust to these perturbations. For the last test, we consider as the best strategy the periodic switching (computing from case 1), which is changing the regimen once a month. We can notice that in 70% of the cases, the periodic switching performance is not too far from the optimal. Nonetheless, it has to be remarked that there are some cases where the viral load is very high, that is when treatments do not affect the highly resistant mutant with the same intensity, then it could be suggested to avoid periodic treatment in those situations.

4.7 Concluding Remarks

In this chapter we have considered the optimal control problem of positive switched linear systems. We have focused specifically on the fixed-horizon problem. The major conclusions made in the chapter are listed below.

- Using a generalized solution of the HJE, for continuous and discrete-time we have obtained the optimal solution. We pointed out that the solution results in a two point boundary value problem, and it can not be solved using regular integration techniques.
- Under certain symmetry assumptions in the proliferation rate and the mutation graph, we presented the main result of this chapter, which reveals that the optimal control on this class of positive switched systems is given by the Filippov trajectory along the plane $x_2 = x_3$.
- Necessary conditions for optimality in a more general permutation problem were introduced, the solution also remains in a sliding surface. Such behavior suggests that in the absence of other practical constraints switching rapidly between therapies may be desirable.
- The numerical solution of the optimal control problem could result in an exponential growth in computational demands. We derived different algorithms to try to avoid the "curse of dimensionality". These strategies were based on a LP problem in order to remove redundant columns. Using forward and backward approaches, these algorithms relieve computational time issues.
- A robustness study demonstrated that given an optimal control history, small perturbations in the control should have vanishing effect on the cost. More precisely, necessary conditions usually indicate that the cost function's linear sensitivity to control variation about the optimum is zero.
- For the clinical point of view, we concluded that it is very important to change therapy in the right moment in order to impact the appearance of high resistant genotypes. Switched on failure is a conservative treatment, which could be improved using a proactive switching as was previously propose in the SWATCH treatment. Robustness tests showed that periodic treatment has good performance in most cases examined. Notwithstanding, it could be possible that certain number of patients were not eligible for the proactive switching. This is when high resistant genotype is affected with different intensity by distinct treatments. In those cases, a specific regimen should be designed for the patient.

Chapter 5

Suboptimal Control Strategies

In this chapter we provide a brief review of results on the stability of switched systems that are available in the literature. In addition we present results for state-feedback stabilization of autonomous positive switched systems through piecewise co-positive Lyapunov functions in both continuous and discrete time. The action of this control need not be optimal but provides a solution which guarantees a level of performance. For comparison purposes, we examine the efficacy of model predictive control applied to the HIV treatment regimen problem. Using control strategies based on a switched linear system we conclude the chapter with the application of these techniques to a nonlinear mutation model.

5.1 Introductory remarks

Switched systems present interesting theoretical challenges and are important in many real-world problems [83]. Stability is a fundamental requirement for all control systems and switched systems are no exception. Furthermore, stability issues become very important in switched systems; for instance, switching between individually stable subsystems may cause instability and conversely, switching between unstable subsystems may yield a stable switched system. This kind of phenomena justifies the recent interest in the area of switched systems. In particular, stability analysis of continuous time switched linear systems has been addressed by different authors [93], [94], [95], [96], [97]. Moreover there have been advances in discrete-time, for example [98], [99], [100] and [101] provide excellent overviews. Stabilization of positive systems has been studied since it is problematic to fulfill the positivity constraint on the input variables [102], [103] and [104]. A few recent works in switched positive systems [105] and [106] study the stability problem using co-positive Lyapunov functions.

As previously discussed in Chapter 4, the difficulty of determining optimal trajectories for switched systems has been studied by different authors [85], [86], [87] and [88]. Nonetheless, there is no general readily computable solution for the optimal control. In the previous chapter, we dealt with the optimal control problem for a particular class of positive switched systems, we unveiled the difficulties in either analytical or numerical solutions to the problem.

Consequently, we now consider other control options which might not exhibit optimal performance, but may achieve reasonable results close to the optimal one. To this end, we introduce a guaranteed cost algorithm associated with the optimal control problem in continuous and discrete-time, that was proposed for a general class of switched systems in infinite-time horizon by [107]. However, because of the biological importance of designing a finite number of decisions, we study the finite-time horizon guaranteed cost control. In addition, we explore the well known Model Predictive Control, which appears to be suitable for a suboptimal application to the biomedical area, due to its robustness to disturbances, model uncertainties and the capability of handling constraints.

5.2 Continuous-time Guaranteed cost control

In this section, we extend the stabilization work proposed by [107], which provided a result on state-feedback stabilization of autonomous linear positive switched systems through piecewise linear co-positive Lyapunov functions. This was accompanied by a side result on the existence of a switching law which can guarantee an upper bound to the achievable performance over an infinite horizon. However, for the mitigation of the viral escape problem discussed in the previous chapters, we noted that the system is not stabilizable. Therefore we consider is necessary to follow finite time horizon strategies. For this purpose, let us take the simplex in the form

$$\Lambda := \left\{ \lambda \in R^N : \sum_{i=1}^{N} \lambda_i = 1,\ \lambda_i \geq 0 \right\} \tag{5.1}$$

which allows to introduce the piecewise linear Lyapunov function:

$$v(x) := \min_{i=1,\ldots,N} \alpha_i' x = \min_{\lambda \in \Lambda} \left(\sum_{i=1}^{N} \lambda_i \alpha_i' x \right) \tag{5.2}$$

The Lyapunov function in (5.2) is not differentiable everywhere, then we need to use the upper Dini derivative expressed by D^+ [82]. In particular, let us define the set $I(x) = \{i : v(x) = \alpha_i' x\}$. Then $v(x)$ fails to be differentiable precisely for those $x \in R_+^n$ such that $I(x)$ is composed of more than one element, that is in the conjunction points of the individual Lyapunov functions $\alpha_i' x$. Now we denote by $\mathscr{M}$ the subclass of Metzler matrices with zero column sum, that is all matrices $P \in R^{N \times N}$

with elements p_{ji}, such that

$$p_{ji} \geq 0 \ \forall j \neq i, \quad \sum_{j=1}^{N} p_{ji} = 0 \ \forall i. \tag{5.3}$$

As a consequence, any $P \in \mathscr{M}$ has an eigenvalue at zero since $c'P = 0$, where $c' = [1 \cdots 1]$. We are now ready to formulate the main result on the guaranteed cost control of the system (4.1).

Theorem 5.1 *Finite horizon Guaranteed Cost*
Consider the linear positive switched system (4.1) and let the nonnegative vectors q_i be given. Moreover, take any $P \in \mathscr{M}$, and let $\{\alpha_1(t), \ldots, \alpha_N(t)\}$, $\alpha_i(t) : [0, t_f] \to R_+^n$ be any positive solutions of the coupled differential inequalities

$$\dot{\alpha}_i + A_i'\alpha_i + \sum_{j=1}^{N} p_{ji}\alpha_j + q_i \preceq 0, \quad i = 1, \ldots, N \tag{5.4}$$

with final condition $\alpha_i(t_f) = c$, $\forall i$. Then, the switching rule

$$\sigma(x(t)) = \arg \min_{i=1,\ldots,N} \alpha_i'(t)x(t) \tag{5.5}$$

is such that

$$\int_0^{t_f} q_{\sigma(\tau)}'x(t)dt + x(t_f)'c \leq \min_{i=1,\ldots,N} \alpha_i'(0)x_0 \tag{5.6}$$

Proof Consider the Lyapunov function

$$v(x,t) = \min_{\ell=1,\ldots,N} \alpha_\ell'(t)x(t)$$

and let $i(t) = \arg\min_l \alpha_l'(t)x(t)$. Then,

$$\begin{aligned} D^+(v(x),t) &= \min_k (\dot{\alpha}_k'(t) + \alpha_k'(t)A_i x) \leq \dot{\alpha}_i' + \alpha_i'(t)A_i x \\ &\leq -p_{ii}\alpha_i'(t)x - \sum_{j\neq i} p_{ji}\alpha_j'(t)x - q_i'x \\ &\leq -p_{ii}\alpha_i'(t)x - \sum_{j\neq i} p_{ji}\alpha_i'(t)x - q_i'x = -q_i'x \end{aligned}$$

Hence, for all $\sigma(t)$,

$$D^+(v(x)) \leq -q_{\sigma(t)}'x(t)$$

which, after integration, gives

$$\begin{aligned} v(x(t_f)) - v(0) &= \int_0^{t_f} D^+v(x(\tau))d\tau \\ &\leq -\int_0^{t_f} q_{\sigma(\tau)}'x(\tau)d\tau \end{aligned}$$

Therefore,

$$\int_0^{t_f} q'_{\sigma(\tau)} x(\tau) d\tau + c' x(t_f) \leq v(0) = \min_{i=1,\ldots,N} \alpha_i'(0) x_0$$

This concludes the proof. ∎

Notice that (5.4) requires the preliminary choice of the parameters p_{ij}. In particular, the search for p_{ij} and α_i that satisfy Theorem 5.1 is a bilinear matrix inequality. We can, at the cost of some conservatism in the upper bound, reduce these parameters to a single one, say ζ, so allowing an easy search for the best ζ as far as the upper bound is concerned.

Corollary 5.1 *Let $q \in R_+^n$ and $c \in R_+^n$ be given, and let the positive vectors $\{\alpha_1, \ldots, \alpha_N\}$, $\alpha_i \in R_+^n$ satisfy for some $\zeta > 0$ the modified coupled co-positive Lyapunov differential inequalities*

$$\dot{\alpha}_i + A_i' \alpha_i + \zeta(\alpha_j - \alpha_i) + q_i \preceq 0 \qquad i \neq j = 1, \ldots, N. \tag{5.7}$$

with final condition $\alpha_i(t_f) = c$, $\forall\, i$. Then the state-switching control given by (5.5) is such that

$$\int_0^{t_f} q'_{\sigma(\tau)} x(t) dt + c' x(t) \leq \min_{i=1,\ldots,N} \alpha_i'(0) x_0 \tag{5.8}$$

Proof Consider any matrix p_{ij} chosen such that $p_{ii} = -\zeta$, therefore

$$\zeta^{-1} \sum_{j \neq i = 1}^{N} p_{ji} = 1 \qquad \forall i = 1, \ldots, N \tag{5.9}$$

Using (5.9), equations (5.4) and (5.7) are equivalent, hence the upper bound of Theorem 5.1 holds. ∎

The result shown in Corolary 5.8 is relevant to the problem of mitigation of HIV escape, in the sense that the switching rule (5.5) may be easy to compute. That is, we consider (5.7) as an equation, and we solve for α_i. The performance might not be optimal but we can know in advance an upper bound on the cost function (5.8). This is very helpful because when a treatment is computed using (5.5), knowledge of a bound on the worst case scenario in the total viral load can be obtained.

5.3 Discrete-time guaranteed cost control

The biological problem of mitigating HIV mutation was described in continuous time. However, in practice, measurements can only reasonably be made infrequently. For this purpose, we consider the discrete time switched system (4.34), clearly, (4.35) constrains $A_{\sigma(k)}$ to jump among the N

vertices of the matrix polytope $A_1, ..., A_N$. We assume that the full state vector is available and the control law is a state feedback

$$\sigma(k) = u(x(k)) \tag{5.10}$$

The control will be a function $u(\bullet)$: $R^N \to \{1, ..., N\}$. Consider the simplex (5.1) and let us introduce the following piecewise co-positive Lyapunov function:

$$\upsilon(x(k)) := \min_{i=1,...N} \alpha_i' x(k) = \min_{\lambda \in \Lambda} \sum_{i=1}^{N} \lambda_i \alpha_i' x(k) \tag{5.11}$$

In a similar vein to continuous time, we need to find a class of matrices $\mathscr{M}$, consisting of all matrices $P \in R^{N \times N}$ with elements p_{ij} such that inequality (5.3) is satisfied. Consequently we shall provide a sufficient condition for the existence of a switching rule that stabilizes the discrete-time system (4.34).

Theorem 5.2 *Stability Theorem in Discrete-time*
Assume that there exist a set of positive vectors $\alpha_1, ..., \alpha_N$, $\alpha_i \in R_+^n$, and $p \in \mathscr{M}$, satisfying the coupled co-positive Lyapunov inequalities:

$$(A_i - I)' \alpha_i + \sum_{j=1}^{N} p_{ji} \alpha_j \prec 0 \tag{5.12}$$

The state-switching control with

$$u(x(k)) = \operatorname*{argmin}_{i=1,...,N} \alpha_i' x(k) \tag{5.13}$$

makes the equilibrium solution $x = 0$ of the system (4.34) globally asymptotically stable (in the positive orthant), with Lyapunov function $\upsilon(x(k))$ given by (5.11).

Proof Recalling that (5.3) is valid for $P \in \mathscr{M}$ and that $\alpha_j' x(k) \geq \alpha_{\sigma(k)}' x(k)$ for all $j = i = 1, ..., N$, we have

$$\begin{aligned} \Delta\upsilon(k) = \upsilon(x(k+1)) - \upsilon(x(k)) &= \min_{j=1,...,N} \{\alpha_j' x(k+1)\} - \min_{j=1,...,N} \{\alpha_j' x(k)\} \\ &= \min_{j=1,...,N} \{\alpha_j' A_{\sigma(k)} x(k)\} - \min_{j=1,...,N} \{\alpha_j' x(k)\} \end{aligned}$$

By definition of $\sigma(k)$ we have $\min_{j=1,...,N} \{\alpha_j' x(k)\} = \alpha_{\sigma(k)}' x(k)$ and therefore

$$\begin{aligned} \Delta\upsilon(k) \quad &\leq \alpha_{\sigma(k)}' A_{\sigma(k)} x(k) - \alpha_{\sigma(k)}' x(k) \\ &\leq \alpha_{\sigma(k)}' (A_{\sigma(k)} - I) x(k) \end{aligned}$$

From (5.12), with $x(k) \neq 0$, it follows

$$\begin{aligned}
\Delta v(k) \qquad &< -\sum_{j=1}^{N} p_{j\sigma(k)} \alpha_j' x(k) \\
&= -p_{\sigma(k)\sigma(k)} \alpha_{\sigma(k)}' x(k) - \sum_{j \neq \sigma(k)}^{N} p_{j\sigma(k)} \alpha_j' x(k) \\
&\leq -p_{\sigma(k)\sigma(k)} \alpha_{\sigma(k)}' x(k) - \sum_{j \neq \sigma(k)}^{N} p_{j\sigma(k)} \alpha_{\sigma(k)}' x(k) \\
&\leq -\sum_{j=1}^{N} p_{j\sigma(k)} \alpha_{\sigma(k)}' x(k) \\
&= 0
\end{aligned}$$

which proves the proposed theorem.

∎

In a similar vein, it is possible to assure an upper bound on an optimal cost function. Let q_i be positive vectors, $i = 1, 2, \cdots, N$, and consider the cost function;

$$J = \sum_{k=0}^{\infty} q_{\sigma(k)}' x(k) \tag{5.14}$$

then, the following result provides an upper bound on the optimal value J^o of J.

Lemma 5.1 *Upper Bound for Infinite Horizon*
Let $q_i \in R_+^n$ be given. Assume that there exist a set of positive vectors $\{\alpha_1, ...\alpha_N\}$, $\alpha_i \in R_+^n$ and $p \in \mathscr{M}$, satisfying the coupled co-positive Lyapunov inequalities;

$$(A_i - I)' \alpha_i + \sum_{j=1}^{N} p_{ji} \alpha_j + q_i \prec 0 \ , \ \forall i \tag{5.15}$$

The state-switching control given by (5.13) makes the equilibrium solution $x = 0$ of the system (4.34) globally asymptotically stable and

$$J^o \leq \sum_{k=0}^{\infty} q_{\sigma(k)}' x(k) \leq \min_{i=1,...,N} \alpha_i' x_0 \tag{5.16}$$

Proof If (5.15) holds, then (5.12) holds as well, then we can say that the equilibrium point $x = 0$ for system (4.34) is globally asymptotically stable. In addition, by mimicking the proof of Theorem

5.2, we can prove that

$$\begin{aligned}\Delta v(x(k)) &= v(x(k+1)) - v(x(k)) \\ &\leq -q'_{\sigma(k)}x(k)\end{aligned}$$

Hence

$$\sum_{k=0}^{\infty}\Delta v(x(k)) \leq -\sum_{k=0}^{\infty}q'_{\sigma(k)}x(k)$$

$$\sum_{k=0}^{\infty}q'_{\sigma(k)}x(k) \leq v(x(0)) - v(x(\infty))$$

therefore

$$\sum_{k=0}^{\infty}q'_{\sigma(k)}x(k) \leq \min_{i=1,\ldots,N}\alpha'_i x_0$$

∎

Remark 5.1 *For fixed p_{ji} in order to improve the upper bound provided by Lemma 5.1, one can minimize* $\min_i \alpha'_i x_0$ *over all possible solutions of the linear inequalities* (5.15)*.*

Coupled co-positive Lyapunov functions can also be used to compute a lower bound on the optimal cost.

Lemma 5.2 *Lower Bound for Infinite Horizon*
Assume that there exist a set of positive vectors $\alpha_1, ..., \alpha_N$, $\alpha_i \in R^n_+$ and $p \in \mathscr{M}$, satisfying the coupled co-positive inequalities:

$$(A_j - I)'\alpha_i + \sum_{m=1}^{N} p_{mi}\alpha_m + q_i \succeq 0\ ,\ \forall i, j \tag{5.17}$$

Then, for any state trajectory such that $x(k) \to 0$,

$$\sum_{k=0}^{\infty}q'_{\sigma(k)}x(k) \succeq \max_{i=1,\ldots,N}\alpha'_i x_0 \tag{5.18}$$

Proof Let

$$v(x(k)) = \max_i \alpha'_i x(k) \tag{5.19}$$

then

$$\begin{aligned}
\upsilon(x(k+1)) &= \max_{i=1,\dots,N}\{\alpha_i' x(k+1)\} \\
&= \max_{i=1,\dots,N}\{\alpha_i' A_{\sigma(k)} x(k)\} \\
&\geq \left(\alpha'_{\sigma(k)} - \sum_{m=1}^{N} p_{m\sigma(k)}\alpha'_m\right) x(k) - q'_{\sigma(k)} x(k) \\
&\geq \left(\alpha'_{\sigma(k)} - p_{\sigma(k)\sigma(k)}\alpha'_{\sigma(k)} - \sum_{m\neq\sigma(k)}^{N} p_{m\sigma(k)}\alpha'_m\right) x(k) - q'_{\sigma(k)} x(k) \\
&\geq \left(\alpha'_{\sigma(k)} - p_{\sigma(k)\sigma(k)}\alpha'_{\sigma(k)} - \sum_{m\neq\sigma(k)}^{N} p_{m\sigma(k)}\alpha'_{\sigma(k)}\right) x(k) - q'_{\sigma(k)} x(k) \\
&\geq \alpha'_{\sigma(k)} x(k) - q'_{\sigma(k)} x(k)
\end{aligned}$$

which implies

$$\upsilon(x(k+1)) - \upsilon(x(k)) \geq -q'_{\sigma(k)} x(k)$$

so that

$$\sum_{k=0}^{\infty} q'_{\sigma(k)} x(k) \geq \max_{i=1,\dots,N} \alpha_i' x_0$$

∎

Remark 5.2 *Notice that inequalities (5.12) are not LMI, since the unknown parameters p_{ji} multiply the unknowns vectors α_j. If all matrices A_i are Schur matrices, then a possible choice is $p_{ji} = 0$, $i, j = 1, 2, \cdots, N$, so that inequalities (5.12) are satisfied by $\alpha_i = (I - A_i)^{-1}\bar{q}_i$, where $\bar{q}_i \succ q_i$.*

Remark 5.3 *Lemma 5.2 may be used to guarantee an upper bound to the finite-time optimal cost*

$$J_{FT} = c' x(t_f) \tag{5.20}$$

where t_f is the finite time and $c \succeq 0$ is a weight on the final state $x(t_f)$. Assume that inequalities (5.12) *are feasible. Hence, thanks to linearity of (5.12) in α, it is possible to find $\alpha_i \succeq 0$ such that* (5.12) *are satisfied along with the additional constraint $c \preceq \alpha_i$, $\forall i$. Then $c'x(t_f) \leq \min_i \alpha_i' x(t_f) = \upsilon(x(t_f)) \leq \upsilon(x(0)) = \min_i \alpha_i' x(0)$.*

The theorems and lemmas presented above refer to a cost function over an infinite time horizon. However, it is possible to slightly modify the relevant inequalities to account for finite time horizon functionals. To be precise, consider the system (4.34), the cost function

$$J = c'x(t_f) + \sum_{k=0}^{t_f-1} q'_{\sigma(k)}x(k) \tag{5.21}$$

and the difference equations, for $i = 1, 2, \cdots, N$

$$\alpha_i(k) = A'_i\alpha_i(k+1) + \sum_{j=1}^{N} p_{ji}\alpha_j(k) + q_i, \quad \alpha_i(t_f) = c \tag{5.22}$$

The following result holds.

Theorem 5.3 *Finite-Horizon Guaranteed cost control*
Let $q_i \in R^n_+, i = 1 \dots N$ be given. Let $\{\alpha_1(k), ...\alpha_N(k)\}$, $\alpha_i(k) \in R^n_+$ be a set of nonnegative vectors satisfying (5.22) where $p \in \mathscr{M}$. The state-switching control

$$\sigma(k) = \underset{i=1,\dots,N}{\operatorname{argmin}}\, \alpha'_i(k)x(k) \tag{5.23}$$

is such that

$$c'x(t_f) + \sum_{k=0}^{t_f-1} q'_{\sigma(k)}x(k) \leq \min_{i=1,\dots,N} \alpha'_i(0)x_0 \tag{5.24}$$

Proof Let $v(x(k), k) = \min_i\{x(k)'\alpha_i(k)\}$. Then

$$\begin{aligned}
v(x(k+1), k+1) &= \min_i\{x(k+1)'\alpha_i(k+1)\} = \min_i\{x(k)'A'_{\sigma(k)}\alpha_i(k+1)\} \\
&\leq x(k)'A'_{\sigma(k)}\alpha_{\sigma(k)}(k+1) \\
&\leq v(x(k), k) - x(k)'q_{\sigma(k)} - x(k)'\sum_{r=1}^{N} p_{r\sigma(k)}\alpha_r(k) \\
&\leq v(x(k), k) - x(k)'q_{\sigma(k)} - x(k)'\alpha_{\sigma(k)}(k)\sum_{r=1}^{N} p_{r\sigma(k)} \\
&\leq v(x(k), k) - x(k)'q_{\sigma(k)}
\end{aligned}$$

so that

$$\begin{aligned}
J &= c'x(t_f) + \sum_{k=0}^{t_f-1} q'_{\sigma(k)}x(k) \\
&\leq c'x(t_f) - \sum_{k=0}^{t_f-1} v(x(k+1), k+1) - v(x(k), k) \\
&\leq c'x(t_f) - v(x(t_f), t_f)) + v(x_0, 0) \\
&\leq \min_i\{x'_0\alpha_i(0)\}
\end{aligned}$$

∎

Remark 5.4 *Note that in the infinite horizon case, the conditions* (5.17)*, may be infeasible. However in the finite horizon case,* (5.22)*, the equations are always feasible (for example taking* $p_{ji} = 0$*), and for any fixed* t_f *can be solved by the reversed time difference equation* (5.22)*. If* A_i *are Schur matrices, then in the limit and with* $p_{ji} = 0$*,* $\lim_{t_f \to \infty} \alpha_i(0) = (I - A_i)^{-1} q_i$*.*

Corollary 5.2 *Let* $q \in R_+^n$ *and* $c \in R_+^n$ *be given, and let the positive vectors* $\{\alpha_1, \ldots, \alpha_N\}$*,* $\alpha_i \in R_+^n$ *satisfy for some* $\zeta > 0$ *the modified coupled co-positive Lyapunov difference equations:*

$$\alpha_i(k) = A_i' \alpha_i(k+1) + \zeta(\alpha_j(k) - \alpha_i(k)) + q_i \qquad i \neq j = 1, \ldots, N. \tag{5.25}$$

with final condition $\alpha_i(t_f) = c$*,* $\forall i$*. Then the state-switching control given by (5.23) is such that*

$$c' x(t_f) + \sum_{k=0}^{t_f - 1} q'_{\sigma(k)} x(k) \leq \min_{i=1,\ldots,N} \alpha_i'(0) x_0 \tag{5.26}$$

The proof of Corollary 5.2 is in similar vein as Corollary 5.1. For the numerical solution of (5.25), we consider a fixed ζ.

5.4 Model Predictive Control

More than 25 years ago MPC appeared in industry as an effective algorithm to deal with multivariable constrained control problems. Much progress has been made on feasibility of the on-line optimization, stability and performance for linear systems. A thorough overview of the MPC history can be found in [108]. However, many systems are in general inherently nonlinear and accompanied with the high product specifications in the process industry make non-linear MPC systems a difficult problem.

Model predictive control involves solving an on-line finite horizon open-loop optimal control problem subject to system dynamics and constraints involving states and controls. The essence of MPC is to optimize, over the manipulable inputs, forecasts of process behavior. The forecasting is achieved with a process model, and therefore a good model is required to represent the problem under study. However, models are never perfect, and therefore there will inevitably be some forecasting errors. Feedback can help overcome these effects [109]. A fundamental question about MPC is its robustness to model uncertainty and noise. When we say that a control system is robust we mean that stability is maintained and that the performance specifications are met. Although a lot of research has been conducted to check robustness in linear systems, very little is known about the robust control of linear systems with constraints [108].

MPC is based on measurements obtained at time t. The controller then predicts the future

dynamic behavior of the system over a prediction horizon T_p and computes an open-loop optimal control problem with control horizon T_c, to generate both current and future predicted control signals. A general picture of MPC scheme can be seen in Fig.5.1.

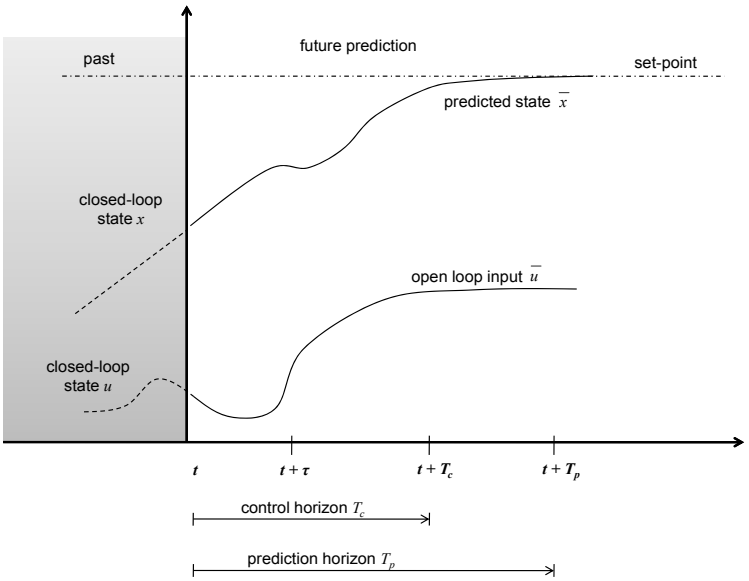

Fig. 5.1: Model Predictive Control strategy

Due to disturbances, measurement noise and model-plant mismatch, the true system behavior is different from the predicted one. To incorporate a feedback mechanism, the first step of the optimal control sequence is implemented. When the next measurement becomes available, at time $t + \tau$, the whole procedure -prediction and optimization- is repeated to find a new input function with the control and prediction horizons moving forward.

It is clear that the shorter the horizon, the less computational time of the on-line optimization problem. Therefore, it is desirable from a computational point of view to implement MPC using short horizons. However, when a finite prediction horizon is used, the actual closed loop input and state trajectories will differ from the predicted open-loop trajectories even if no model plant mismatch and no disturbances are present [113].

Notice that the goal of computing a feedback such that performance objective over infinite horizon of the closed loop is not achieved. In general it is by no means true that a repeated minimization over a finite horizon objective in receding horizon manner leads to an optimal solution for the infinite horizon problem, in fact the two solutions differ significantly if a short horizon is chosen. Moreover, if the predicted and actual trajectories differ, there is no guarantee that the closed-loop system will be stable [114].

MPC has been mainly applied to many problem in the industry. However, because of its good performance this technique has been applied to other areas, for instance aerospace, biology, electronic devices and many others can be found in [113]. Recently, biology problems have been a productive application area for MPC [110], [111] and [112]. Nevertheless, modeling in biology is a difficult task: low-order models are usually too simple to be useful, conversely, high order models are too complex for simulation purposes and have too many unknown parameters requiring identification [112].

In this work, we are interested in the use of MPC techniques to plan treatment applications for HIV. This idea is not new, for example a feedback-based treatment scheduling for HIV patients is summarized in [111]. MPC strategies have been applied to the control of HIV infection, with the final goal of implementing an optimal structured treatment interruptions protocol [112]. Nevertheless, clinicians have been solidly against interruption treatments [5]. Moreover, the models used in these previous approaches do not accurately reflect the interaction between different genotypes and drug treatments, and consequently do not predict the possibility of the appearance of highly resistant genotypes.

5.4.1 Mathematical Formulation of MPC

From the biological nature of HIV infection, the system (4.34) is unstable and in fact not stabilizable. This is because of the existence of a highly resistant genotype that is not affected by any treatment. Therefore, once the highly resistant mutant has "emerged" the population will explode after a period of time. The objective of MPC is to suppress the total viral load as shown in (4.15). In order to distinguish the real system and the system model used to predict the future for the controller, we denote the internal variables in the controller by a bar $(\bar{x}, \bar{\sigma})$, where $x(t) \in \mathcal{X} \subseteq R^n$ and $\sigma(\bullet) \in \mathcal{U} \subseteq R^m$. We can formulate the following model predictive control problem.

Problem 5.1 *Find*

$$\min_{\bar{\sigma}} J(x(t), \bar{\sigma}(\bullet); T_c, T_p),$$

with

$$J(x(t), \bar{\sigma}(\bullet); T_p, T_c) := cx(t + T_p)$$

subject to:

$$\bar{x}(k + h + 1/k) = A_{\bar{\sigma}(k+h/k)}\bar{x}(k + h/k)$$

$$\bar{\sigma}(k + h/k) \in \mathcal{U}, \ \ \forall h \in [0, T_c]$$

$$\bar{x}(k + h/k) \in \mathcal{X}, \ \ \forall h \in [0, T_p]$$

where T_p and T_c are the prediction and the control horizon with $T_c \leq T_p$. The bar denotes internal controller variables, the distinction between the real system and the variables in the controller is necessary since the predicted values, even in the nominal undisturbed case, in generally will not be

the same as the actual close-loop values, since the optimal is recalculated at every sampling instance. For numerical solution, we shall use the following algorithm;

MPC Algorithm

i. Given $x(k)$ at time k, compute the open-loop optimal control $\bar{\sigma}(\bullet)$ for a receding horizon T_p

ii. Apply only the first input of the optimal command sequence to the system

iii. The remaining optimal inputs are disregarded

iv. Collect the new measurement from the system and increment k

v. Continue with point (i) until the final time is reached

■

In this algorithm, T_p has to be chosen in advance. As was previously mentioned, the shorter the horizon, the less costly the solution of the on-line optimization problem. The method to solve the open-loop optimal problem using (4.42) has an exponential growth. Therefore, it is desirable to use short horizons MPC schemes for computational reasons. In general, it is not true that a repeated minimization over a finite horizon objective in a receding horizon manner leads to an optimal solution for the the infinite horizon problem [114]. In fact, both solutions differ significantly if a short horizon is chosen.

5.5 Comparisons for the 4 variant model

First we introduce continuous-time guaranteed cost results. The switching rule presented is computed using (5.5), where $\alpha(t)$ can be obtained from the inequality (5.4), which an easy way to be solve it is considering $p_{ji} = 0$. Fig.5.2 shows the performance of the optimal control for scenario 1. Using a symmetric cost function weighting as $c = [1, 1, 1, 1]'$, an upper bound can be computed, for such control a performance no worse than 2432.07 copies/ml is obtained. However, the final cost for a simulation period of 12 months is 1367.31 copies/ml, this result is exactly the same as the optimal control performance.

Simulation results show that at least in some cases, guaranteed cost control capture's the possible sliding mode behavior of the optimal control law. Indeed, consider a matrix $P \in \mathscr{M}$ and its Frobenius eigenvector β, i.e. such that $P\beta = 0$. It is known that β is a nonnegative vector and it is possible to choose it in such a way that $\sum_{i=1}^{N} \beta_i = 1$. Now, it is easy to see that the solution of the differential equations (5.4) associated with the choice $\gamma\Pi \in \mathscr{M}$ are such that $\lim_{\gamma\to\infty} \alpha_i(t) = \bar{\alpha}(t)$, $\forall i$. In order

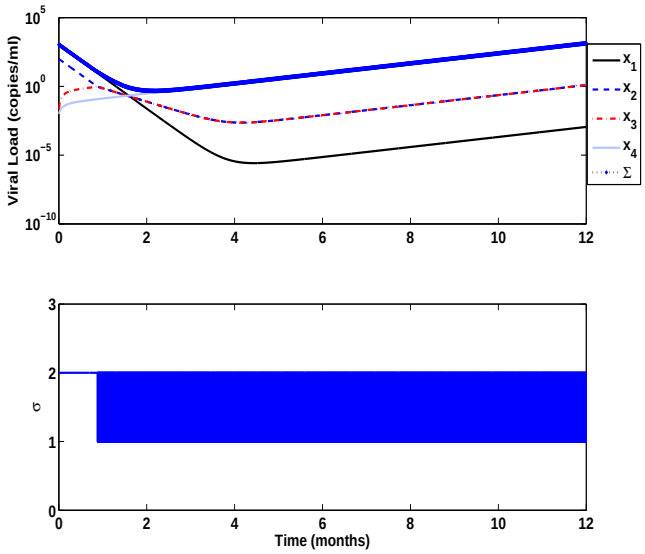

Fig. 5.2: Guaranteed cost control

to characterize the limit function $\bar{\alpha}$, multiply each equation (5.4) by β_i and sum up all of them. Since $\sum_{i=1}^{N} \beta_i p_{ji} = 0$, and $\alpha_i(t) = \bar{\alpha}(t)$, it results:

$$-\dot{\bar{\alpha}}(t) = \left(\sum_{i=1}^{N} \beta_i A_i \right) \bar{\alpha}(t) + \sum_{i=1}^{N} \beta_i q_i$$

This equation is analogous to the equation of the costate time evolution along a sliding mode. Therefore, the guaranteed cost control is capable of generating the possible sliding behavior as exhibited by the optimal trajectories satisfying, in some time interval, the equation $\dot{\bar{x}}(t) = \left(\sum_{i=1}^{N} \beta_i A_i \right) \bar{x}(t)$.

For comparison purposes, we introduce the use of model predictive control which typically achieves superior performance with respect to other control strategies when manipulated and controlled variables have constraints to meet. However, for this particular application the system is not stabilizable. The MPC objective is to delay as far as possible the escape of the system. In general, the finite set of possible control values causes problems for many control techniques. Nevertheless in the cause of MPC, having a finite set of options may be an advantage in making the optimization easier to solve.

In Table 5.1 we show the performance for all the proposed strategies designed to mitigate the viral escape in the model (3.30). For Scenario 1, it can be observed that all the strategies present an optimal behavior with the exception of the switch on failure scheme. The best switching regimen would consist of switching as soon as possible for the next regimen. This recycling treatment can potentially decrease the viral load through the years and delay the appearance of resistant mutants.

Table 5.1: Total viral load at the end of treatment using model (3.30)

Scenario	Switch on failure	SWATCH	Optimal	Guaranteed	MPC
1	344.25	45.35	45.35	45.35	45.35
2	919.29	60.59	57.55	73.92	57.62
3	1.2437×10^4	1045.27	55.56	83.14	55.56

For scenario 2, we noticed that the switch on failure strategy performs worse than proactive switching. For instance, the optimal strategy is very close to undetectable levels where the detection threshold is approximately 50 copies/ml. Numerical results illustrate the good performance of MPC since the viral load achieved is very close to the optimal one. The guaranteed cost control has a good behavior for this scenario, even though its simple design is able to maintain reasonably good results when compared to the optimal with much less computational time. Scenario 3 unveils that both suboptimal strategies have good performance when compared with the optimal. Furthermore, MPC shows for this example an optimal behavior, then we may conjecture that MPC is a good strategy to deal with the mitigation of viral escape.

5.6 Comparisons for the macrophage mutation model

It was previously shown that using the macrophage mutation model (3.33), the first virological failure is presented after six years of treatment, then the second therapy may last for 5 years before viral explosion is presented. Numerical results are consistent with clinical observation. In addition the SWATCH treatment outperformed the switch on failure treatment. This motivates the study of a more structured method to design a treatment regimen aimed at minimizing the viral load. Therefore we explore the optimal treatment and suboptimal strategies to mitigate the viral escape in HIV. Using 10 months as prediction horizon for MPC, we observe in Fig.5.3 the closed-loop response of T_i, M_i, V and the switched drug therapy over a period of 20 years. The MPC algorithm achieves the goal of containing the viral load for a long period. For this example, MPC has the same performance as SWATCH. This coincidence suggests that oscillating between one treatment and the other will improve the viable treatment duration.

Table 5.2 shows the total viral load using optimal and suboptimal strategies. We note that the suboptimal strategies have a similar performance to the optimal strategy; for instance, guaranteed cost control slightly outperforms MPC and SWATCH. Using guaranteed cost control we know in advance an upper bound on the performance achieved by the controller. We remark that using optimal and suboptimal strategies we can delay the appearance of a virologic failure approximately three years compared to the switch on failure strategy.

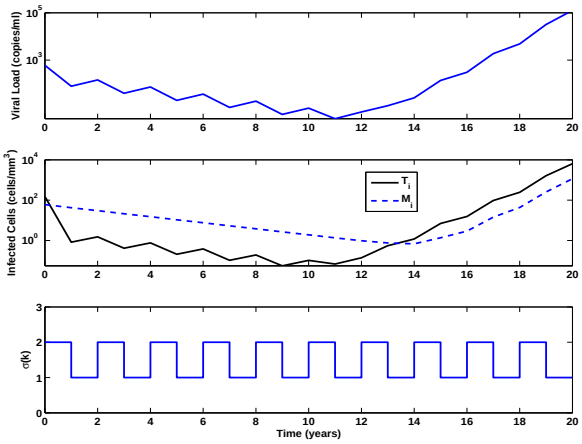

Fig. 5.3: Closed loop using MPC for the macrophage mutation model

Table 5.2: Simulation results for 7 year treatment period using 3 month decision time

Strategy	Viral Load
Virologic Failure	780
SWATCH	25.8
Optimal Control	9.9
Guaranteed Cost	13.38
MPC	25.53

5.7 Comparisons for the Latently infected CD4+T cell model

In the latently infected CD4+T cell model we consider three different therapies. Using the virologic failure treatment, there are three changes in therapy in a period of 4 years. The first therapy keeps the viral concentration below 1000 copies/ml for one year, however resistant genotypes appear. Therefore the second treatment is introduced, the viral population is again decreased for a while, but because of the existence of a high concentration of infected cells, virological failure occurs in a shorter time period. It is then necessary to introduce the third treatment. An important fact is that latently infected cells remain almost constant, this fits with clinical and theoretical studies which agree that these cells play an important role for the late stage in HIV infection. Using 10 months as prediction horizon for MPC, we present in Fig.5.4 the closed-loop response of T_i, L, V and the switched drug therapy over a period of 14 year. The MPC algorithm accomplishes the main goal of containing the viral load as long as possible. In fact, for this example, virologic failure would be present after 12 years, which means that we could extend the duration of virologic control by 8 years compared to the clinical assessment. In addition the total population of infected CD4+T cells is decreased for a period of 6 years. These results are consistent with the preliminary clinical trial

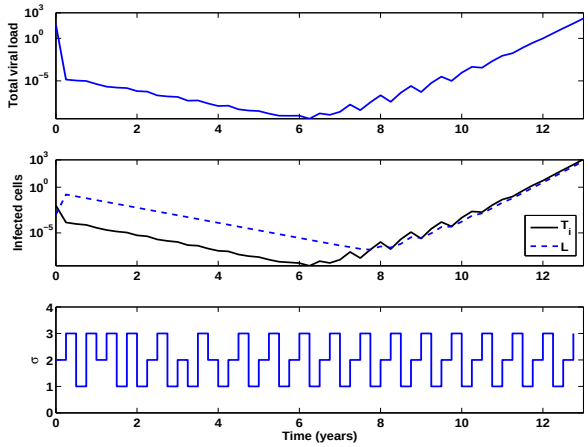

Fig. 5.4: Closed loop using MPC

SWATCH [8], which concluded that proactive alternation of antiretroviral regimens might extend the long-term effectiveness of treatment options without adversely affecting patients' adherence or quality of life.

Table 5.3: Simulation Results for 5 year treatment period using 3 month decision time

Strategy	Viral Load
Virologic Failure	5.14e28
SWATCH	6.22e-9
Optimal Control	2.20e-9
Guaranteed Cost	2.53e-4
MPC	2.31e-9

We notice in Fig.5.4 how the switching is irregular for the first 4 years, but it remains quite regular for the remaining years. This means that oscillating treatment might be a good strategy to mitigate the viral replication when it is not possible to measure the complete HIV state. Table 5.3 shows that the oscillating drug regimen provides very close results to both MPC and optimal control. Based on simulation results and clinical trials we could suggest that this approach may minimize the emergence of drug-resistant strains better than frequent monitoring for viral rebound. Moreover, we test the guaranteed cost strategy, which requires very low computational resources and exhibits good performance with respect to a switch on virologic failure treatment protocol.

5.8 A Nonlinear Mutation Model Study

It was previously shown that the proposed controllers based on a switched linear exhibit a good performance to decrease viral load and overperformed clinically used common strategies. However, all comparisons were made on switched linear systems, which we consider represent adequately the HIV dynamics when the patient is under treatment. However, it is very important to verify the effectiveness of these strategies in a more realistic situation. For this reason, based on the proposed model (3.12) and using proliferation terms (3.27) and (3.28), we suggest the following nonlinear mutation model:

$$\begin{aligned}
\dot{T} &= s_T + \frac{\rho_T}{C_T + V_T} T V_T - \sum_{i=1}^{n} k^i_{T,\sigma} T V_i - \delta_T T \\
\dot{M} &= s_M + \frac{\rho_M}{C_M + V_T} M V_T - \sum_{i=1}^{n} k^i_{M,\sigma} M V_i - \delta_M M \\
\dot{T}^*_i &= k^i_{T,\sigma} T V_i + \sum_{j=1}^{n} \mu m_{i,j} V_j T - \delta_{T^*} T^*_i \\
\dot{M}^*_i &= k^i_{M,\sigma} M V_i + \sum_{j=1}^{n} \mu m_{i,j} V_j M - \delta_{M^*} M^*_i \\
\dot{V}_i &= p^i_{T,\sigma} T^*_i + p^i_{M,\sigma} M^*_i - \delta_V V_i
\end{aligned} \tag{5.27}$$

where $V_T = \sum_{i=1}^{n} V_i$. Therapies are composed of reverse transcriptase inhibitors and protease inhibitors, that are represented by $k^i_{T,\sigma} = k_T f_i \eta^T_{\sigma,i}$, $k^i_{M,\sigma} = k_M f_i \eta^M_{\sigma,i}$, $p^i_{T,\sigma} = p_T f_i \theta^T_{\sigma,i}$, and $p^i_{M,\sigma} = p_M f_i \theta^M_{\sigma,i}$. $\eta_{\sigma,i}$ is the infection efficiency for genotype i under treatment σ, and $\theta_{\sigma,i}$ expresses the production efficiency for the genotype i under treatment. We assume that in the absence of treatment, mutation reduces the fitness of the genotype. Thus we use linear decreasing factors f_i, which represents the fitness of the genotype i. For simulation purposes, we suggest a 4 variant, 2 drug combination model as was presented in Chapter 3. The linear decreasing factors are $f_i = [1, 0.83, 0.83, 0.77]$ and the treatment efficiencies are: $\eta^T_{\sigma,1} = \theta^T_{\sigma,1} = [0.8, 0, 0.7, 0]$, $\eta^T_{\sigma,2} = \theta^T_{\sigma,2} = [0.8, 0.7, 0, 0]$, $\eta^M_{\sigma,1} = \theta^M_{\sigma,1} = [0.7, 0, 0.6, 0]$ and $\eta^M_{\sigma,2} = \theta^M_{\sigma,2} = [0.7, 0.6, 0, 0]$.

In our test scenario we assume that the patient is untreated during the initial 4 years. We make this assumption since the guidelines for the use of antiretroviral agents HIV-1 [5] recommends antiretroviral therapy for patients with CD4+T counts between 350 and 500 $cells/mm^3$. After 4 years we introduce the common practice regimens in the model (5.27). Fig.5.5 presents results for the virological failure and oscillating treatment. When virologic failure treatment is introduced after the fourth year, there is a fast recovering in CD4+T cells counts and a sharp drop in viral load to undetectable levels as reported in clinical studies [3]. Clinical markers are in acceptable levels to maintain good immunological responses before the first virological failure is presented at

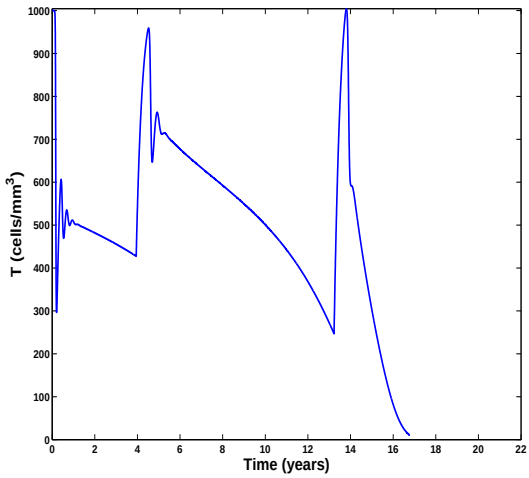

(a) CD4+T cells using virologic failure

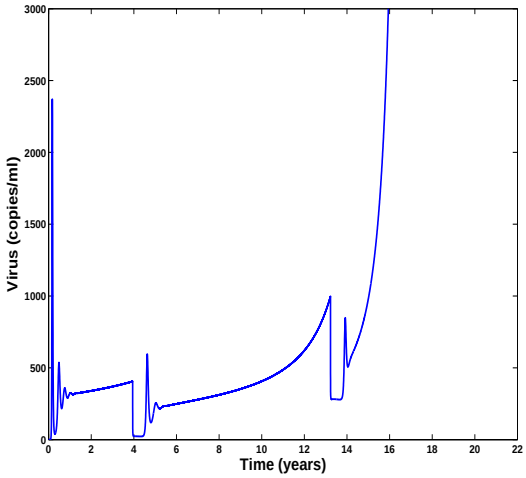

(b) Viral load using virologic failure

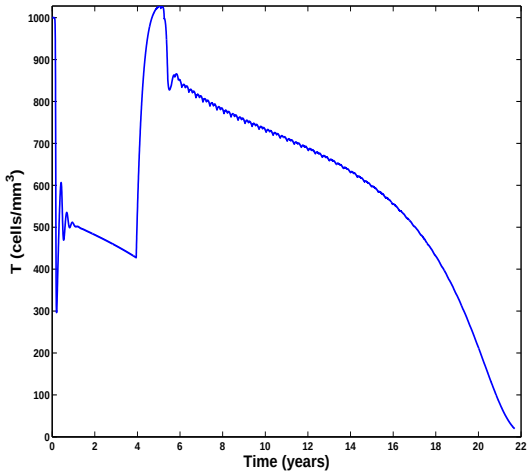

(c) CD4+T cells using SWATCH

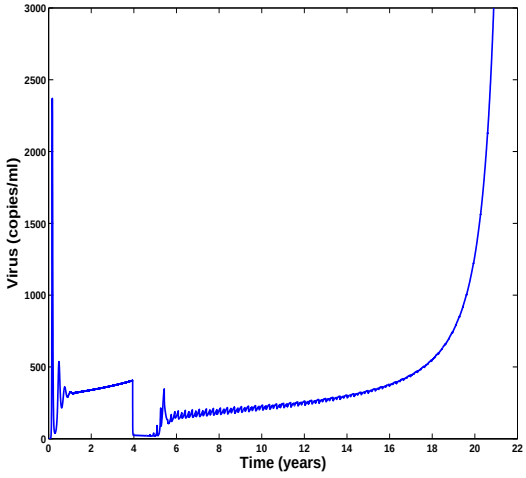

(d) Viral load using SWATCH

Fig. 5.5: Virologic on failure and SWATCH applied to the nonlinear model (5.27)

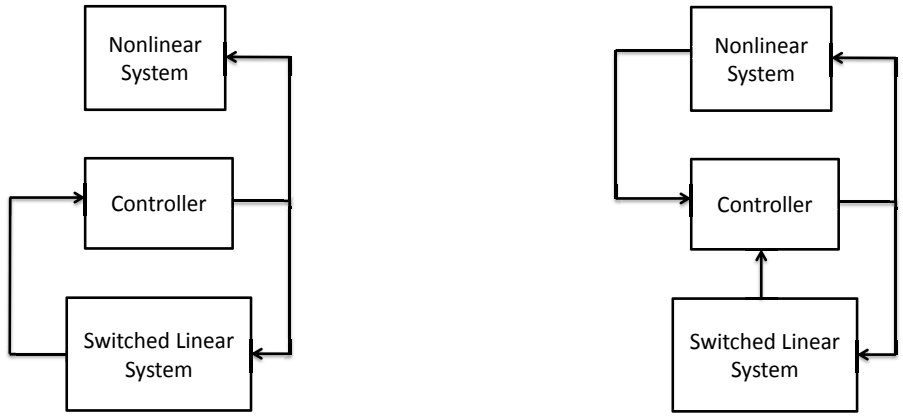

(a) Offline Controller (b) Online Controller

Fig. 5.6: Switched linear strategies applied on a nonlinear model

approximately 10 years. To avoid the collapsing of CD4+T cells, the introduction of the second therapy is necessary. However, the persistent low-level viremia cause a second virological failure after two years. Time scales are consistent with the clinical work of [76].

Using a proactive switching as proposed in [8], we note in Fig.5.5d that virological failure is delayed until 19 years. This numerical results reveal the importance of proactive switching to extend good health conditions. In comparison with the virological failure, SWATCH treatment extended the time to virological failure by four years. Moreover, Fig.5.5c reveals that CD4+T cells counts are maintained in good levels (over 400 $cells/mm^3$) for longer period than with the virological failure treatment.

In order to check the applicability of the optimal and suboptimal strategies proposed before, we introduce the strategies after 4 years and keep them for a period of 6 years. That is because in this period cells are maintained almost constant. Therefore, the switched linear system (3.33) could be used to design switching trajectories. For this end, we simulate the nonlinear mutation model (5.27) without any treatment during 4 years, then we collect the final values of infected cells and virus, which will serve as initial condition for the switched system. CD4+T cells and macrophages are considered constant, with values 700 $cells/mm^3$ and 740 $cells/mm^3$ respectively.

After the fourth year we compute the switching rule based on the switched linear system (3.33) using two different approaches, see Fig.5.6. For the first one, we compute the whole switching trajectory using only the switched system, then the whole switching trajectory is implemented in the nonlinear system as is shown in Fig.5.6a, this is called offline control. The second approach is based on the switched linear system, the difference is that at every decision step the output of

Table 5.4: Simulation results for symmetric case

Strategy		Viral Load	CD4+T cells
Virologic Failure		405.7	500.9
SWATCH		230.9	731.4
Optimal Control	Offline	243	648.1
	Online	376	583.4
Guaranteed Cost	Offline	408	570
	Online	410	568.5
MPC		231	511

the nonlinear system updates the controller which computes the next input for the nonlinear model as is shown in Fig.5.6b. Simulation results reveal that proactive switching overperformed virologic failure treatment. In Table 5.4 we consider a 10 year treatment period and 3 month decision time. Linear switched strategies present values very closed to the SWATCH treatment, where the offline optimal strategy has the best performance compared to the other strategies based on the switched linear model.

It is observed in Table 5.4 that SWATCH treatment had the best performance, that is because we considered a symmetric treatment scenario. Nevertheless, in practice different therapies can affect with different intensities the genotypes presented in the patient. For this end, we suggest the following asymmetric treatment efficiencies: $\eta^T_{\sigma,1} = \theta^T_{\sigma,1} = [0.8, 0.01, 0.4, 0.01]$, $\eta^T_{\sigma,2} = \theta^T_{\sigma,2} = [0.8, 0.8, 0.01, 0.1]$, $\eta^M_{\sigma,1} = \theta^M_{\sigma,1} = [0.7, 0.01, 0.3, 0.01]$ and $\eta^M_{\sigma,2} = \theta^M_{\sigma,2} = [0.7, 0.7, 0.03, 0.1]$.

For the asymmetric case, we proposed that the highly resistant genotype is partially affected by treatments, but not with enough strength to affect the final viral escape. Notice in Fig.5.7b how the first virological failure is presented after ten years, that is, slightly larger than in the symmetric case. The second therapy does not last more than three years before a virological failure. Therefore the total time before the viral load escapes is approximately 16 years. On the other hand, the SWATCH strategy exhibits a duration of 30 years before virological failure occurs. For this asymmetric example, SWATCH treatment provides good levels in CD4+T cell count and viral load for almost 25 years. We can conclude from this example that even though the therapies were more efficient, the switch on virological failure does not promote any improvement in the extension of the viral escape. Proactive switching might make a difference in time scales to preserve safe in infected people with HIV.

For the symmetric case, the SWATCH treatment option provides the best performance. Linear switching strategies had slightly worse performance than the SWATCH strategy. Nevertheless, when therapies are asymmetric, the proposed strategies present different performances as is shown in Table 5.5. At the end of 6 year period treatment, virological on failure treatment exhibits slightly less concentration in viral load than the SWATCH strategy. However if optimal and suboptimal strategies based on a switched systems are used, we may notice that MPC provides the best result

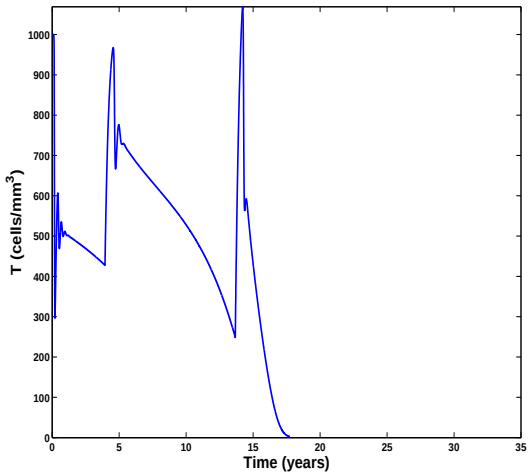

(a) CD4+T cells using virologic failure treatment

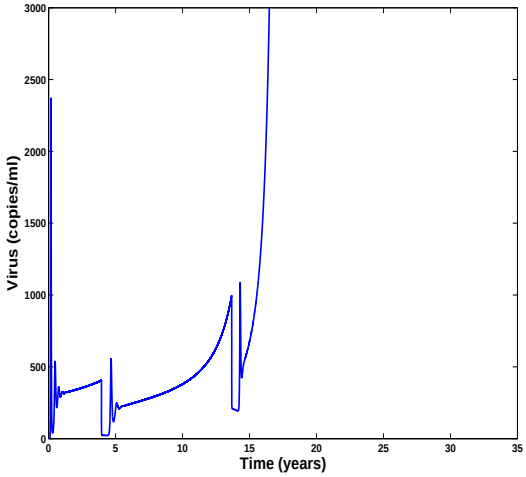

(b) Viral load using virologic failure treatment

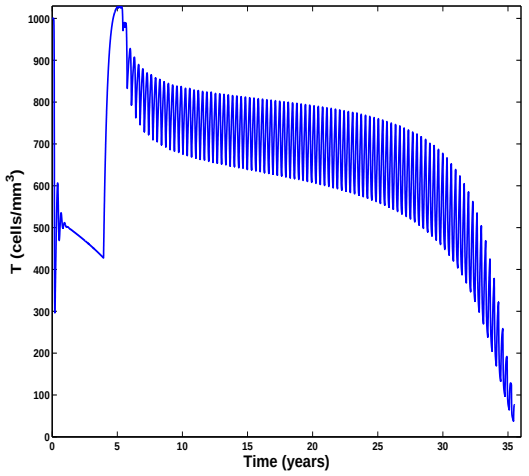

(c) CD4+T cells using SWATCH

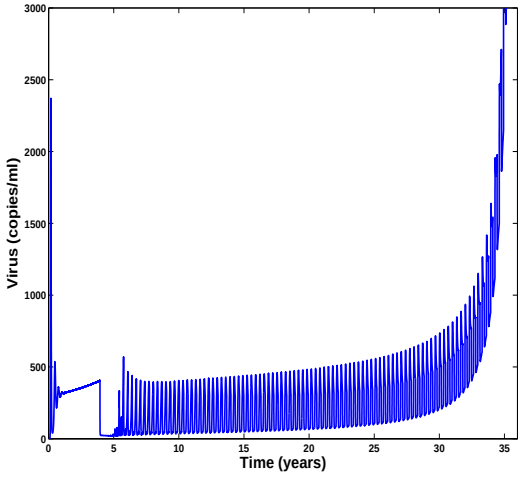

(d) Viral load using SWATCH

Fig. 5.7: Virologic on failure and SWATCH for an asymmetric case in the model (5.27)

Table 5.5: Simulation results for asymmetric case

Strategy		Viral Load	CD4+T cells
Virologic Failure		380	527.4
SWATCH		410	724.4
Optimal Control	Offline	50.98	727
	Online	264	639
Guaranteed Cost	Offline	397.8	563.6
	Online	314.17	646.03
MPC		49.08	733.622

with undetectable levels of virus and high concentration in CD4+T cells. Offline optimal control supplies inconsiderably higher concentrations in viral load than MPC. Numerical results for both examples show that feedback does not provide any improvement to optimal control. We consider this bad performance is due to decision variables are very close each other using online optimal control, together the use of a model approximation of the real system and measurements are made infrequently.

Even though guaranteed cost strategies provide less viral load than virologic failure treatment, they present the worst performance compared with the other suboptimal strategies for this example. We remark that optimal control present an optimal trajectory for the linear system, that does not mean it is going to be optimal when we apply it to the nonlinear case. Actually, there is no guarantee that it will provide better results than other strategies.

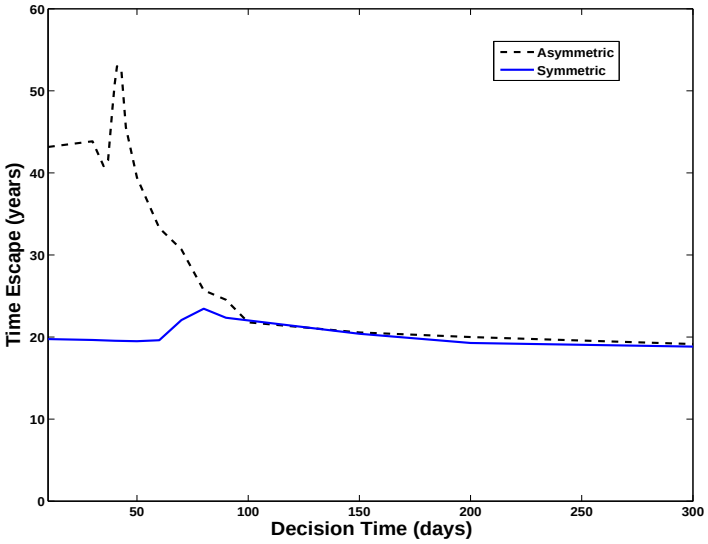

Fig. 5.8: Viral time escape as a function of the decision time

Numerical results suggest that proactive switching is important to maintain low levels of viral load for a long period of time. In general, switching every three months between two therapies appears to be suitable for the last two examples. Since measurements are expensive and cumbersome for the patient, viral and CD4+T cell count are recommended every three to six months, depending on the patient's health status.

Using the model (5.27) we can examine how decision time affects the markers for very long period treatments. In Fig.5.8 we may notice how the viral escape is affected by the decision time when SWATCH treatment is used. Simulation results reveal for the symmetric case a maximum in the viral time escape, using a decision time of approximately 80 days the viral escape might be extended nearby 53 years. Comparing with the recommended decision time of three months [8], we obtain an extension of 4 years in the escape time. In the asymmetric case, the maximum escape time is approximately 53 years using a decision time of 40 days.

Results show that the design of proactive switching is not trivial, and the decision time should be carefully designed for each patient. These examples suggest that decision time should be between 1 and 4 months. For both cases, proactive switching provides the same results when the decision time is more than 4 months. Based on this, we might suggest avoiding long decision times for proactive switching, whilst decision time does not make a big difference in the case of switch on virological failure treatment.

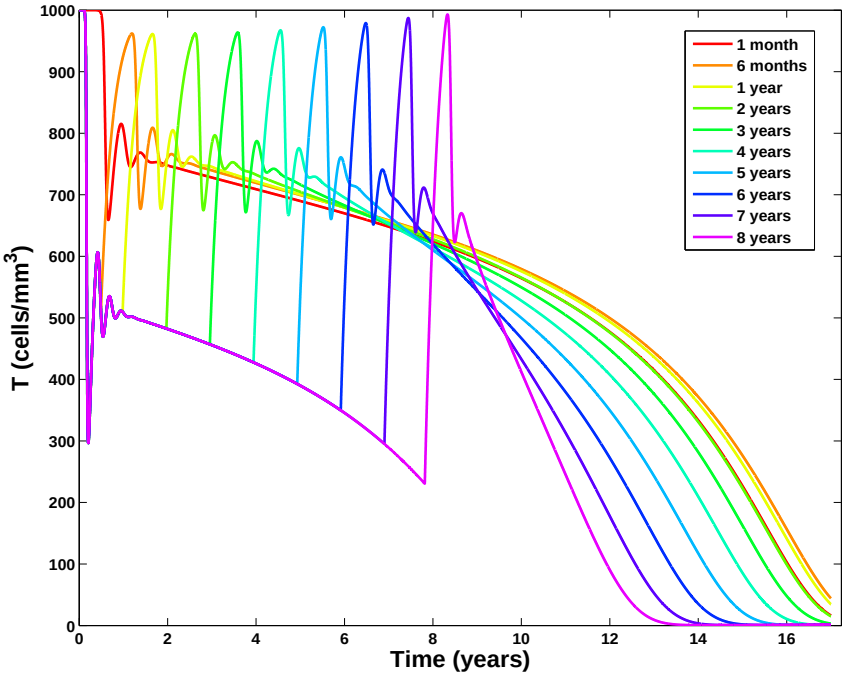

Fig. 5.9: Treatment introduction

Over the last 20 years, several changes have been made to the recommendations on when to start therapy. The standard procedure for the Panel [5] has not been agree when to start therapy. However, there is a general consensus that antiretroviral therapy should be initiated in all patients with a history of an AIDS-defining illness or CD4+T counts are less than 350 cells/mm^3.

Using the nonlinear mutation model (5.27) we also analyze the question when to initiate therapy. We consider therapy 1 for the asymmetric case, then we introduce treatment in different periods of the infection. On one hand, numerical results in Fig.5.9 suggest that there is very little advantage in the time to viral escape as a result of introducing HAART in the early stages of infection, that is during the first 4 years. In fact, when we introduce treatment in the primary infection stage, first month, the viral escape is slightly faster than introducing the treatment later. This is because in the early stage we suppress the wild type genotype, and this might help the emergence of other strains with long term resistant.

On the other hand, patients should not be initiated treatment in later stages of infection. If treatment is introduced approximately in the sixth year or after of the infection, the progression to AIDS is faster. This is because treatments are of reduced efficacy in macrophages and can not help to delay the progression.

5.9 Concluding Remarks

In this chapter we have considered alternatives to the optimal control problem for positive switched linear systems. Specifically we have concentrated on guaranteed cost control which provides an upper bound on the cost function and the well known model predictive control strategy. The major conclusions made in the chapter are listed below.

- Using a piecewise co-positive Lyapunov function, we provide sufficient conditions for stability in positive switched linear systems for continuous and discrete time.
- We derive in both continuous and discrete time a switching rule which guarantees a bound on the achieved performance. This means that we know in advance the worst achievement of the controller. At the cost of some conservatism in the upper bound, we may reduce the parameters in the controller to a single one, allowing an easy computation line search for a single parameter.
- Due to the biological application, we need to design a switching treatment for a specific period of time, therefore we extend the guaranteed cost control to a finite horizon. Numerical results reveal that guaranteed cost control achieves good results with minimal computational resources. Moreover, this strategy could exhibit an optimal performance for some symmetric cases, and very close results to the optimal for some asymmetric cases.
- The model predictive control application was explored to mitigate the viral escape. Simulation results exhibit the effectiveness of this method. MPC gave similar performance to the optimal control, with the advantage that MPC requires less computational resources than the optimal strategy and it can handle constraints.
- From a clinical point of view, we conclude that macrophages occupy a unique place in the viral escape, these treatments are not completely efficient to clear the infected macrophages causing the final transition to AIDS.
- Using a more realistic scenario, we applied optimal and suboptimal strategies based on a switched linear system to a nonlinear mutation model. Simulation results suggest that proactive switching is important to extend the viral time escape. MPC technique showed the best performance and was able to maintain undetectable viral levels for the asymmetric case. Slightly less than MPC, guaranteed cost and optimal control revealed good results for the escape time problem. Suboptimal strategies might be important for the design of switching treatments, in the majority of the cases, MPC presents the best performance. Therefore, we conclude that MPC might be consider in the future for a possible application.
- The clinical trial SWATCH suggests a switching time of 3 months, however, simulation results suggest that the election of decision time is not trivial for the efficacy in the proactive switching. From the study examples, long decision times (more than 4 months) should be avoided, because they reduce the benefits in extending the viral escape time.

- When to start therapy? is a difficult question to answer for clinicians. Based on this numerical study, we suggest that there is not any reason to expose the patient to the strong effects of HAART therapy during the first three years of infection. We did not find any evidence that an early therapy would help in the long-term for the viral escape. However, treatment should not be delay for later stages (more than 7 years), that is because HAART is still not effective for long-term reservoirs.

Chapter 6

Conclusions and Open Questions

The motivation and background for the study of the HIV infection was presented in the opening two chapters. In particular, motivated by the worldwide problem in health caused by HIV, we described several issues related to this infection. To tackle this biological problem, we follow a mathematical approach. Toward this end we divided the thesis work in two parts. The first part introduces the biological background and the mathematical models, which are fundamental for the HIV infection study. Using a control theoretic approach, the second part of this work is composed of optimal and suboptimal strategies to mitigate viral escape in HIV infection.

In **Chapter 3**, motivated by the work in [4], we proposed a mathematical model (3.12) able to represent the whole trajectory in HIV infection: primary infection, asymptomatic and symptomatic stage. Compared with other works, the proposed model based on the latent reservoir theory exhibits the complete course of the infection with a robust behavior to parameter variations. Numerical results suggest that HIV dynamics might be divided in two coupled feedback paths. One path provides the fast dynamics presented in the early stages of infection as a result of a strong inhibition to CD4+T cells. The second feedback path sustains a slow but constant process of infection in macrophages. In this way, infected macrophages induce growth in the viral load in the last stages of the infection. Incorporating cell proliferation terms, the dynamics of CD4+T cells and virus match better clinical observations and preserve the property of robustness in the model. However, the proposed model (3.12) needs more work to represent other mechanisms in HIV infection, for instance immune responses, CD4+T cell activation, homing theory, and dendritic cell role. Then, it might be possible to understand how other mechanisms affect the transition to AIDS.

Mathematical analysis of HAART regimens reveals that the longer the delay before initiating therapy, the greater the number of new infections of cells and long-term reservoirs. Consequently a longer period treatment is needed to clear the virus. When the patient is undergoing therapy and prior to virologic failure, we make the assumption that non-infected CD4+T cell and macrophage

counts are approximately constant. Then the model (3.12) may be reduced to a switched linear system. We proposed three different switched systems using different mutation trees to explore treatment regimens: the switch on failure which is common in clinical practice and the alternating regimen SWATCH. Simulation results exposed the relevance of proactive switching to decrease viral load maximally. SWATCH approach appears to give superior results to the classical switch on failure approach. Nonetheless, periodic alternating treatments might not always provide good performance when the available treatment options have unequal effects on the proliferation rate of the resistant genotypes.

To obtain models capable of reproducing the long term clinical observations for the responses of patients under treatment, we followed two different cells to match these dynamics: latently infected CD4+T cells and macrophages. Simulations show that macrophages are necessary to obtain the appropriate time scales and treatments responses. Consequently, we suggest that macrophages may be an important component of the dynamics in HIV infection for both non-treated and treated patients.

Because periodic alternating treatments does not always provide the best response, in the second part of the thesis we examine the problem of treatment scheduling to mitigate viral escape in HIV infection using optimal and suboptimal strategies. In **Chapter 4** we provided the relevant background to address the optimal control question. Using the Pontryagin principle we established the optimal control problem for positive switched systems for a finite horizon which results in a two point boundary value problem. Under certain conditions of symmetry in the viral proliferation rate, we prove that the solution of the optimal control problem lies on a sliding surface. The biological relevance resides when the resistant genotypes are affected with the same intensity by their respective treatment, then it is important to switch proactively instead of using the current clinical practice of switching on virological failure. In fact, optimally switching should occur as soon as one genotype exceeds the concentration of the other and vice versa. This provides the idea that a periodic switched treatment might be applied to different cases. In some asymmetric examples the optimal solution is still switching, however, we have not been able to establish general results.

In a similar vein, we approach the discrete-time optimal control, where the problem also results in a two point value problem. A possible numerical solution is an exhaustive search, however the computational demands of this approach grow exponentially with the number of decisions. To tackle computational time issues, we derived different algorithms based on linear programming to "prune" partial control sequences that are provably sub-optimal. Depending on the number of decisions, these algorithms offer faster solutions than an exhaustive search algorithm. A numerical robustness study shows that optimal trajectories are robust to parameter variation, and therefore these strategies might be relevant for treatment scheduling in HIV.

Many problems remain open for the optimal control area. For the continuous time case, it is still needed to find the optimal solution for asymmetric cases, we conjecture that the solution lies on a sliding mode but more work is necessary. The optimal solution in the discrete time version,

even for the symmetric case, is difficult to prove analytically. An interesting question is to analyze the optimal control using different cost functions. In this work we focus on a terminal penalty cost function. However it might be important to analyze an integral term, that requires minimization of aggregate the viral load. This might be relevant for the treatment scheduling. For the numerical part, simulations showed that the algorithm proposed based on LP are good at "pruning" suboptimal solutions. However, when we include higher order models with more species, MATLAB optimization toolbox provides results with warnings of numerical difficulties in solving the optimization. Therefore it might be important to find other strategies or formulations to achieve longer and faster simulations.

Regarding a practical application, optimal control strategies are very demanding. At the cost of some conservatism in the optimality, in **Chapter 5**, we used suboptimal strategies that might not provide an optimal performance, but whose solution may lie close to an optimal behavior. These approaches have a dramatic reduction in use of computational resources. On one hand, using a piecewise co-positive Lyapunov function, we give suboptimal strategies with a guaranteed cost control. This guarantees a certain performance, therefore we can compute in advance the worst scenario that this control might provide. The guaranteed cost control was presented for both finite and infinite horizon cases.

Numerical results show that in the examples considered, guaranteed cost control achieves good results compared with the optimal one, with minimal computational resources. In fact, for some examples this strategy is able to reproduce optimal switching trajectories. However we have not been able to establish which conditions are necessary for such behavior. On the other hand, model predictive control appears to be a suitable suboptimal strategy for treatment scheduling. Simulations reveal that MPC achieves similar performance to the optimal control, but MPC uses less computational resources. It is difficult to choose which suboptimal strategy is better than the other. In several numerical cases, MPC outperformed guaranteed cost control.

Using a more realistic scenario, we analyzed optimal and suboptimal strategies based on a switched linear system but applied to a nonlinear mutation model. Simulations suggest that proactive switching is important to extend the time to viral escape. The MPC technique proved the most effective strategy. Slightly worse than MPC, guaranteed cost and optimal control revealed good results for the escape time problem. We should remark about the robustness of the proposed strategies, even though they were designed for a switched linear system, they present an acceptable performance.

Suboptimal strategies based on a switched linear system present good performance, in most of the cases they obtained similar results to the optimal one, independently of the complexity of the mutation tree and nonlinearities. However, it might be important to explore control strategies based on the nonlinear model. There are some works for the guaranteed cost control for a particular class of nonlinear models, so it is necessary to adapt for nonlinear positive switched systems. MPC has been shown to work well for nonlinear models, for instance in control process. Therefore it is interesting to check MPC based on the nonlinear model.

Simulation studies on the nonlinear mutation model advice us about the election of decision time, which is important for the efficacy in the proactive switching. An example study showed that long decision times (more than 4 months) should be avoided, because they do not provide any considerable extension in the viral time escape. The clinical trial SWATCH suggests a switching time of 3 months, however, based on simulation results we suggest that the decision time should be analyzed for every case. This problem could be consider as an oscillating control, which can be formalized and might provide good results in treatment scheduling.

Based on the nonlinear mutation model, we investigated when infected people with HIV should start therapy. The question is still a point of discussion between clinicians and no general consensus has been achieved. Simulation results suggest that there is no reason to expose the patient to the strong effects of HAART therapy during the first three years of infection. This is because CD4+T cell counts are over acceptable levels (more than 400 copies/ml) and we could not find any evidence that an early therapy would help in the long-term for the viral escape. Nevertheless, treatment can not be delay for later stages (more than 7 years). HAART is still not effective for long-term reservoirs, which promotes the last depletion in CD4+T cells.

A very important problem which remains open is the design of observers in HIV, that is some cells can not be measured frequently and other like macrophages are very difficult to estimate. In practice, state observer based switching control may provide a suitable and implementable therapeutic strategy.

Bibliography

[1] UNAIDS/WHO, AIDS Epidemic Update, 2007.

[2] S.H. Bajaria, G. Webb, M. Cloyd and D. Kirschner, "Dynamics of Naive and Memory CD4+ T Lymphocytes in HIV-1 Disease Progression", *JAIDS*, 30:41–58, 2002.

[3] 20 year of HIV, *Nature Medicine*, 9, 803-891, 2003

[4] M. Hadjiandreou, R. Conejeros and V. Vassiliadis, "Towards a Long-Term Model Construction for the Dynamic Simulation of HIV Infection", *Mathematical Bioscience and Engineering*, 4:489–504, 2007.

[5] Panel of Antiretroviral Guidelines for Adults and Adolescents, "Guidelines for the use of Antiretroviral agents in HIV-1 infected adults and adolescents", *Department of Health and Human Services*, December 1, 2009

[6] A. Molla, M. Korneyeva, Q. Gao et al., "Ordered Accumulation of Mutations in HIV Protease Confers Resistance to Ritonavir", *Nature Med.*, 2: 760–766, 1996

[7] R.M. D'Amato, R.T. D'Aquila and L.M. Wein, "Management of Antiretroviral therapy for HIV infection: modelling when change therapy", *Antivir. Ther.*, 3: 147–158, 1998

[8] J. Martinez-Cajas and M.A. Wainberg, "Antiretroviral Therapy: Optimal Sequencing of Therapy to Avoid Resistance", *Drugs*, 139: 81–89, 2003

[9] J. Martinez-Picado, E. Negredo et al., "Alternation of Antiretroviral Drug Regimens for HIV infection", *Annals of Internal Medicine*, 68(1): 43–72, 2008

[10] K. Murphy, P. Travers and M. Walport, Immunobilogy, *Garland Science*, New York and London, 2008.

[11] M.J. Bevan, "Helping the CD8(+) T-cell response", *Nat. Rev. Immunol.*, 4(8): 595-602, 2004.

[12] M.D. Hazenberg, S.A. Otto, B.H.B. van Benthem, M.T.L. Roos, R.A. Coutinho, J.M.A. Lange, D. Hamann, M. Prins, and F. Miedema, "Persistent immune activation in HIV-1 infection is associated with progression to AIDS", *Nat. AIDS*, 17(13): 1881-8, 2003.

[13] K. Blum and R. Pabst, "Lymphocyte numbers and subsets in human blood, Do they mirror the situation in all organs?", *Immunology Letters*, 108: 45–51, 2007.

[14] F. Barre-Sinoussi, L. Montagnier et al., "Isolation of a T-lymphotropic retrovirus from a patient at risk for acquired immune deficiency syndrome (AIDS)", *Science*, 220: 868-871, 1983.

[15] A.M. Jeffrey, A Control Theoretic Approach to HIV/AIDS Drug Dosage Design and Timing the Initiation of Therapy, PhD Dissertation Thesis, University of Petroria, 2006.

[16] B.D. Jamieson, D.C. Douck, S. Killian and L.E. Hultin, "Generation of Functional thymocytes in the human adult", *Immunity*, 10: 569-575, 1999.

[17] P. Ye, D.E. Kirschner and A. Kourtis "The thymus during HIV disease: Role in pathogenesis and in Immune Recovery", *Current HIV Research*, 2: 177-183, 2004.

[18] D.R. Clark, N.M. Ampel, C.A. Hallett, V. Yedavalli, N. Ahmad and D. De Luca, "Peripheral blood from human immunodeficiency virus type 1-infected patients displays diminished T cell generation capacity", *Journal of Infectius Diseases*, 176: 649-65, 1997.

[19] S.M. Schnittman, K.H. Singer and J.J. Greenhouse, "Thymic microenvironment induces HIV expression", *Journal of Immunology*, 147:2553-2558, 1991.

[20] L. Wang, "HIV induces homing of resting T lymphocytes to lymph nodes", *Virology*, 228: 141–152, 1997.

[21] L. Wang, "A Novel Mechanism of CD4 lymphocyte depletion involves effects of HIV on resting lymphocytes: induction of lymph node homing and apoptosis upon secondary signaling through homing receptors", *J. Immunol*, 162: 266–276, 1999.

[22] M. Cloyd, J. Chen and L. Wang, "How does HIV cause AIDS? The homing theory", *Molecular Medicine Today*, 6: 108–113, 2000.

[23] W. Ford and J. Gowans, "The traffic of lymphocytes", *Semin. Hematol.*, 6: 67–83, 1969.

[24] S.G. Turville, P.U. Cameron, A. Handley, G. Lin, S. Pohlmann, R.W. Doms and A.L. Cunningham, "Diversity of receptors binding HIV on dentritic cell subsets", *Nat. Immunology*, 3: 975–983, 2002.

[25] D.S. Kwon, G. Gregorio, N. Bitton, W.A. Hendrickson and D.R. Littman, "DC-SIGN mediated internalization of HIV is required for trans-enhancement of T cells infection", *Immunity*, 16: 135–1443, 2002.

[26] C. Chougnet and S. Gessani, "Role of gp120 in dentritic cell dysfunction in HIV infection", *J. Leukoc. Bio.*, 80: 994–1000, 2006.

[27] M.D. Hazenberg, D. Hamann, H. Schuitemaker, and F. Miedema, "T cell depletion in HIV-1 infection: how CD4+T cell go out of stock", *Nature Immunology*, 1(4): 285-289, 2000.

[28] N. Letvin and B. Walker, "Immunopathogenesis and Immunotherapy in AIDS virus infections", *Nature Medicine*, 9(7): 861-866, 2003.

[29] T.W. Chun, L. Stuyver, S. Mizell et al., "Presence of an inducible HIV-1 latent reservoir during HAART", *Proc. Natl. Acad. Sci.*, 94: 13193–13197, 1997.

[30] D. Finzi, M. Hermankova, T. Pierson and et al., "Identification of a reservoir for HIV-1 in patients on HAART", *Science*, 278: 1295–1300, 1997.

[31] J. M. Orenstein, "The Macrophage in HIV infection", *Immunobiology*, 204: 598–602, 2001.

[32] E.M. Connor et al., "Reduction of maternal-infant transmission of human immunodeficiency virus type 1 with zidovudine treatment", *N. Engl. J. Med.*, 331: 1173-1180, 1994

[33] B. Autran et al., "Positive effects of combined antiretroviral therapy on CD4+T cell homeostasis and function in advanced HIV disease", *Science*, 277: 112-116, 1997

[34] J.M. Emmelkamp and J.K. Rockstroh, "CCR5 antagonists: comparison of efficacy, side effects, pharmacokinetics and interactions–review of the literature", *Eur. J. Med. Res.*, 12(9): 409-417, 2007

[35] D.L. Robertson, B.H. Hahn and P.M. Sharp, "Recombination in AIDS viruses", *J. Mol. Evol.*, 40(3): 24959, 1995

[36] M. von Kleist, Combining pharmacology and mutational dynamics to understand and combat drug resistance in HIV, PhD Dissertation Thesis, National University of Ireland Maynooth, 2010.

[37] D. Ho, "Time to hit HIV, early and hard", *N. Engl. J. Med.*, 333: 1450–451, 1995

[38] S. Haggerty and M. Stevenson "Predominance of distinct viral genotypes in brain and lymph node compartments of HIV infected individuals", *Viral Immunology*, 4: 123–131, 1991

[39] H. Zhan et al., "Human immunodeficiency virus type 1 in the semen of men receiving highly active antiretroviral therapy", *N. Engl. J. Med.*, 339: 1803–1809, 1998

[40] M. Thompson, *AIDS 2010: XVIII International AIDS Conference*, Vienna, Austria, 2010.

[41] J. Lisziewicz, E. Rosenberg and J. Lieberman, "Control of HIV despite discontinuation of antiretroviral therapy", *NEJM*, 340: 1683–1684, 1999

[42] T. Harrer and et al., "Strong cytotoxic T cell and weak neutralizing antibody responses in a subset of persons with stable nonprogressing HIV type 1 infection", *Aids research and Human Retroviruses*, 12(7): 585-592, 1996

[43] M SMARTgroup, "CD4 Count-guided Interruption of Antiretroviral Treatment. The Strategies for Management of Antiretroviral Therapy (SMART) Study Group", *NEJM*, 355: 2283-2296, 2006

[44] J. Ananworanich, A. Gayet, M. Braz et al., "Staccato Study and Swiss HIV Cohort Study, CD4-guided scheduled treatment interruptions compared with continuous therapy for patients infected with HIV-1: results of the Staccato randomised trial", *Lancet*, 368: 459-465, 2006

[45] F. Maggiolo, D. Ripamonti, G. Gregis, G. Quinzan, A. Callegaro and F. Suter, "Effect of prolonged discontinuation of successful antiretroviral therapy on CD4 T cells: A controlled, prospective trial", *AIDS*, 18(3): 439–446, 2004

[46] C. Danel, R. Moh, A. Minga, A. Anzian et al., "Trivacan ANRS 1269 trial group, CD4-guided structured antiretroviral treatment interruption strategy in HIV-infected adults in west Africa (Trivacan ANRS 1269 trial): a randomised trial", *Lancet*, 367: 1981–1989, 2006

[47] J. Barbour, T. Wrin, R. Grant et al., "Evolution of phenotypic drug susceptibility and viral replication capacity during long-term virologic failure of protease inhibitor therapy in HIV infected adults", *Virol.*, 76(21): 11104–11112, 2002

[48] M. Nowak and R. May, Virus Dynamics: Mathematical Principles of Immunology and Virology, *Oxford University Press*, New York, 2000.

[49] D. Kirschner, "Using Mathematics to Understand HIV Immune Dynamics", *AMS*, 43:191–202, 1996.

[50] D.S. Callaway and A. Perelson, "HIV-1 infection and low steady state viral loads", *Bull. Math. Biol.*, 64: 29-64,2002.

[51] D. Kirschner and A. Perelson, "A Model for the Immune System Response to HIV: AZT Treatment Studies", *Winnepeg: Wuerz Publishing Ltd*, 1995.

[52] A. Perelson and P. Nelson, "Mathematical Analysis of HIV-1 Dynamics in Vivo", *SIAM Review*, 41: 3–44, 1999.

[53] X. Xia, "Modelling of HIV infection: Vaccine readiness, drug effectiveness and therapeutical failures", *Journal of Process Control*, 17: 253–260, 2007.

[54] F. Campello, "Modelling the Dynamics of HIV-1 and CD4 and CD8 Lymphocytes", *IEEE Engineering in Medicine and Biology Magazine*, 18: 21–24, 1999.

[55] B. Adams, H. Banks, H. Kwon and H. Tran, "Dynamic Multidrug Therapies for HIV: Optimal and STI Control Approaches", *Mathematical Biosciences and Engineering*, 1: 223–241, 2004.

[56] G. Stan, F. Belmudes, R. Fonteneau, F. Zeggwagh, M. Lefebvre, C. Michelet and D. Ernst, "Modelling the Influence of activation-induced apoptosis of CD4+ and CD8+ T cells on the immune system response of a HIV-infected patient", *IET System Biology*, 2: 94–102, 2007.

[57] W. Tan and H. Wu, "Stochastic Modeling of the Dynamics of CD4 + T-Cell Infection by HIV and Some Monte Carlo Studies", *Mathematical Biosciences*, 147(2): 173–205, 1998

[58] N. Dalal, D. Greenhalgh and X. Mao, "A stochastic model for internal HIV dynamics", *Journal of Mathematical Analysis and Application*, 341: 1084-1101, 2008

[59] R. Zorzenon dos Santos, "Dynamics of HIV Infection: A Cellular Automata Approach", *Phisical Review Letters*, 87(16): 168102–4, 2001

[60] E.G. Burkheada, J.M. Hawkinsb and D.K. Molinekc, "A Dynamical Study of a Cellular Automata Model of the Spread of HIV in a Lymph Node", *Bulletin of Mathematical Biology*, 71: 2574, 2009

[61] D. Kirschner, G. Webb and M. Cloyd, "Model of HIV-1 Disease Progression Based on Virus-Induced Lymph Node Homing and Homing-Induced Apoptosis of CD4 Lymphocytes", *JAIDS*, 24: 352–362, 2000.

[62] D. Kirschner, R. Mehr and A. Perelson, "Role of the Thymus in Pediatric HIV-1 Infection", *JAIDS*, 18: 195–109, 1998.

[63] I. Hougue, S. Bajaria, B. Fallert, S. Qin, T. Reinhart and D. Kirschner, "The dual role of dentritic cells in the immune response to human immunodeficiency virus type 1 infection", *Journal of General Virology*, 89: 1–12, 2008.

[64] L. Zhang, C. Chung, B. Hu, T. He, Y. Guo, A.J. Kim, E. Skulsky, X. Jin, A. Hurley, B. Ramratnam, M. Markowitz and D.D. Ho, "Genetic characterization of rebounding HIV-1 after cessation of highly active antiretroviral therapy", *J. Clin. Invest.*, 106:839-845, 2000.

[65] T.C. Greenough, D.B. Brettler, F. Kirchhoff et al., "Long-Term Non-Progressive Infection with Human Immunodeficiency Virus Type in A Hemophilia Cohort", *Journal of Infectious Diseases*, 180: 1790–1802, 1999.

[66] A.S. Fauci, G. Pantaleo, S. Stanley et al., "Immunopathogenic Mechanisms of HIV Infection", *Annals of Internal Medicine*, 124: 654–663, 1996.

[67] S. Lawn, D. Roberts, E. Griffin, T. Folks and T. Butera, "Cellular compartments of HIV type 1 replication in vivo: determination by presence of virion-associated host proteins and impact of opportunistic infection", *Journal Virology*, 74: 139–145, 2000.

[68] C. Chougnet and S. Gessani, "Role of gp120 in dendritic cell dysfunction in HIV infection", *Journal of Leukocyte Biology*, 80: 994–1000, 2006.

[69] A. Brown, H. Zhang, P. Lopez, C.A. Pardo and S. Gartner, "In vitro modeling of the HIV-macrophage reservoir", *Journal of Leukocyte Biology*, 80: 1127–1135, 2006.

[70] K. Takahashi, S. Wesselingh, D.E. McArthur et al., "Localization of HIV-1 in human brain using polymerase chain reaction/in situ hybridization and immunocyto-chemestry", *Ann. Neurology*, 39: 705–711, 1996

[71] M. Meltzer and D. Skillman, "Macrophages and HIV", *Immunology Today*, 6: 217–223, 1990

[72] T. Igarashi, C.R. Brown, Y. Endo et al., "Macrophages are the Principal Reservoir and Sustain High Virus Loads in Rhesus Macaques following the depletion of CD4+T Cells by a Highly Pathogen SHIV: Implications for HIV-1 Infections of Man", *Proc Natl Acad Sci*, 98:658–663, 2001

[73] H. Chang and A. Astolfi, "Control of HIV Infection Dynamics", *IEEE Control Systems Magazine*, 28-39, 2008

[74] A.M. Elaiw, "Global Properties of a Class of HIV models", *Nonlinear Analysis: Real World Applications*, 11: 2253-2263, 2010

[75] M. Barao and J.M. Lemos, "Nonlinear control of HIV-1 infection with a singular perturbation model", *Biomedical Signal Processing and Control*, 2:248–257, 2007.

[76] S. Sungkanuparph, R.K. Groger, E. Overton, J. Fraser, W. Powderly et al., "Persistent Low-Level Viraemia and Virological Failure in HIV-1 infected Patients Treated with HAART", *HIV Medicine*, 7: 7437-7441, 2006

[77] A. Locatelli, *Optimal Control: An introduction.* Basel: Birkauser, 2001.

[78] D. Kirk, *Optimal Control Introduction*, Dover Publication, New york, 1970

[79] L.S. Pontryagin, *The Mathematical Theory of Optimal Processes*, Gordon and Breach Science Publishers, 1986

[80] R. Bellman, *Dynamic Programming*, Dover Publications, 2003

[81] R.B. Vinter, *Optimal Control*, Birichauser, Boston, 2000

[82] F.H. Clarke, *Nonsmooth Analysis and Control Theory*, Springer, 1997

[83] D. Liberzon, *Switching in Systems and Control.* Systems and control:Foundations and Applications, 2003

[84] L. Farina and S. Rinaldi, *Positive Linear Systems.* Willey-Interscience Series, 2000

[85] W. Spinelli, P. Bolzern and P. Colaneri, "A note on optimal control of autonomous switched systems on a finite time interval", *Proceedings of American Control Conference*, Minnesota, USA, 2006

[86] M. Branicky, V. Bokar and S. Mitter, "A unified framework for hybrid control:model and optimal control theory", *IEEE Trans. Automat. Contr.*, 43(1):31–45, 1998

[87] C. Cassandras, D. Pepyne and Y. Wardi, "Optimal control of a class of hybrid systems", *IEEE Trans. Automat. Contr.*, 46(3):398–415, 2001

[88] X. Xu and P. Antsaklis, "Optimal control of switched systems based on parameterization of the switched instants", *IEEE Trans. Automat. Contr.*, 49(1), 2004

[89] H. Sussmann, "A maximum principle for hybrid optimal control problems", *Proceedings of Conference Decision and Control*, Phoenix, USA, 1999

[90] B. Piccoli, "Necessary conditions for hybrid optimization", *Proceedings of Conference Decision and Control*, Phoenix, USA, 1999

[91] J. Murray, M. Elashoff, L.C. Iacono and et al., "The use of plasma HIV RNA as a study endpoints in efficacy trials of antiretroviral drugs", *AIDS*, 13(7): 797–804, 1999

[92] F. Blanchini and S. Miani, Set-theoretic methods in control, Birkhauser, 2008

[93] M.S. Branicky, "Multiple Lyapunov functional and other analysis tools", *IEEE Trans. Automat. Contr.*, 43: 475–482, 1998

[94] J.P. Hespanha, "Uniform stability of switched linear systems: extensions of LaSalle's principle", *IEEE Trans. Automat. Contr.*, 49: 470–482, 2004

[95] J. Hockerman-Frommer, S.R. Kulkarni and P.J. Ramadge, "Controller switching based on output predictions errors", *IEEE Trans. Automat. Contr.*, 43: 596–607, 1998

[96] M. Johansson and A. Rantzer, "Computation of piecewise quadratic Lyapunov functions for hybrid systems", *IEEE Trans. Automat. Contr.*, 43: 555–559, 1998

[97] D. Liberzon and A.S. Morse, Basic problems in stability and design of switched systems. *IEEE Control System Magazine*, 19: 59–70, 1999

[98] J.C. Geromel and P. Colaneri, "Stability and stabilization of discrete-time switched systems", *International Journal of Control*, 79(7): 719–728, 2006

[99] R.A. De Carlo, M.S. Branicky, S. Pettersson and B. Lennartson, "Perspectives and results on the stability and stabilizity of hybrid systems", *Proceedings of the IEEE*, 88:1069–1082, 2000

[100] J. Daafouz and J. Bernussou, "Parameter dependent Lyapunov functions for discrete-time systems with time varying parametric uncertainties", *Systems and Control Letters*, 43:355–359, 2001

[101] G.M. Xie and L. Wang, "Reachability realization and stabilizability of switched linear discrete-time systems", *Journal of Math. Analysis and Applications*, 280:209–220, 2003

[102] V.G. Rumchev and D.J. James "Spectral characterization and pole assignment for positive linear discrete-time system", *International Journal Systems Science*, 26(2):295–312, 1995

[103] T. Kaczoreck, "Stabilization of positive linear systems", *Proceedings of Conference Decision and Control*, Florida, USA, 1998

[104] P.D. Leenheer and D. Aeyels, "Stabilization of positive linear systems", *Systems and Control Letters*, 44(4):259–271, 2001

[105] L. Gurvits, R. Shorten and O. Mason, "On the stability of switched positive linear systems", *IEEE Transactions on Automatic Control*, 52(6):1099–1103, 2007

[106] F. Knorn, O.Mason and R. Shorten, "On linear co-positive Lyapunov functions for sets of linear positive systems", *Automatica*, 45(8):1943–1947, 2009

[107] A. Zappavigna, P. Colaneri, J. Geromel and R. Middleton, "Stabilization of continuous-time switched linear positive systems", *Proceedings of The American Control Conference*, Baltimore, USA, 2010

[108] M. Morari and J.H. Lee, "Model Predictive Control: past, present and future", *Computers & Chemical Engineering*", 667–682, 1999

[109] R. Findeisen and F. Allgower, "An introduction to Nonlinear Model Predictive Control", *21st Benelux Meeting on Systems and Control*, Veldhoven, 2002

[110] S.M. Lynch and B.W. Bequette "Model Predictive Control of Blood Glucose in Type I Diabetics Using Subcutaneous Glucose Measurements", *Proceedings of The American Control Conference*, 4039–4043, 2002

[111] R. Zurakowski and A.R. Teel "A Model Predictive Control based scheduling method for HIV therapy", *Journal of Theoretical Biology*, 238: 368–382, 2006

[112] G. Pannocchia, M. Laurino and A. Landi "A Model Predictive Control Strategy Toward Optimal Structured Treatment Interruptions in Anti-HIV Therapy", *IEEE Transactions on Biomedical Engineering*, 57(5): 1040–1050, 2010

[113] F. Allgower, T.A. Badgwell, J.S. Qin, J.B. Rawlings, and S.J. Wright, "Nonlinear predictive control and moving horizon estimation - An introductory overview", *Advances in Control, Highlights of ECC*, Springer, 1999

[114] R. R. Bitmead, M. Gevers and V. Wertz, "Adaptive Optimal Control", *The thinking Man's GPC*, Prentice Hall, New york, 1990